An Experimental and Theoretical Study on Piezoelectric Ceramic Processing

by

Hatem El-Lakany
B.Sc., The American University in Cairo, 1992

A Thesis Submitted in Partial Fulfillment of the
Requirements for the Degree of

MASTER OF APPLIED SCIENCE

in the Department of Mechanical Engineering

We accept this thesis as conforming
to the required standard

[redacted]

Dr. S. Dost, Supervisor (Department of Mechanical Engineering)

[redacted]

Dr. Y. Stepanenko, Co-Supervisor (Department of Mechanical Engineering)

[redacted]

Dr. Z. Dong, Departmental Member (Department of Mechanical Engineering)

[redacted]

Dr. A. Zielinski, Outside Member (Department of Electrical Engineering)

[redacted]

Dr. H. Kwok, External Examiner (Department of Electrical Engineering)

Supervisors: Dr. Sadik Dost and Dr. Yury Stepanenko

Abstract

Piezoelectricity is the ability of some solid materials to convert a mechanical deformation into an electric charge and vise versa. In recent years, piezoelectric ceramics have gained great importance in high precision actuating and sensing applications. As a part of the IRIS (MSA-6) project, this research is aimed at building an understanding of these materials as well as their processing and characterization techniques. In order to achieve this objective, a combined theoretical and experimental study was conducted by doing the following: the design and construction of experimental facilities for processing and characterizing piezoceramics, the documentation of a detailed theoretical background on piezoelectric materials and the selection of the most suitable ceramic for the planned purpose. This was followed by the processing and characterization of ten batches of piezoceramics. This application-oriented research has established the required background and expertise that will make it possible to repeatedly process the piezoceramic PZT in our laboratory.

Examiners:

[redacted]

Dr. S. Dost, Supervisor (Department of Mechanical Engineering)

[redacted]

Dr. Y. Stepanenko, Co-Supervisor (Department of Mechanical Engineering)

[redacted]

Dr. Z. Dong, Departmental Member (Department of Mechanical Engineering)

[redacted]

Dr. A. Zielinski, Outside Member (Department of Electrical Engineering)

[redacted]

Dr. H. Kwok, External Examiner (Department of Electrical Engineering)

Table of Contents

Preliminary Pages

List of Figures

List of Tables

Acknowledgments

I would like to thank Dr. A. Prasad, Dr. F. El-Guibaly, Dr. A. Zielinski and Dr. Z. Dong for their assistance and advise. I would also like to thank the members of the Materials and Mechatronics research group, especially N. Audit, for their technical assistance and support. Thanks most weightily to my supervisors Dr. S. Dost and Dr. Y. Stepanenko for their patience, guidance and support. This work is funded by the Institute for Robotics and Intelligent Systems (IRIS), and the support has been much appreciated.

1 Introduction

1.1 History of Piezoelectric Materials

The ability of some crystals to produce an electric field (potential) proportional to an applied mechanical deformation is called the "direct piezoelectric effect". The discovery of this phenomenon is attributed to the Curie brothers in 1880. In their earlier research, they discovered this property in crystals such as sodium chlorate, boracite, tourmaline, quartz and Rochelle salt. The Curie brothers were later able to measure the polarization quantitatively and verify the mechanical deformation produced upon the application of an electric field (converse effect). The piezoelectric effect remained a scientific curiosity until a third of a century later when its practical use was investigated during the First World War. In France, Langevin used quartz crystals to emit and later receive high-frequency sound waves under water for the detection of submarines. Later, the examination of the electric behavior of piezoelectric crystals around the neighborhood of their mechanical resonance frequencies led to the development of the piezoelectric resonator. This research was used in developing oscillators, stabilizers and filters [1].

The discovery of the first piezoelectric ceramic, barium titanate ($BaTiO_3$) in 1940 was an important development in this area. Barium titanate showed piezoelectric properties comparable to Rochelle salt. Moreover, it was easy to produce, it could withstand higher temperatures and was not water-soluble. It was followed by other man-made piezoelectric materials called piezoceramics, such as lead zirconate titanate which showed better physical and piezoelectric properties [3].

1.2 Applications

Recently, piezoelectric materials have been characterized as belonging to the so-called "smart materials". These are materials that can sense changes in their environment and react to them in a useful manner [24]. This has made them useful in a multitude of applications which are divided into: sensing, and actuation [5]. A piezoactuator is a device that accurately converts an electric signal into mechanical energy (displacement and/or force). They are usually constructed of several piezoelectric elements configured to get maximum displacement at the highest accuracy. PZT actuators are the most widely used ones and they will be discussed in detail in Chapter 5. Although piezoactuators produce displacements in the order of microns, their high accuracy has made them useful in many high precision positioning applications such as micro-robotics and micro-machining. These applications include:

Piezomotors: They convert high frequency (> 20 kHz) vibratory motion into continuous or stepping motion [8].

Impact Dot-Matrix Printers: They are faster, use less energy and produces less heat than conventional printers [23].

Deformable Mirrors: These mirrors are used in telescopes to rectify the images of distant objects. The mirrors are deformed using the piezoelectric effect to compensate for image distortions caused by the earth's atmosphere.

1.3 Current State of Research

Currently, research in piezoelectric materials is carried out in three main categories:

- The improvement of the physical, electrical and piezoelectric properties of ceramics made of existing materials. This is done by optimizing their composition and processing parameters and/or by combining them with other materials to form composites with superior qualities.
- The synthesis of new classes of piezoelectric materials such as polymers and organic jells.
- The development of new applications for new and improved piezoelectric materials.

1.4 Scope and Objectives of the Present Investigation

The research described in this thesis is an integral part of the materials research of the IRIS[1] (MSA-6) project aiming at the development of actuators for robotics applications. The main objectives of this thesis work were to:

- set up the planned "Piezoelectric Materials Processing and Characterization Laboratory" to be a part of the Materials and Mechatronics Laboratories[2], and
- develope the required expertise to produce desired piezoceramics materials for the IRIS project.

---

1. IRIS stands for the Institute for Robotics and Intelligent Systems, a Canadian Federal Government Network of Centers of Excellence dedicated to funding research collaboration efforts between Canadian universities and industry.
2. The Materials and Mechatronics Laboratory was founded in 1994 for research into smart materials and their use in micro-robotics and medical applications.

In order to achieve these objectives, a combined theoretical and experimental study was conducted. First, a literature survey was carried out to build a theoretical background on piezoelectricity and piezoelectric materials. This was followed by the selection of the material best suited for our applications. A detailed study of the chosen material, its use in actuators and the effect of processing parameters on its properties was conducted. The next step was to design and implement the processing and characterization system of the chosen material (the piezoceramic PZT). After the laboratory became operational, about ten batches of PZT were processed and characterized to optimize the processing parameters. As shown later, the last two batches showed satisfactory results indicating the success of processing. The experience gained through this research makes us confident towards the production of repeatable piezoelectric ceramics (PZT) with desired characteristics in our laboratory.

2 Piezoelectricity

2.1 Introduction

The purpose of this chapter is to provide a brief review of the theory behind the piezoelectric effect. It begins by explaining this effect in atomic scale and its relation to crystal structure. Section 2.2.2 shows how piezoelectricity is induced in ceramics by poling, while 2.2.4 and 2.2.5 explain the direct and indirect piezoelectric effects in ceramics on a macroscopic scale. Section 2.3 is a brief explanation of the derivation of the nonlinear piezoelectric equations. The linear equations are discussed in Section 2.4 along with the conventions used in naming the material constants.

2.2 The Piezoelectric Effect in Atomic Scale

Although piezoelectricity was first discovered in naturally occurring crystals like quartz, piezoceramics will be taken as the model on which the effect will be explained. Later, in Chapter 3, we will discuss the advantages of piezoceramics over other piezoelectric materials and why they were chosen for this project.

2.2.1 Polarization

When materials of a non-centrosymmetric crystal structure are cooled from high temperatures through their Curie point (a characteristic temperature for each material) their crystal structure changes. This results in the center of the positive charge being different from the center of the negative charge, giving rise to an electric dipole [5].

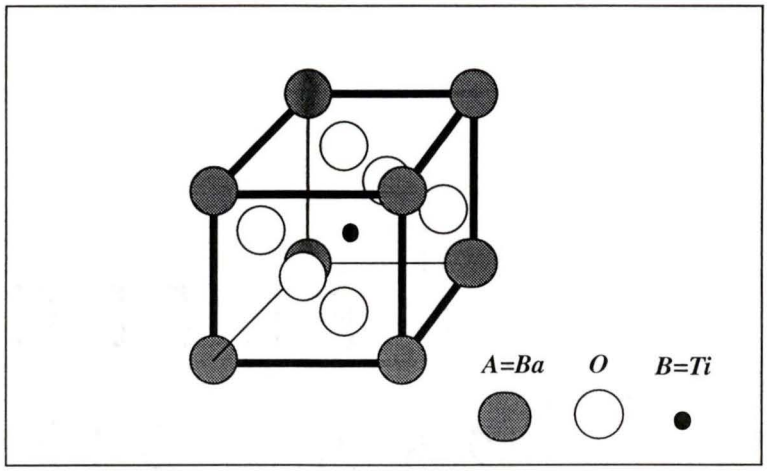

Figure 2.1: Peroveskite structure of $BaTiO_3$ above its Curie point [6]

An example of a non-centrosymmetric crystal structure is the barium titanate peroveskite structure shown in Figure 2.1. It changes from its neutral cubic structure into a polarized tetragonal one as it cools down from above 130 ^oC as shown in Figure 2.2. At room temperature, the polarization is caused by the displacement of the titanium cation relative to the oxygen anion. This causes a dipole moment equal to the product of the charge by the distance between them as shown in Figure 2.2 [6].

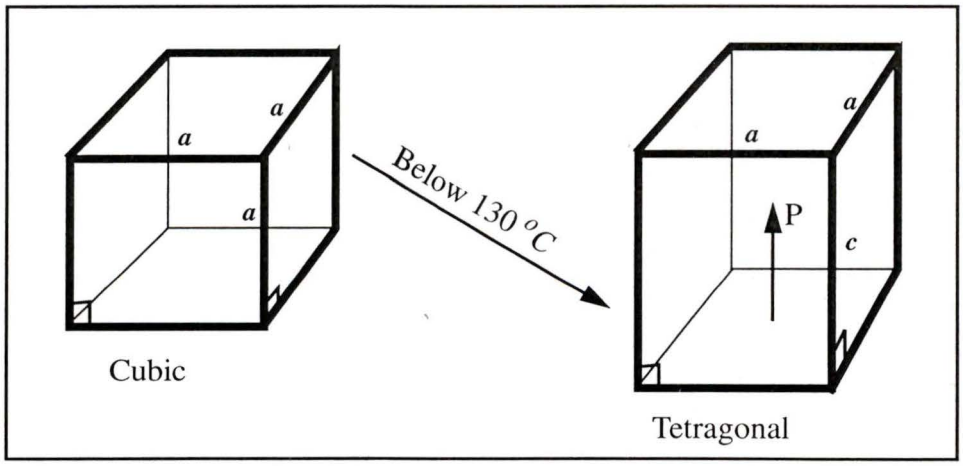

Figure 2.2: Change in Peroveskite crystal structure with temperature [6]

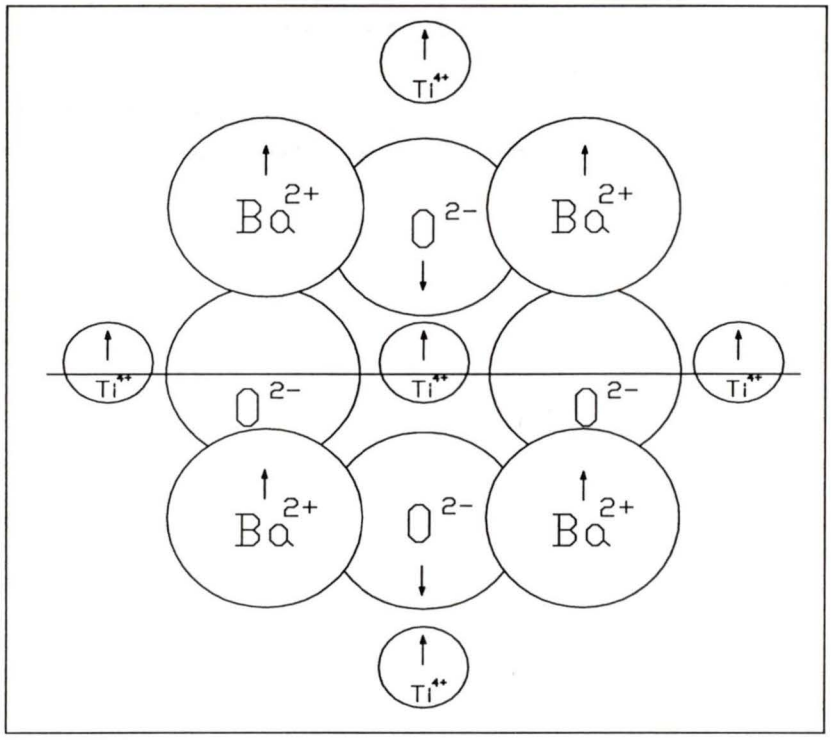

Figure 2.3: Polarization on an atomic scale in $BaTiO_3$ below its Curie point

These dipoles cause an external charge on the surface of the crystal called polarization. If the magnitude of this dipole can be changed by an externally applied stress, the crystal is said to be piezoelectric [3].

2.2.2 Inducing Polarization in Ceramics

A ceramic, which is composed of a mixture of piezoelectric crystals, does not show piezoelectric properties because the polar direction of each domain is randomly oriented, cancelling each other out as shown in Figure 2.4a. The direction of the dipoles can be switched in ferroelectric materials by a process called poling [6]. In this process, a high electric field is applied to switch the direction of the dipoles in the general direction of the applied electric field as shown in Figure 2.4b[5].

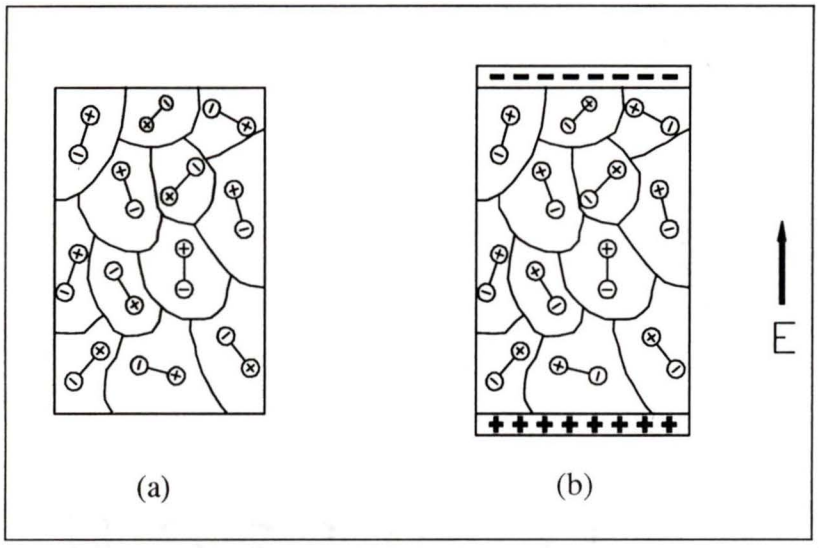

Figure 2.4: Poling of ceramics a) Spontaneous polarization b) Application of an electric field

2.2.3 Energy Considerations

The switching of dipole direction during poling does not involve any physical rotation of domains. What happens is that the *Ti* cations are displaced in the opposite direction relative to the oxygen anions. This occurs when they gain enough energy from the poling electric field to pass over the hump of the W shaped energy curve shown in Figure 2.5.

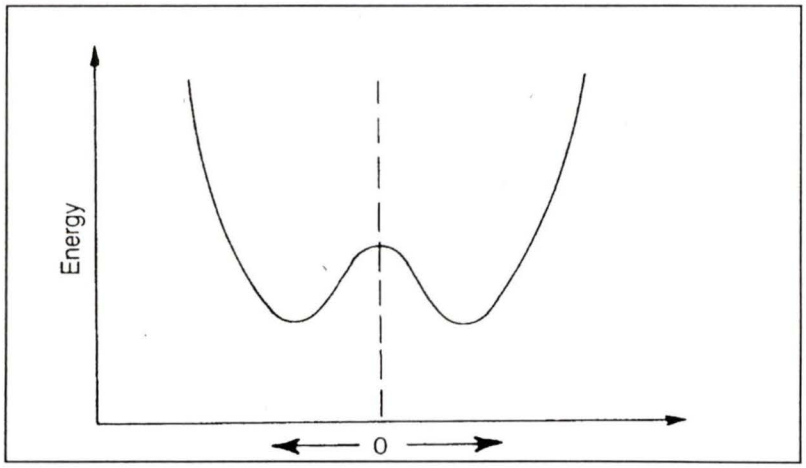

Figure 2.5: Variation in the potential energy of a *Ti* ion along the c axis

2.2.4 The Direct Piezoelectric Effect

Now that the ceramic has a net polarization in the field direction, an external stress along the same direction will change the distance between the unit dipoles. A compressive stress will reduce the overall dipole moment per unit volume, thus changing the charge density at the ends of the sample as shown in Figure 2.6 [12]. This is what is known as the direct effect and it is useful in producing sensors such as accelerometers.

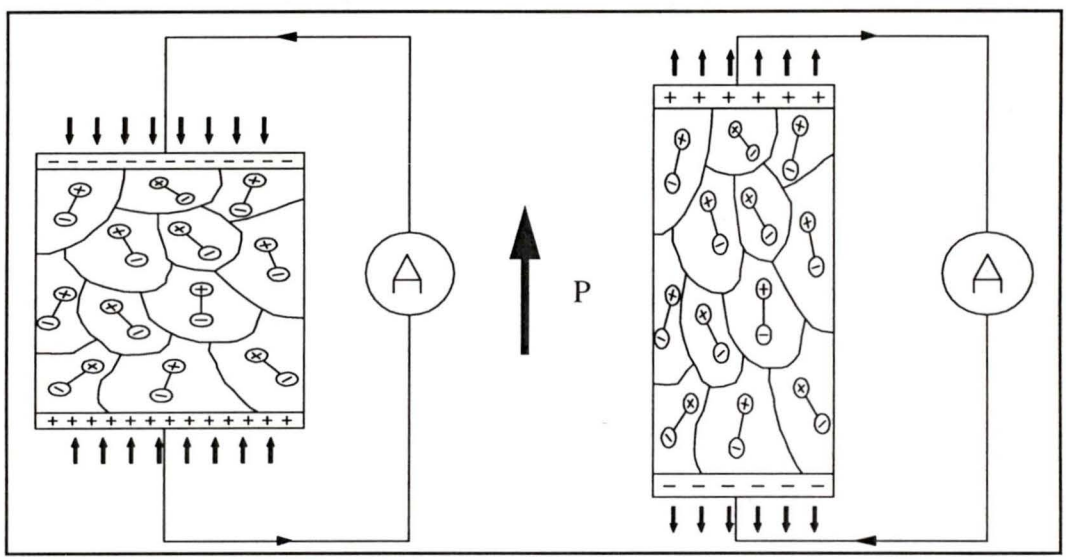

Figure 2.6: The direct piezoelectric effect

2.2.5 The Indirect Effect

Conversely, an applied electric field will change the charge density at the ends. If the electric field is in the direction of poling, the ceramic will elongate due to the positively charged electrode attracting the negative poles of the dipoles. An exaggeration of the indirect effect is shown in Figure 2.7 [12]. This effect is the principle behind piezoelectric actuators, which will be discussed later in detail.

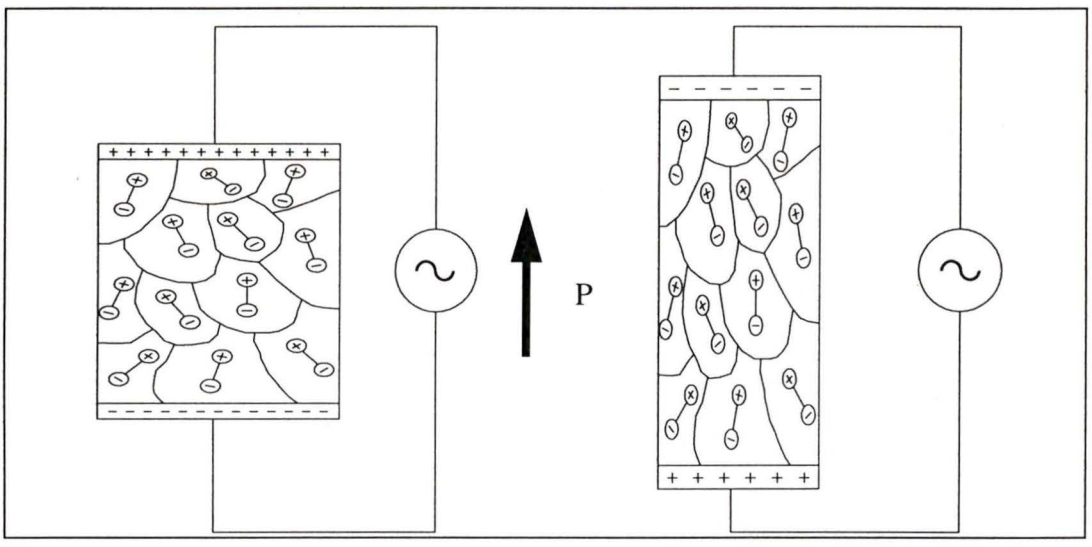

Figure 2.7: The indirect piezoelectric effect

2.3 Nonlinear Piezoelectric Relation

In this section, we briefly introduce the nonlinear piezoelectric effect in piezoceramics. This is done within the frame work of the principles of continuum mechanics.

2.3.1 Basic Principles of Continuum Mechanics

In microscopic scale, matter is actually composed of discrete constituents. However, as in many engineering applications, piezoelectric materials can be modeled as a continuum when we deal with their macroscopic phenomena. This assumption is absolutely valid for various aspects of engineering materials as long as the characteristic length of the problem is very large compared with atomic distances. With the continuity assumption, various properties of their materials such as mass, displacement and velocity can be assumed to be expressed in space in terms of their time averaged values. There are two sets of equations in continuum mechanics. The first set consists of those basic equations obtained from the fundamental axioms of continuum mechanics, which are valid regardless of material

structure. The second set is the constitutive equations expressing the response of material to external effects such as motion, temperature change, electric field, etc. These two sets of equations are solved in conjunction with appropriate boundary conditions, including initial and interface if appropriate, to predict the behavior of different materials [9].

2.3.2 Derivations

Piezoelectric relations can be derived from the basic laws of continuum physics which apply to all materials. They consist of four equalities which are the conservation of mass, balance of momentum, balance of moment of momentum and conservation of energy. The fifth principle yields the well-known inequality describing the change in entropy [9]. For electromagnetic materials, the basic principles of electrodynamics, which lead to the well-known Maxwell's equations, must be added to the list. These laws have no proof except the fact that they have not been proven wrong for the kind of materials and conditions considered in this field [9]. Piezoelectric materials, which we are concerned with, are non-magnetizable, dielectric materials. Therefore all magnetic effects can be dropped. We also assume no external heat flux when applying the balance laws. These equations will not be presented here for the sake of space, but the resulting constitutive equations are briefly presented due to the importance of some material coefficients in analyzing the piezoelectric effect.

Table 2.1: Symbols used in derivations

Symbol	Description
θ	Temperature
t_{ij}	Stress tensor
E_{ij}	Electric field
e_{ij}	Strain tensor
D_{ij}	Dielectric displacement (the density of electric flux per unit area)

Table 2.1: Symbols used in derivations

Symbol	Description
η	Entropy density
ρ_o	Initial density
q_f	Volume free charge density

Introducing the terms in Table 2.1, and upon the application of the axioms of the constitutive theory to piezoelectric materials, the entropy inequality takes the following form:

$$\left(t_{ij}-\rho_o\frac{\partial\psi}{\partial e_{ij}}\right)\dot{e}_{ij}+\left(E_i-\rho_o\frac{\partial\psi}{\partial D_i}\right)\dot{D}_i+\rho_o\left(-\eta-\frac{\partial\psi}{\partial\theta}\right)\dot{\theta}-\rho_o\frac{\partial\psi}{\partial\theta_{,i}}\dot{\theta}_{,i}+\frac{1}{\theta}q_k\theta_{,k}\geq 0 \qquad (2.1)$$

The entropy inequality is linear in $\dot{e}_{ij}$, $\dot{D}_{ij}$, $\dot{\theta}$, $\dot{\theta}_{,i}$, and the free energy function (Ψ) is independent of these quantities. Therefore, in order for the inequality to be satisfied for any independent thermodynamic processes, the coefficients of these terms must vanish. This restriction yields:

$$\begin{aligned} t_{ij} &= \rho_o\frac{\partial\psi}{\partial e_{ij}} \qquad E_m = \rho_o\frac{\partial\psi}{\partial D_m} \\ \eta &= -\frac{\partial\psi}{\partial\theta} \qquad \frac{\partial\psi}{\partial\theta_{,i}} = 0 \end{aligned} \qquad (2.2)$$

which implies that:

$$\begin{aligned} \psi = \psi(e_{ij},\theta,D_i) &= \frac{\Sigma}{\rho_o}(e_{ij},\theta,D_i) \\ t_{ij} = t_{ij}(e_{ij},\theta,D_i) &\qquad \text{stress tensor} \\ E_m = E_m(e_{ij},\theta,D_m) &\qquad \text{electric field} \end{aligned} \qquad (2.3)$$

By expanding the internal energy (Σ) into a Taylor series and assuming an unbiased reference state at which there is no initial strain ($e_0 = 0$) or electric displacement ($D_0 = 0$), at initial temperature (θ_0) we obtain (see details in [9] and chapter 10 of [20]):

$$
\begin{aligned}
\Sigma = \Sigma_o &+ \left(\frac{\partial \Sigma}{\partial e_{ij}}\right)_0 e_{ij} + \left(\frac{\partial \Sigma}{\partial D_i}\right)_0 D_i + \left(\frac{\partial \Sigma}{\partial \theta}\right)_0 (\theta - \theta_o) \\
&+ \frac{1}{2}\left(\frac{\partial^2 \Sigma}{\partial e_{ij}\partial e_{kl}}\right)_o e_{ij}e_{kl} + \frac{1}{2}\left(\frac{\partial^2 \Sigma}{\partial D_m \partial D_k}\right)_o D_i D_m + \frac{1}{2}\left(\frac{\partial^2 \Sigma}{\partial \theta \partial \theta}\right)_o (\theta - \theta_o)^2 \\
&+ \frac{1}{2}\left(\frac{\partial^2 \Sigma}{\partial e_{ij}\partial D_m}\right)_o e_{ij}D_m + \frac{1}{2}\left(\frac{\partial^2 \Sigma}{\partial D_m \partial \theta}\right)_o D_m (\theta - \theta_o) + \frac{1}{2}\left(\frac{\partial^2 \Sigma}{\partial e_{ij}\partial \theta}\right)_o e_{ij}(\theta - \theta_o) \\
&+ \frac{1}{6}\left(\frac{\partial^3 \Sigma}{\partial e_{ij}\partial e_{kl}\partial e_{mn}}\right)_o e_{ij}e_{kl}e_{mn} + \frac{1}{6}\left(\frac{\partial^3 \Sigma}{\partial D_m \partial D_k \partial D_i}\right)_o D_m D_k D_i \\
&+ \frac{1}{6}\left(\frac{\partial^3 \Sigma}{\partial \theta^3}\right)_o (\theta - \theta_o)^3 + \frac{1}{6}\left(\frac{\partial^3 \Sigma}{\partial e_{ij}\partial e_{kl}\partial D_m}\right)_o e_{ij}e_{kl}D_m \\
&+ \frac{1}{6}\left(\frac{\partial^3 \Sigma}{\partial e_{ij}\partial D_m \partial D_k}\right)_o e_{ij}D_m D_k + \frac{1}{6}\left(\frac{\partial^3 \Sigma}{\partial e_{ij}\partial D_m \partial \theta}\right)_o e_{ij}D_m(\theta - \theta_o) \\
&+ \frac{1}{6}\left(\frac{\partial^3 \Sigma}{\partial \theta \partial D_m \partial D_k}\right)_o (\theta - \theta_o) D_m D_k + \frac{1}{6}\left(\frac{\partial^3 \Sigma}{\partial e_{ij}\partial e_{kl}\partial \theta}\right)_o e_{ij}e_{kl}(\theta - \theta_o) \\
&+ \frac{1}{6}\left(\frac{\partial^3 \Sigma}{\partial e_{ij}\partial \theta \partial \theta}\right)_o e_{ij}(\theta - \theta_o)^2 + \frac{1}{6}\left(\frac{\partial^3 \Sigma}{\partial D_m \partial \theta \partial \theta}\right)_o D_m (\theta - \theta_o)^2
\end{aligned}
\tag{2.4}
$$

Thus, the stress tensor (t_{ij}) can be obtained by using Equations (2.4) in (2.2) as:

$$
\begin{aligned}
t_{ij} = \frac{\partial \Sigma}{\partial e_{ij}} &= \left(\frac{\partial \Sigma}{\partial e_{ij}}\right)_0 I + \left(\frac{\partial^2 \Sigma}{\partial e_{ij}\partial e_{kl}}\right)_o e_{kl} + \frac{1}{2}\left(\frac{\partial^2 \Sigma}{\partial e_{ij}\partial D_m}\right)_o D_m \\
&+ \frac{1}{2}\left(\frac{\partial^2 \Sigma}{\partial e_{ij}\partial \theta}\right)_o (\theta - \theta_o) + \frac{1}{2}\left(\frac{\partial^3 \Sigma}{\partial e_{ij}\partial e_{kl}\partial e_{mn}}\right)_o e_{kl}e_{mn} \\
&+ \frac{1}{3}\left(\frac{\partial^3 \Sigma}{\partial e_{ij}\partial e_{kl}\partial D_m}\right)_o e_{kl}D_m + \frac{1}{6}\left(\frac{\partial^3 \Sigma}{\partial e_{ij}\partial D_m \partial D_k}\right)_o D_m D_k \\
&+ \frac{1}{6}\left(\frac{\partial^3 \Sigma}{\partial e_{ij}\partial D_m \partial \theta}\right)_o D_m (\theta - \theta_o) + \frac{1}{3}\left(\frac{\partial^3 \Sigma}{\partial e_{ij}\partial e_{kl}\partial \theta}\right)_o e_{kl}(\theta - \theta_o) \\
&+ \frac{1}{6}\left(\frac{\partial^3 \Sigma}{\partial e_{ij}\partial \theta \partial \theta}\right)_o (\theta - \theta_o)^2
\end{aligned}
\tag{2.5}
$$

and similarly the electric field from Equation (2.2) as:

$$
\begin{aligned}
E_m = \frac{\partial \Sigma}{\partial D_m} = \left(\frac{\partial \Sigma}{\partial D_i}\right)_0 I + \left(\frac{\partial^2 \Sigma}{\partial D_m \partial D_k}\right)_o D_k + \frac{1}{2}\left(\frac{\partial^2 \Sigma}{\partial e_{ij} \partial D_m}\right)_o e_{ij} \\
+ \frac{1}{2}\left(\frac{\partial^2 \Sigma}{\partial D_m \partial \theta}\right)_o (\theta - \theta_o) + \frac{1}{2}\left(\frac{\partial^2 \Sigma}{\partial D_m \partial \theta}\right)_o (\theta - \theta_o) \\
+ \frac{1}{6}\left(\frac{\partial^3 \Sigma}{\partial e_{ij} \partial e_{kl} \partial D_m}\right)_o e_{ij} e_{kl} + \frac{1}{3}\left(\frac{\partial^3 \Sigma}{\partial e_{ij} \partial D_m \partial D_k}\right)_o e_{ij} D_k + \frac{1}{6}\left(\frac{\partial^3 \Sigma}{\partial e_{ij} \partial D_m \partial \theta}\right)_o e_{ij} (\theta - \theta_o) \\
+ \frac{1}{3}\left(\frac{\partial^3 \Sigma}{\partial \theta \partial D_m \partial D_k}\right)_o (\theta - \theta_o) D_k + \frac{1}{6}\left(\frac{\partial^3 \Sigma}{\partial D_m \partial \theta \partial \theta}\right)_o (\theta - \theta_o)^2
\end{aligned}
\tag{2.6}
$$

The above equations are the nonlinear constitutive equations for the stress and electric field in dielectric materials.

2.3.3 Non-linear Equations

By introducing the notation used in Table 2.2, we can further simplify Equations (2.5) and (2.6).

Table 2.2: Non-linear equation coefficients

Tensor	Significance
$c^D_{ijkl} = \left(\frac{\partial^2 \Sigma}{\partial e_{ij} \partial e_{kl}}\right)_o$	Elasticity coefficients
$h_{ijm} = -\frac{1}{2}\left(\frac{\partial^2 \Sigma}{\partial e_{ij} \partial D_m}\right)_o$	Piezoelectric coefficients
$\beta^{\varepsilon}_{mk} = \left(\frac{\partial^2 \Sigma}{\partial e_{ij} \partial e_{kl}}\right)_o$	Dielectric impermittivities
$c^D_{ijklmn} = \frac{1}{4}\left(\frac{\partial^3 \Sigma}{\partial e_{ij} \partial e_{kl} \partial e_{mn}}\right)_o$	Nonlinear elastic constants

Table 2.2: Non-linear equation coefficients

Tensor	Significance
$h_{ijklm} = -\frac{1}{6}\left(\frac{\partial^3 \Sigma}{\partial e_{ij}\partial e_{kl}\partial D_m}\right)_o$	Nonlinear piezoelectric constants
$\varepsilon_{ijmk} = -\frac{1}{12}\left(\frac{\partial^3 \Sigma}{\partial e_{ij}\partial D_m \partial D_k}\right)_o$	Electrostriction coefficients
$\beta^{\varepsilon}_{mki} = \frac{1}{4}\left(\frac{\partial^3 \Sigma}{\partial D_m \partial D_k \partial D_i}\right)_o$	Electro-optical coefficients
$\theta_m = -\frac{1}{2}\left(\frac{\partial^2 \Sigma}{\partial D_m \partial \theta}\right)_o$	Pyroelectricity
$\tau_{KL} = -\frac{1}{2}\left(\frac{\partial^2 \Sigma}{\partial e_{ij}\partial \theta}\right)_o$	Thermoelastic coefficient

These coefficients represent various physical effects observed in piezoceramics. Their appearance depends on the nature of the ceramic and the operating conditions. Some of the most important ones, other than piezoelectricity, are:

Pyroelectricity: A state of electric polarity produced on crystal structures containing a unique polar axis due to a change in temperature [1].

Electrostriction: Deformation produced in a material which is directly proportional to the square of an applied electric field and thus not dependant on its direction [3].

Using the terms in Table 2.2, the piezoelectric relations for the stress and the electric field, Equations (2.5) and (2.6), can be expressed as:

$$t_{kl} = \left(c^{D}_{ijkl} + c^{D}_{ijklmn}e_{mn} - h_{ijklm}D_m\right)e_{kl} - \left(h_{ijm} + h_{ijklm}e_{kl} - \varepsilon_{ijmk}D_k\right)D_m - \tau_{KL}(\theta - \theta_o) \tag{2.7}$$

and

$$E_m = (-h_{mlk} - h_{ijklm}e_{ij} - \varepsilon_{klmi}D_i)\,e_{kl} + \left(\beta^{\varepsilon}_{mi} - \varepsilon_{klmi}e_{kl} + \beta^{\varepsilon}_{mki}D_k\right)D_i - \theta_m(\theta - \theta_o) \tag{2.8}$$

The second and third terms in each bracket (nonlinear terms) in Equations (2.7) and (2.8) are the corrections (higher order terms) for the linear relations expressing the dependance of the stress and electric field on the strain and electric displacement. These corrections are summarized in the following table:

Table 2.3: Correction for linear constants [10]

Tensor	Describes the change in	Due to
$c^{D}_{ijklmn}e_{mn}$	Elastic constants	Crystal deformation
$h_{ijklm}D_m$	Elastic constants	Electric displacement
$\varepsilon_{ijmk}D_k$	Piezoelectric constants	Electric displacement
$h_{ijkln}e_{kl}$	Piezoelectric constants	Strain
$\beta^{\varepsilon}{}_{mki}D_k$	Dielectric impermittivities	Electric displacement
$\varepsilon_{iklm}e_{kl}$	Dielectric impermittivities	Mechanical strains

2.4 Linear Piezoelectric Calculations.

2.4.1 One Dimensional Equations

In order to have a physical insight into the indirect and direct piezoelectric effects, we consider one dimensional linear constitutive equations by simply neglecting the nonlinear material coefficients listed in Table 2.3. The indirect effect can be better understood if the one dimensional form of Equation (2.7), in the absence of temperature dependence, is rearranged to express the strain as:

$$e = s^{E}t + dE \qquad \text{Indirect effect} \tag{2.9}$$

Similarly, for the direct effect, Equation (2.8) is arranged for the electric displacements as [5]:

$$D = \varepsilon^T E + dt \qquad \text{Direct effect} \tag{2.10}$$

where d is the one dimensional piezoelectric constant which is described later. The elastic compliance s^E denotes the interaction between the stress and strain under constant (usually zero) electric field, i.e. short circuit conditions. On the other hand, ε^T is the permittivity at constant stress, i.e. clamped sample [5].

2.4.2 Piezoelectric Constants

The piezoelectric constant *(d)* is the most important property in the design of actuators. Other constants may be significant in different applications. Some of these constants along with their relevance and units are listed in Table 2.4

Table 2.4: Piezoelectric constants [6]

Constant	Direct Effect	Indirect Effect	Units	Application
Strain (d)	$\left(\frac{\partial D}{\partial t}\right)_{E,\theta}$	$\left(\frac{\partial e}{\partial E}\right)_{t,\theta}$	*m/V=C/N*	Actuators
Voltage (g)	$-\left(\frac{\partial E}{\partial t}\right)_{D,\theta}$	$\left(\frac{\partial e}{\partial D}\right)_{t,\theta}$	*Vm/N=m2/C*	Sensors
Stiffness (h)	$-\left(\frac{\partial E}{\partial D}\right)_{D,\theta}$	$-\left(\frac{\partial t}{\partial D}\right)_{e,\theta}$	*V/m=N/C*	

where the subscripts denote the quantities that were kept constant in the evaluation of the quantities in brackets. These subscript notations are summarized in Table 2.5.

Table 2.5: Subscript notations (measurement constraints)

Subscript	Denotes Constant	i.e.
θ	Temperature	Isothermal conditions
e	Strain	Clamped sample

Table 2.5: Subscript notations (measurement constraints)

Subscript	Denotes Constant	i.e.
t	Stress	Free sample
E	Electric field	Short circuit
D	Electric displacement	Open circuit

2.4.3 Matrix Form of Constitutive Equations

The material constants in Equations (2.9) and (2.10) (ε, d and s) are second, third and fourth order tensors, possessing, in general, 9, 27 and 81 different values respectively. Although the crystal structure of piezoceramics is initially isotropic, poling ends the isotropy in the direction of the electric field. The resulting cylindrical polar symmetry leads to the simplification of the material tensors. This is because many of its components vanish while others are replaced by their duplicates such as d_{31} for d_{32}. Other simplifications result from loading constraints during the measurements of elastic compliance[1] and permittivity[2] [5]. The previous simplifications leave us with only ten independent non-zero terms in Equations (2.7) and (2.8) consequently they are expanded as follows:

$$\begin{bmatrix} D_1 \\ D_2 \\ D_3 \end{bmatrix} = \begin{bmatrix} 0 & 0 & 0 & 0 & d_{15} & 0 \\ 0 & 0 & 0 & d_{15} & 0 & 0 \\ d_{31} & d_{31} & d_{33} & 0 & 0 & 0 \end{bmatrix} \begin{bmatrix} t_1 \\ t_2 \\ t_3 \\ t_4 \\ t_5 \\ t_6 \end{bmatrix} + \begin{bmatrix} \varepsilon_1 & 0 & 0 \\ 0 & \varepsilon_1 & 0 \\ 0 & 0 & \varepsilon_3 \end{bmatrix} \begin{bmatrix} E_1 \\ E_2 \\ E_3 \end{bmatrix} \tag{2.11}$$

1. Elastic compliance coefficients are measured under the application of a single stress while others are fixed, leading to the interchangeability of stress and strain (e.g. $s_{13} = s_{31}$).
2. Non-diagonal permittivity constants vanish in the absence of oblique forces or electric fields.

$$\begin{bmatrix} e_1 \\ e_2 \\ e_3 \\ e_4 \\ e_5 \\ e_6 \end{bmatrix} = \begin{bmatrix} s_{11} & s_{12} & s_{13} & 0 & 0 & 0 \\ s_{12} & s_{11} & s_{13} & 0 & 0 & 0 \\ s_{13} & s_{13} & s_{33} & 0 & 0 & 0 \\ 0 & 0 & 0 & s_{44} & 0 & 0 \\ 0 & 0 & 0 & 0 & s_{44} & 0 \\ 0 & 0 & 0 & 0 & 0 & 2(s_{11}-s_{12}) \end{bmatrix} \begin{bmatrix} t_1 \\ t_2 \\ t_3 \\ t_4 \\ t_5 \\ t_6 \end{bmatrix} + \begin{bmatrix} 0 & 0 & d_{31} \\ 0 & 0 & d_{31} \\ 0 & 0 & d_{33} \\ 0 & d_{15} & 0 \\ d_{15} & 0 & 0 \\ 0 & 0 & 0 \end{bmatrix} \begin{bmatrix} E_1 \\ E_2 \\ E_3 \end{bmatrix} \tag{2.12}$$

Thus after eliminating the zero terms, the constitutive equations of piezoelectric materials takes the following form:

$$\left.\begin{aligned} D_1 &= \varepsilon_1 E_1 + d_{15} t_5 \\ D_2 &= \varepsilon_1 E_2 + d_{15} t_4 \\ D_3 &= \varepsilon_3 E_3 + d_{31}(t_1 + t_2) + d_{33} t_3 \end{aligned}\right\} \quad \text{Direct effect} \tag{2.13}$$

$$\left.\begin{aligned} e_1 &= s_{11} t_1 + s_{12} t_2 + s_{13} t_3 + d_{31} E_3 \\ e_2 &= s_{12} t_1 + s_{11} t_2 + s_{13} t_3 + d_{31} E_3 \\ e_3 &= s_{13}(t_1 + t_2) + s_{33} t_3 + d_{33} E_3 \\ e_4 &= s_{44} t_4 + d_{15} E_2 \\ e_5 &= s_{44} t_5 + d_{15} E_1 \\ e_6 &= 2(s_{11} - s_{12}) t_6 \end{aligned}\right\} \quad \text{Indirect effect} \tag{2.14}$$

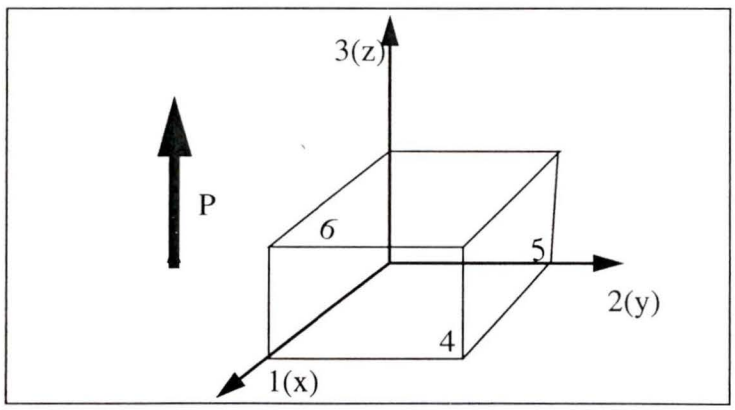

Figure 2.8: Naming conventions

For a better understanding of the subscript notation of the terms used in Equations (2.12) to (2.14), we examine a typical piezoceramic shown in Figure 2.8. The numbers 1, 2 and 3 denote the directions of the x, y and z Cartesian axes, while 4, 5 and 6 denote the z-y, x-z and x-y planes respectively. The direction 3 (z) is always the poling direction. In the dependent variables (stress t, strain e, electric displacement D and electric field E), the subscripts 1 to 6 simply denotes the direction in which they act. For example, e_3 is the strain in the poling direction (z), while t_4 is the shear stress acting in the y-z plane. On the other hand, for the material constants (piezoelectric d, elastic compliance s and permittivity ε), the first subscript denotes the directions of the applied field, while the second subscript denotes the direction of the resulting field. The subscript notations for the material constants used in Equation (2.14) are summarized in Table 2.6 for easy reference.

Table 2.6: Subscript notations (direction)

Constant	First Subscript denotes the direction of applied:	Second Subscript denotes the direction of resulting:
d	Electric field	Strain
s	Stress	Strain

3 Material Selection

3.1 Introduction

This chapter discusses the necessary properties of the materials used in actuators and identifies materials candidate for such applications. These applications include deformable mirrors, micro-robotics and vibromotors. It then presents the procedure by which the best material for our planned applications is selected. The information presented here is a valuable guide for the subsequent improvement of the processing parameters for the selected material. It should be noted that the selection requirements were kept here as general as possible with keeping in mind that additional criteria must be introduced for specific actuation applications when appropriate.

3.2 Selection Criteria

These criteria are divided into the categories of rigid and soft (relative) requirements as shown in Figure 3.1. As the name implies, rigid requirements are those properties that a material must posses in order to be considered in the selection process. On the other hand, soft requirements are the optimizable properties that differentiate between the candidate materials [11]. The materials best suited for actuators are those possessing the highest "maximum value required properties" and the lowest "minimum value required properties".

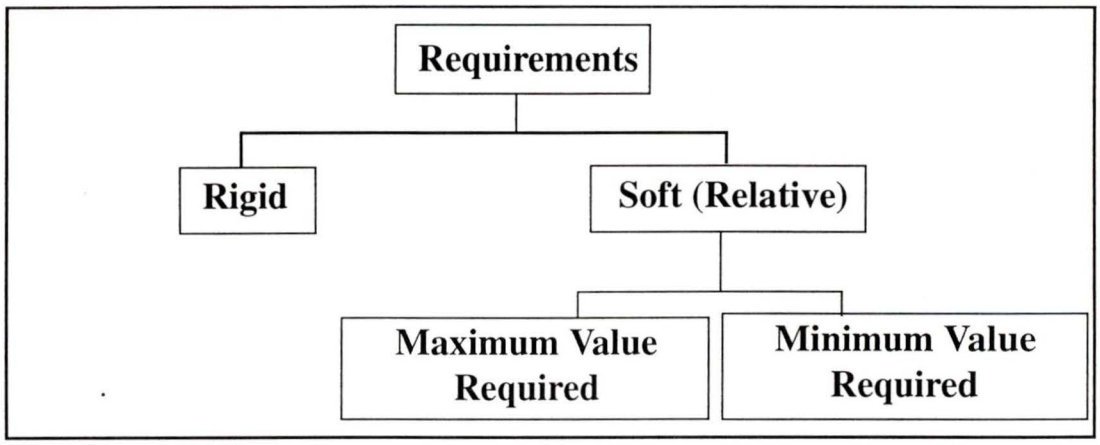

Figure 3.1: Selection criteria

3.2.1 Rigid Requirements

Most materials in which strain can be induced by a change in the materials environment, such as temperature or electric field, can be used as actuators. Piezoelectric materials, where strain is induced by a change in the electric field, stand out as the most accurate and efficient of these materials. Thus piezoelectricity is a rigid requirement in actuator materials and the following are its main properties:

Non-centrosymmetric Crystal Structure: These materials have a crystal structure with no center of symmetry which results in electric dipoles. An example is the tetragonal structure of barium titanates below 130 ^{o}C, shown in Figure 2.2.

Ferroelectricity: In ferroelectric materials the direction of the dipoles can be switched by the application of a high electric field [5].

3.2.2 Maximum Value Required Properties

They are the optimizable properties that differentiate between candidate materials satisfying the rigid requirements. They help us narrow down the selection to a certain material

with a specific composition. The chosen material must have the highest values of the following properties:

Piezoelectric Constant (*d*): The ratio between the applied electric field and the resulting strain is the most important property of piezoelectric materials. In these anisotropic materials, the greatest displacement occurs in the poling direction as a result of an electric field in the same direction. Thus d_{33} is the most important piezoelectric constant, especially in stacked actuators[1] where it is the only measure of displacement. In other actuator designs[2], d_{31} is also considered to be a contributor to the displacement achieved [23].

Electromechanical Coupling Factor (*k*): For a piezoceramic, it measures the strength of the piezoelectric effect and the success of poling [5]. In the direct effect, it is expressed as [3]:

$$k^2 = \frac{\text{Mechanical energy converted to electrical energy}}{\text{Input mechanical energy}} \tag{3.1}$$

while in the indirect effect [3]:

$$k^2 = \frac{\text{Electrical energy converted to mechanical energy}}{\text{Input electrical energy}} \tag{3.2}$$

Curie Point: The Curie point is the temperature above which piezoelectric materials lose their piezoelectric properties due to the change in crystal structure. The higher this point is, the wider the operating temperature range and the more stable an actuator is.

---

1. See "Stacked Actuators" on page 50.
2. Moonie and bimorph designs to be discussed in Chapter 5.

Dielectric Strength: The dielectric strength is the maximum electric field a material can stand before electrically breaking down and conducting. During poling, a high electric field is needed as it produces more dipole reorientation. Later during operation, it produces high displacement.

The Mechanical Quality Factor (Q_m): A high ratio of the strain in-phase to the strain out-of-phase with stress is important in actuator materials to reduce losses [6].

Stiffness Coefficient (Force, Natural Frequency, Response Time): It is desirable for the selected piezoelectric material to have a small elastic coefficient (s). In this case, it would have a large stiffness coefficient (c_T) which will:

- limit the effects of the external forces,
- increase the actuating force, and
- increase the natural frequency which reduces the response time (one third of the cycle length) [29].

3.2.3 Minimum Value Required Properties

The effect of certain parameters, other than the applied electric field, on the piezoelectric materials response are not desirable and should be minimized. This is because these dependencies affect the accuracy of an actuator adversely. These undesired dependencies are:

Temperature Dependence

The properties of piezoelectric materials used as actuators are highly dependent on the operating temperature. This is because of the change in properties caused by temperature

fluctuations and ultimately the threat of thermal breakdown. The best actuator material will then be the one least dependent on temperature within the operating temperature range. It should therefore have the lowest:

- coefficient of thermal expansion, and
- pyroelectric coefficient[1].

Electric Field Direction Dependance

Hysteresis: Most piezoelectric materials show strain-electric field hysteresis which affects their dynamic accuracy adversely. Hysteresis will be discussed in detail in Section 5.3 on page 47, but for now we will state that, in general, low hysteresis is desirable for dynamic actuator applications.

Electrostriction Coefficient: The strain caused by electrostriction is proportional to the square of the electric field, therefore the displacement does not depend on the field direction. This independence will cause inaccuracies in materials with a high electrostriction coefficient.

Time Dependence

Drift Factor: Drift is the extra displacement observed after the applied electric field is removed. It is due to the continuing reorientation of dipoles in the ceramic. This phenomena is a short-term dependance of piezoelectric material properties on time which reduces their accuracy.

---

1. See "Nonlinear Piezoelectric Relation" on page 10.

Aging: The long-term loss of piezoelectric properties with time should also be minimized in actuator materials.

Energy Loses (Tan δ)

The dielectric loss is a measure of the electrical energy converted to heat in each cycle of operation [6]. Large values of this coefficient are particularly dangerous in high frequency operation and can lead to considerable heating in an actuator.

3.3 Selection Process

3.3.1 Materials Satisfying the Rigid Requirements (Piezoelectric)

They are the non-centrosymmetric, ferroelectric, dielectric materials in which an external stress changes their polarization state. There are two kinds of piezoelectrics: naturally occurring and processed materials (ceramics, composites and polymers), as shown in Figure 3.2.

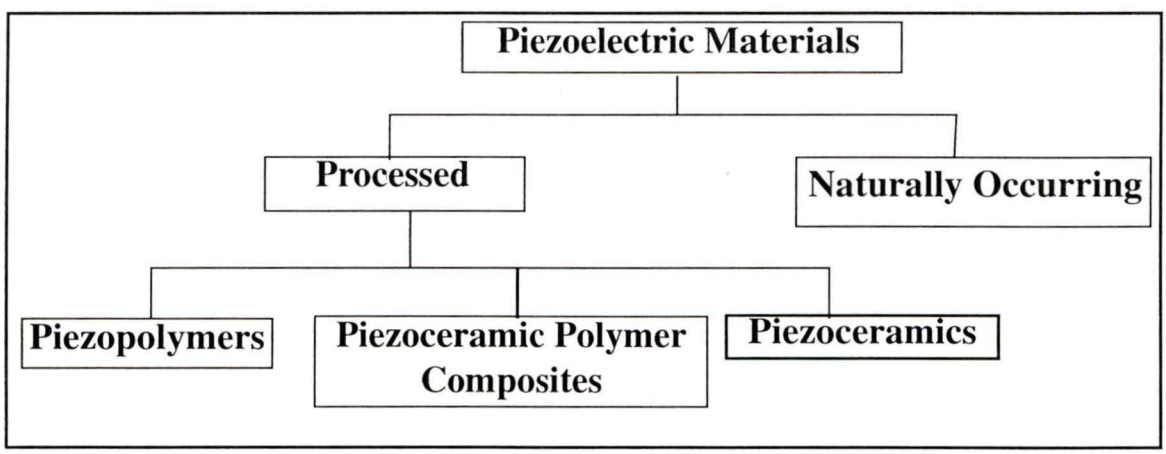

Figure 3.2: Classification of Piezoelectric materials

Naturally Occurring Piezoelectric Crystals: The first discovered piezoelectric materials were composed of naturally piezoelectric single crystals [1]. Some of these crystals are briefly described below.

- **Quartz**, which is a crystal of silicon dioxide that has a series of resonance frequencies, making it useful in filter applications [3].
- **Rochelle salt** is crystallized from a solution of potassium sodium titrate with properties largely dependant on the angle of cutting. Disadvantages of these crystals are its water solubility and low Curie point (45^oC) [3].
- **Ammonium Dihydrogen Phosphate (ADP)** is a crystal that shows properties similar to Rochelle salt but possesses a higher Curie point of 120^oC. These crystals were used in beam light modulation and hydrophones [3].

Piezoceramics: Single piezoelectric crystals were difficult to work with because of their manufacturing constraints, low Curie points, high hysteresis and water solubility. Piezoceramics, the first synthesized piezoelectrics discovered, offered solutions to all these problems. The first ceramic used as a piezoactuator was barium titanate [5]. It offered great advantages over its single crystal counterparts. Later, the superior piezoelectric properties of PZT[1] were discovered, generally replacing barium titanate. Although PZT is still the most widely used ceramic in piezoactuators and sensors, new and promising ceramics are being continuously discovered and improved [24].

1. PZT will be discussed in detail in "Lead Zirconate Titanate (PZT)" on page 39.

Piezoelectric Polymers: In 1969 Kawai [25] discovered that certain polymers exhibit piezoelectric properties when poled by a strong electric field. Piezoelectric polymers such as PVDF (polyvinylidene fluoride) have the advantage of being manufacturable in the form of very thin film. Their piezoelectric coefficients have improved in the last two decades (up to d_{13} of 40 *pC/N* for PVDF) but they are still very low compared to piezoceramics. Another polymer that should be mentioned is P(VDF-Tefe), which can be processed in films of 1 μm thickness and is useful in making high frequency ultrasonic transducers [25].

Piezoceramic-Polymer Composites: These composites are made with specific properties that are controlled by the constituents, their ratios and the configuration in which they are connected. An example is the 1-3 piezoelectric polymer composite that shows high hydrostatic piezoelectric strain constant (d_h), a measure of its sensitivity given by:

$$d_h = d_{33} + 2d_{31} \tag{3.3}$$

As shown in Figure 3.3, this composite material is formed of piezoelectric ceramic rods imbedded in a polymer matrix. The planer coupling which contributed negatively to the hydrophonic piezoelectric constant (d_h) is interrupted by the elastically compliant polymer. This kind of composite is more useful in sensing applications such as hydrophones and medical diagnostic ultrasonic equipment [24].

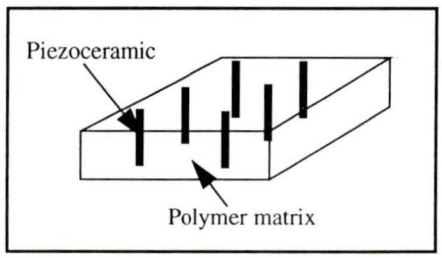

Figure 3.3: Piezoelectric polymer composite

3.3.2 Soft Requirements

All previous classes of materials introduced satisfy the rigid requirements, so we must compare their soft requirements in order to choose the best group. After careful examination, piezoceramics were found to have superior soft requirements as opposed to the other piezoelectric materials. They are the materials best suited piezoelectric actuators for the following reasons:

- They can produce large displacements because of their high piezoelectric coefficients.
- They can be manufactured in different shapes and sizes such as thin discs, hollow tubes or slabs.
- They withstand a wider range of operating temperatures because of their higher Curie points.
- They are not water soluble.
- They show lower hysteresis than other piezoelectric materials.

3.3.3 Final Selection

The final phase of the selection process was to investigate the different types of piezoceramics, compare their soft requirements and choose the best composition for actuator design. Soft requirements were compared by using the Figure of Merit Method suggested in [11]. This method ranks the candidate materials according to the suitability of their properties for the desired application by:

1. Assigning a weight, from 1-10, to each property according to its relative importance in actuator design. The sign of the weight depends on whether it is a maximum or minimum value required property as shown in the third row of Table 3.1 and 3.2.

2. Preparing a table with the values of the properties of each candidate material.

Table 3.1: Maximum value required properties [5] and [6]

Material \ Property	d_{33}	d_{31}	**Curie Point**	k_{33}	*Density*	Q_m
Units	*pC/N*	*pC/N*	^oC		$Mg\ m^{-3}$	
Weight	*10*	*5*	*3*	*7*	*5*	*1*
1) $BaTiO_3$	190	-79	130	0.49	5.7	500
2) $Pb(Ti_{0.48}Zr_{0.52})O_3$	223	-93.5	386	0.67	7.8	500
3) $(Pb_{0.94}Sr_{0.06})(Ti_{0.47}Zr_{0.53})O_3$	289	-123	328	0.70	7.8	500
4) $Pb_{0.988}(Ti_{0.48}Zr_{0.52})_{0.976}Nb_{0.024}O_3$[a]	374	-171	365	0.70	7.8	75
5) $PbNb_2O_6$	80	-11	560	0.38	5.9	11
6) $Na_{1/2}K_{1/2}NbO_3$	160	-50	180	0.53	4.5	240

a. This composition is commercially known as PZT-5.

Table 3.2: Minimum value required properties [5] and [6]

Material \ Property	**Dissipation factor.**	$s_{33}^E 10^{-12}$
Units	**Tan δ**	m^2/N
Weight	*-1*	*-3*
1) $BaTiO_3$	0.007	9.1
2) $Pb(Ti_{0.48}Zr_{0.52})O_3$	0.004	17.1
3) $(Pb_{0.94}Sr_{0.06})(Ti_{0.47}Zr_{0.53})O_3$	0.004	15.5
4) $Pb_{0.988}(Ti_{0.48}Zr_{0.52})_{0.976}Nb_{0.024}O_3$	0.02	18.8

Table 3.2: Minimum value required properties [5] and [6]

Material \ Property	Dissipation factor.	$s_{33}^{E}10^{-12}$
5) $PbNb_2O_6$	0.01	25
6) $Na_{1/2}K_{1/2}NbO_3$	0.01	10

3. The figure of merit for each material is the summation of the products of: the standardized[1] property value by its weight. For example, the figure of merit of barium titanate ($BaTiO_3$) would be:

$$\left|\frac{190}{374}\right| \times 10 + \left|\frac{-79}{-171}\right| \times 5 + \ldots + \left|\frac{9.1}{25}\right| \times -3 \;=\; 16 \tag{3.4}$$

4. The material with the highest figure of merit is the most suitable for the application.

3.3.4 Selection Results

After comparing the soft requirements of the candidate materials, PZT-5 was chosen since it exceeds most other piezoceramics in soft requirements with the highest figure of merit (26) as shown in Figure 3.4.

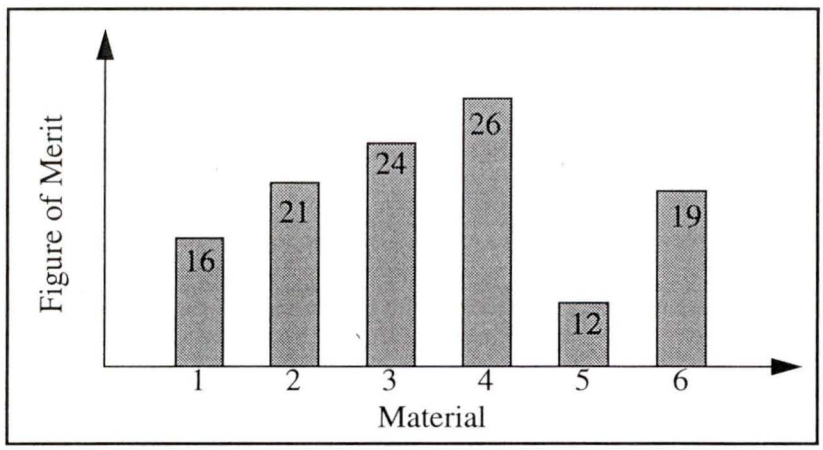

Figure 3.4: Comparison of the figure of merit of candidate piezoceramics

1. The standardized property value is defined as the absolute value of the division of the property value by the maximum value.

3.4 Conclusion

All piezoelectric materials satisfy the rigid requirements set previously, but piezoceramics were found to possess the best soft requirements. After the selection process, shown in Figure 3.5, PZT was recommended as the best material for the project at hand for the following reasons:

- The PZT-5 composition has the highest figure of merit because of its high piezoelectric constants, electromechanical coupling coefficient and Curie point, which makes it the most suitable piezoceramic for actuation applications.
- Its properties can be further improved by controlled doping.
- Low dependence on external factors resulting in high accuracy.
- It is widely used in industry, so the required basic information on its composition and manufacturing process is readily available in the relevant literature (see chapter 11 of [5] and chapter 6 of [6]).

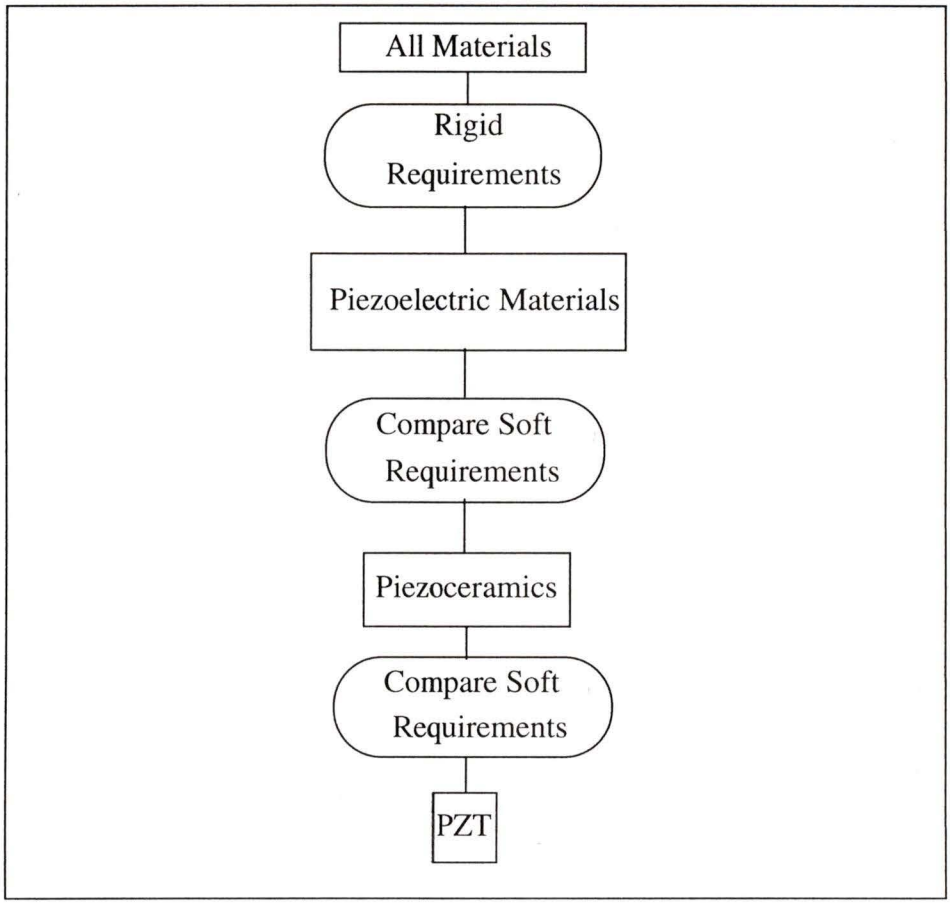

Figure 3.5: Flow chart of the selection process

4 Piezoceramics and PZT

4.1 Introduction

The selection process introduced in the previous chapter revealed that lead zirconate titanate, a class of piezoceramics known as PZT, has the best overall material properties for actuator applications. In this chapter, we discuss their crystal structure, chemical composition, thermal properties and changes in their properties induced by controlled doping. For the sake of shedding light on some terminology, a brief summary of the classification of piezoceramics and their general properties is also provided.

4.2 Classification of Piezoceramics

Piezoceramics can be divided according to their crystal structure into peroveskite and non-peroveskite materials. Ceramics of the peroveskite structure are the most widely used piezoelectric materials.

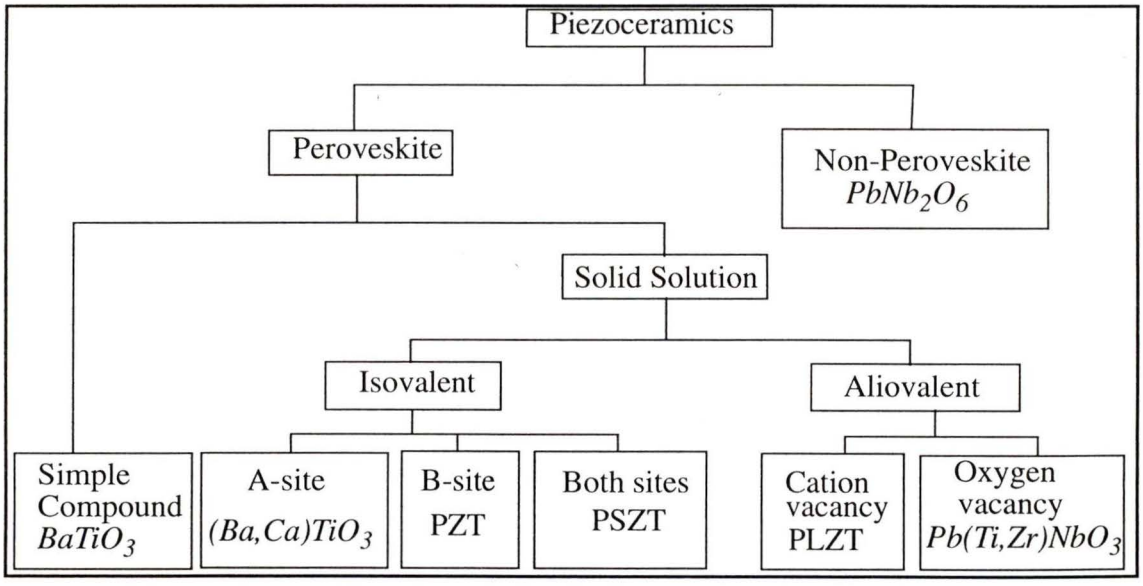

Figure 4.1: Classification of Piezoceramics

Ceramics of the peroveskite crystal structure can be further classified into simple compounds and solid solutions. The latter are, in turn, subdivided according to the kind of substation they undergo. The general classification of piezoceramics is shown in Figure 4.1.

4.2.1 The Peroveskite Crystal Structure

The peroveskite structure, such as that of PZT shown in Figure 4.3, is similar to a simple cubic structure. It has four large cations at the corners (A-site), a smaller cation at the center of the cube (B-site) and one oxygen anion at the center of each face. The crystal structure consists of corner-linked oxygen octahedra, with the small cation filling the octahedral holes and the large cation filling the dodecahedral holes. Any pair of cations can occupy the A- and B-sites as long as their ratio of radii and that of the oxygen anion, R_A, R_B and R_O shown below, is close to one [5].

$$\frac{R_A + R_B}{\sqrt{2}\,(R_B + R_O)} \approx 1 \tag{4.1}$$

4.2.2 Simple Compounds

The ceramics listed in Table 4.1 can be considered simple in the sense that they are formed of a single phase with the A- and B-sites occupied by a single element each. The most famous of these ceramics is barium titanate ($BaTiO_3$), which was the first piezoceramic to be discovered. It was the leading ceramic in the manufacture of sensors and actuators until the discovery of PZT. In its peroveskite structure, barium occupies the A-site and titanium occupies the B-site. Another pair of important peroveskite ceramics are lead titanate and lead zirconate. This is because they are the building blocks of the most important piezoceramic PZT which is the focus of this research effort. These ceramics are formed by react-

ing the powder oxides or carbonates of their constituents at high temperatures (up to 1350 ^{o}C for barium titanate) [5].

Table 4.1: Simple Compounds (peroveskite)

Ceramic	Formula	Structure	Constituents
Barium Titanate	$BaTiO_3$	Peroveskite (tetragonal)	$BaCO_2$ & TiO_2
lead Titanate	$PbTiO_3$	Peroveskite (tetragonal)	PbO & TiO_2
Lead Zicronate	$PbZrO_3$	Peroveskite (orthorhombic)	PbO & ZrO_2

4.2.3 Solid Solutions (Isovalent Substitution)

Solid solutions such as PZT have taken the place of simple compounds because of their superior qualities. In these solid solutions the A- and/or B-sites of the peroveskite structure are shared by different ions having the same valiancy. The properties of the resulting solid solution depends on the nature of the replacement ions and their concentration.

A-site Sharing: The A-site in the peroveskite structure holds the cation of the larger radius which should be divalent. Table 4.2 is a list of the suitable ions for sharing the A-site [6]. They all have the same valiancy of 2^{+} and a relatively large radius that satisfies Equation (4.1).

Table 4.2: Isovalent A-site candidates [12]

Element	Symbol	Atomic #	Ionic radius(nm)	Source
Barium	Ba^{2+}	56	*0.143*	$BaCO_3$
Lead	Pb^{2+}	82	*0.132*	PbO
Calcium	Ca^{2+}	20	*0.106*	CaO
Strontium	Sr^{2+}	38	*0.127*	SrO

B-site Sharing: The B-site in the peroveskite structure is the smaller cation in the center of the cube. This position can be shared by any ion having a valiancy of 4^{+} listed in Table

4.3 [6]. The most well-known example is PZT, where the B-site is shared by titanium and zirconium.

Table 4.3: Isovalent B-site sharing candidates [12]

Element	Symbol	Atomic #	Ionic radius(nm)	Source
Titanium	Ti^{4+}	22	*0.064*	TiO_2
Zirconium	Zr^{4+}	40	*0.087*	ZrO_2
Tin	Sn^{4+}	50	*0.074*	SnO_2
Hafnium	Hf^{4+}	72	*0.084*	TiO_2

A and B-site Sharing: Another possibility is forming a solid solution by sharing both sites between different ions. The candidates are the same as those listed in Table 4.2 and Table 4.3. An example is PSZT, described in Table 4.4, which shows a high piezoelectric constant but lower Curie point [6].

Table 4.4: Isovalent solid solutions

Name	Formula	Constituents
PZT	$Pb(Ti_{0.48},Zr_{0.52})O_3$	$PbO\ ZrO_2\ TiO_2$
BST	$Ba(Sn_{0.15},Ti_{0.85})O_3$	$BaO\ SnO_2\ TiO_2$
PSZT	$(Pb_{0.94},Sr_{0.06})(Ti_{0.47},Zr_{0.53})O_3$	$PbO\ SrO\ ZrO_2\ TiO_2$

4.2.4 Off-Valiancy Additives (Controlled Doping)

In materials processing, the term "doping" is generally used for the process of introducing a small amount of foreign materials into a solid composition. This small amount of materials alter some properties of the host material tremendously while leaving some others unchanged. Controlled doping is also very important in the processing of piezoceramics. We can alter the properties of peroveskite-type piezoceramics by replacing A- and/or B-site cations with ones having different valiancy as long as they have atomic radii within 15% of the original cation [6]. Although doping of peroveskite-type ceramics is not a sim-

ple process, we will try to describe it in general terms. There are two kinds of dopants, donors and acceptors. **Donors** are those of valiancy greater than that of the ion they replace. Thus they are compensated for by cation[1] vacancies. On the other hand, **acceptors** are of valiancy less than that of the ion they replace and are compensated for by oxygen vacancies. Both types of dopant ions form dipolar pairs with the vacancies they cause. Thus the two dipolar pairs are: donor-cation vacancy and acceptor-oxygen vacancy. Each dopant also suppress the vacancies caused by the other. Commonly used dopants for peroveskite-type piezoceramics are listed in Table 4.5. The effects of controlled doping on PZT are discussed in Section 4.3.4 on page 41.

Table 4.5: Commonly used dopants

Type	A-site (2^+)	B-site (4^+)
Donors	*La, Bi, Nd* (3^+)	*Nb, Ta, Sb* (5^+)
Acceptors	*K, Rb* ($^+$)	*Co, Fe, Sc, Ga, Cr, Mn* (3^+)

Soft and Hard Piezoceramics: Dopants will also determine the corrosive field[2] of the ceramic. Hard ceramics are produced by adding acceptor dopants; they have low piezoelectric coefficients but their coercive fields are high. They also show low hysteresis and high Curie points. Soft ceramics result from donor doping and generally have higher d_{33} coefficients, a low coercive field and show high hysteresis [6].

1. Cations are the ions in the A- or B-sites of the peroveskite crystal structure for example, *Ba* and *Ti* in barium titanate.
2. The electric field at zero polarization. See "Inaccuracy Sources (Hysteresis)" on page 47.

4.3 Lead Zirconate Titanate (PZT)

4.3.1 Introduction

The ferroelectric properties of the solid solution of lead zirconate and lead titanate (PZT) was first discovered in Japan in the 1950s. Since then, this group of piezoceramics has been the focus of much research. Certain compositions such as PZT-5 have replaced barium titanate in most piezoelectric applications [5]. In this section, we briefly discuss the effect of crystal structure, stoichiometry, operating temperature and doping on their properties.

4.3.2 Crystal Structure

PZT is a solid solution of the ferroelectric lead titanate and the antiferroelectric lead zirconate. It has a paraelectric simple cubic (P_C) crystal structure above its Curie point. At lower temperatures, the replacement of Zr^{+4} for Ti^{+4} reduces the tetragonal distortion and finally causes the presence of a new ferroelectric rhombohedral phase. Thus compositions rich in $PbZrO_3$ are ferroelectric rhombohedral (F_R), while those rich in $PbTiO_3$ are ferroelectric tetragonal (F_T) as shown in the phase diagram (Figure 4.2). In this configuration, lead occupies the A-site while Ti and Zr share the B-site of the peroveskite crystal structure as shown in Figure 4.2 [5].

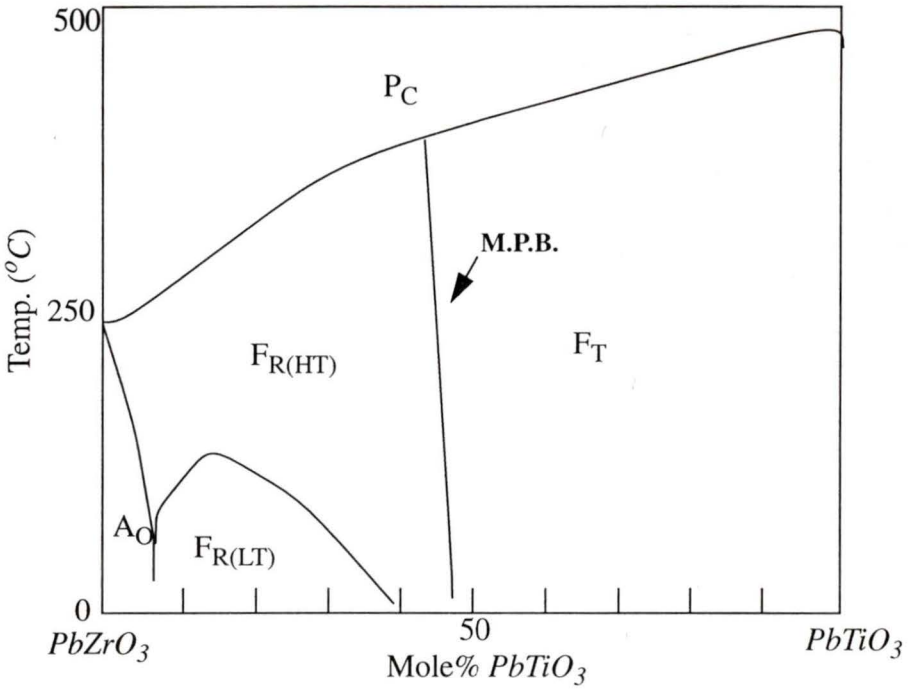

Figure 4.2: Phase diagram of PZT [5]

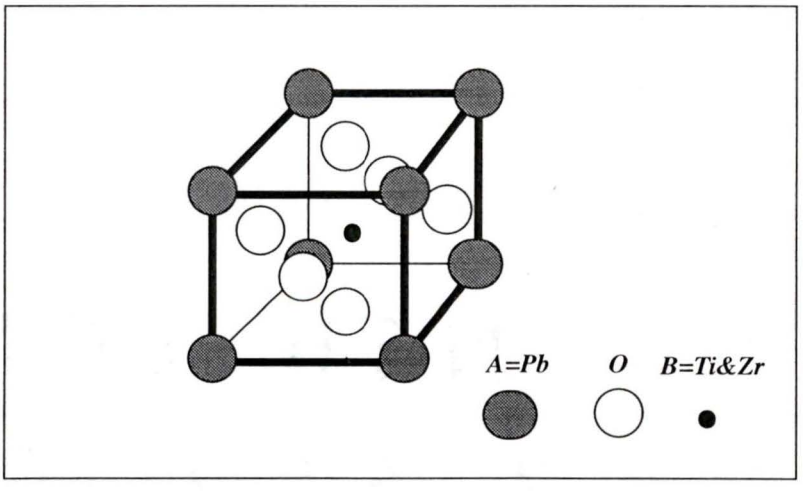

Figure 4.3: Peroveskite structure of *PZT* above its Curie point [6]

4.3.3 Peak Properties

The best piezoelectric properties, lowest impurities and highest density are obtained at the morphotropic phase boundary (M.P.B.) shown in Figure 4.2. In its vicinity, there is nearly equal amounts of tetragonal and rhombohedral phases. Both the dielectric and piezoelectric constants along with the coupling factor peak just on the tetragonal side of the M.P.B. as shown in Figure 4.4. In PZT, this peak can be achieved in the composition $Pb(Ti_{0.48}Zr_{0.52})O_3$ (exact stoichiometry). Table 3.1 on page 30 (2) lists these peak properties for an undoped composition of PZT. High electromechanical properties are attributed in this composition to the ease of reorientation during poling [5].

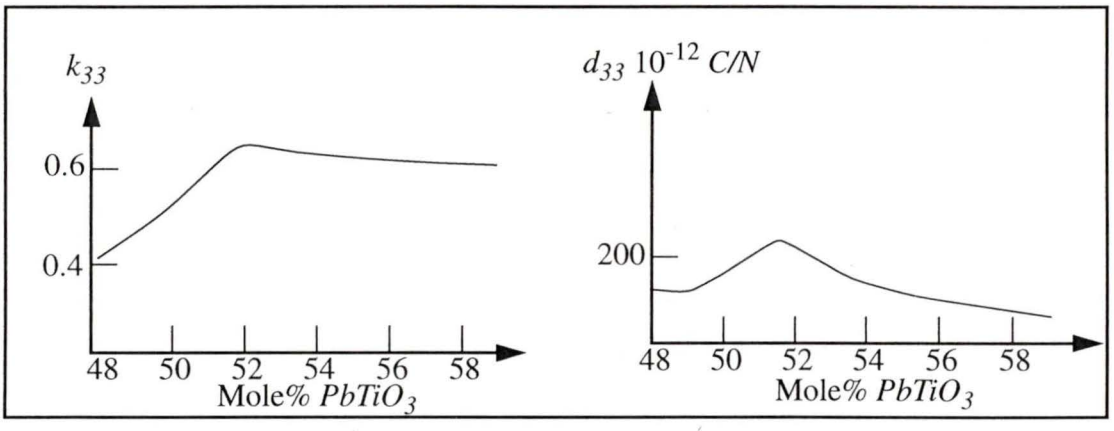

Figure 4.4: Variation of piezoelectric constants with composition [5]

4.3.4 Controlled Doping of PZT

The properties of PZT can be further improved by controlled doping. As mentioned previously, oxygen vacancies are caused by acceptor doping. These vacancies are not separated from oxygen ions in the peroveskite crystal structure, therefore they are more mobile than cation vacancies (caused by donor doping). Once oriented in the same direction, acceptor-oxygen vacancy dipoles will stabilize the domain structure and inhibit wall movement.

Conversely, cations and cation vacancies are separated by oxygen ions which means that they would need higher energy to overcome the resulting energy gap. Donor doping in PZT will reduce the number of domain stabilizing defect pairs. This results in an increase in wall mobility which will lead to the changes in properties listed in Table 4.6 [6].

The higher coupling factor and piezoelectric coefficient will make donor doped PZT ceramics a more suitable material for actuators. An example is the $Pb_{0.988}(Ti_{0.82}Zr_{0.52})_{0.976}Nb_{0.024}O_3$ [5] composition known commercially as PZT-5. This ceramic is widely used in actuator applications and its properties are listed in Table 3.1 on page 30 (4). Another positive effect of donor dopants such as lanthanum is that their excess positive charge will compensate for that of lead lost during sintering [6].

Table 4.6: Effect of dopants on PZT

Type	Higher	Lower
Donors	Piezoelectric coefficient Domain boundary motion, dielectric losses, permittivity, elastic compliance, coupling factor	Aging rates Coercive field (Soft ceramics) Mechanical quality factor (Q)
Acceptors	Strength Coercive field (Hard ceramics) Difficulty in poling Mechanical quality factor (Q)	Domain boundary motion Unite cell size Grain growth in firing Dielectric loses, elastic compliance, electric resistivity, cell size

4.3.5 Effect of Temperature on PZT

The operation and properties of PZT like all piezoceramics, are strongly affected by operating temperature. These effects can be summarized in the following points:

- The change in temperature will change the piezoelectric, electric and mechanical properties of PZT. This occurs because upon heating, a number of the domains will gain enough energy to revert back to their pre-poling direction.
- PZT will gradually lose its piezoelectric properties as its temperature increases, and a complete loss will occur above its Curie point due to changes in crystal structure[1].
- The pyroelectric effect is the small electric field induced in a material when it is heated. This charge can produce excess strain leading to the inaccuracy during operation.
- Linear thermal expansion which is, like other properties of poled PZT, anisotropic.

In general, piezoceramic devices can only be operated in a certain temperature range where the effects of temperature on their accuracy is minimal. This fact gives PZT an advantage over other piezoceramics as it has a high Curie point of about 360 ^{o}C. This gives it temperature stability and a wide operation temperature range.

Note: Heating during operation of piezoceramics result from the input energy converted into heat. This is especially important in high frequency applications as we will see later.

1. See "Polarization" on page 5.

5 Piezoactuators

5.1 Introduction

Piezoelectric actuators employ the indirect piezoelectric effect to accurately convert an applied electric field into displacement. Some piezoactuators can produce a displacement of 10 μm with an accuracy of 0.01 μm in less than 10 μs, even under high stresses [6]. They are used in a variety of precision engineering applications such as micropositioning of lenses, bimorph mirrors and microrobotics. For a better understanding of their operation and its effects on processing, we introduce their operating characteristics, sources of inaccuracy affecting their performance and the construction of some common designs.

5.2 Operation of Piezoactuators

The typical actuator considered in this section is constructed of staked cylindrical piezoceramic discs. It has a total length (L_0) and diameter (D) expressed in meters. In this section, we consider various aspects of their performance under different conditions. Unreferenced material can be attributed to chapter 5 of [29].

5.2.1 Operation Under Load

Generally, the displacement produced by a piezoceramic is proportional to its piezoelectric and stiffness coefficients, the force (F) acting on it and its original length as

$$\Delta L = E \cdot d_{33} \cdot L_o + \frac{F}{c_T} = \Delta L_o + \frac{F}{c_T} \tag{5.1}$$

where d_{33} is in m/V, E in V/m, F in N and c_T in M/m

The stiffness of a piezoactuator (c_T) can be related to its elastic compliance constant (s_{33}) by

$$c_T = \frac{Area}{s_{33} L_o} \tag{5.2}$$

No Load: The increase in length (ΔL_o) under ideal conditions and with no initial loading (see Figure 5.1a) is directly related to the applied electric field (E) by the piezoelectric constant (d_{33}) by

$$\Delta L_o = E \cdot d_{33} \cdot L_o \tag{5.3}$$

Static Load: If piezoactuators are subjected to an electric field while under a static load (M) as shown in Figure 5.1b, its absolute expansion will be the same. However, the displacement will start from a point lower than that of a free element at the amount of

$$\Delta L_n = \frac{Mg}{c_T} \tag{5.4}$$

Variable Load: If the external load is a function of the expansion, as in the case of pressing piezoactuators against a spring of stiffness (c_s), the maximum expansion is reduced by the following ratio [29] (see Figure 5.1c)

$$\Delta L = \Delta L_o \frac{c_T}{c_T + c_s} \tag{5.5}$$

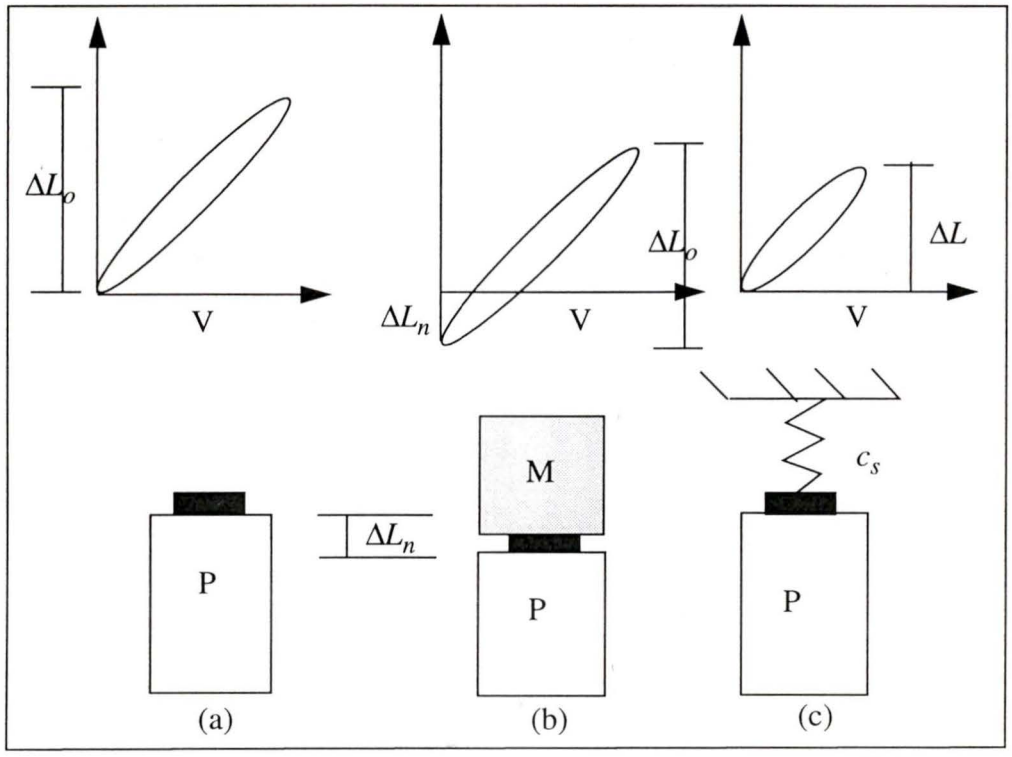

Figure 5.1: Piezoactuator response under different loading conditions

5.2.2 Actuation Force

The effective force produced by a piezoactuator depends on its stiffness and the stiffness of the resistance. Consequently, it is given by

$$F_{eff} = c_T \cdot \Delta L_o \left(1 - \frac{c_T}{c_T + c_s} \right) \tag{5.6}$$

A piezoactuator will produce its maximum force called the blocking force, against an infinitely stiff resistance such as a rigid wall:

$$F_{max} = c_T \cdot \Delta L_o \tag{5.7}$$

Dynamic Forces: If the operating voltage is sinusoidal with a frequency (*f*), the dynamic force is can be expressed by

$$F_{dyn} = \pm 4\pi^2 \cdot m_{eff} \cdot \frac{\Delta L}{2} \cdot f^2 \tag{5.8}$$

where m is in kg and f in s^{-1}

5.2.3 Resonance Frequency

A rough estimate of the resonance frequency (f_r) can be calculated from an actuators stiffness, mass (m) and its loading condition as

$$f_r = \frac{1}{2\pi} \cdot \sqrt{\frac{c_T}{m_{eff}}} \tag{5.9}$$

where $m_{eff} = m/2$

5.2.4 Heating Effect

Usually 5-8% of the electrical energy inputted into the actuator in each cycle is converted into heat. This could cause considerable rise in temperature during high frequency operations. The thermal heat generated (P) in the actuator due to operation at frequency (f) can be approximated by the following equation:

$$P = \tan\delta f C V^2 \qquad \text{where} \quad \begin{matrix} \tan\delta \approx 0.05 \\ C = \text{Capacitance} \end{matrix} \tag{5.10}$$

5.3 Inaccuracy Sources (Hysteresis)

Several sources of inaccuracy have been discussed in chapter 3 under the heading "Minimum Value Required Properties" on page 24. In this section we focus on hysteresis, which

is considered as the major source of error in the operation of piezoactuators. Hysteresis occurs when a piezoelectric ceramic is subjected to a high alternating electric field. In this case, the strain induced while the electric field increases will be higher than that induced when it is decreasing. This phenomena is due to the fact that the electric field will switch the polar directions of an increasing number of dipoles, resulting in the temporary loss of some piezoelectric properties. Hysteresis also occurs in an electric field verses polarization plot, as shown in Figure 5.2, where the area inside the loop represents the energy dissipated during each cycle.

Note: In Figure 5.2 the electric field at zero polarization is called the coercive field [6].

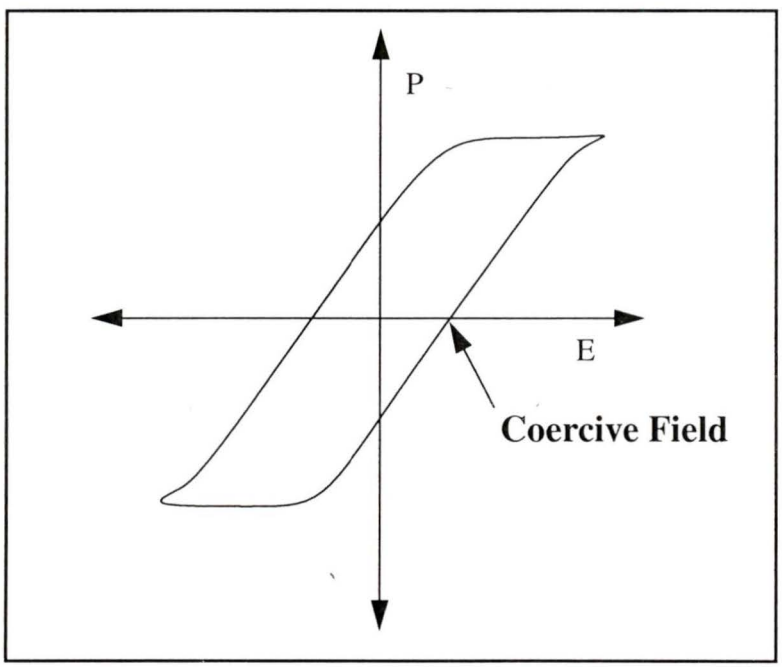

Figure 5.2: Polarization verses electric field hysteresis loop

5.3.1 Evaluating Hysteresis

The magnitude of hysteresis can be assessed by measuring the maximum difference in displacement of the actuator as shown in Figure 5.3. The extent of hysteresis depends on [6]:

- the intensity of the electric field (amplitude),
- the composition of the ceramic, e.g. the amount and kind of dopants, and
- the grain size of the ceramic.

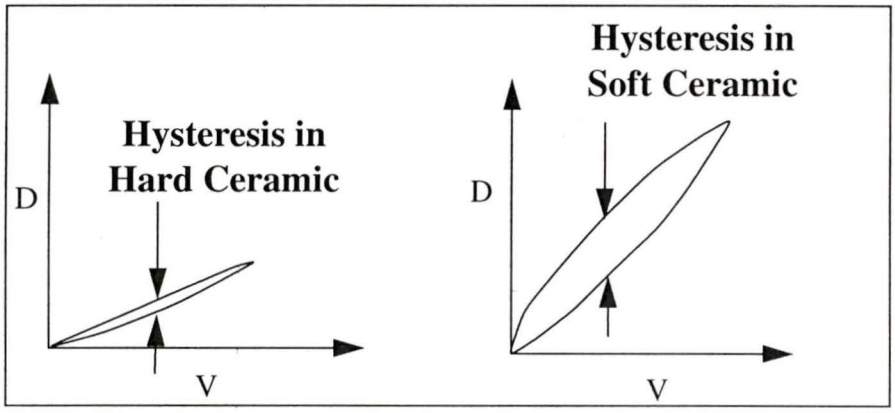

Figure 5.3: Displacement versus voltage hysteresis in soft and hard ceramics

5.3.2 Proposed Solutions

As mentioned previously, hysteresis can produce inaccuracies in the operation of piezoactuators. This is because the displacement is partially dependent on whether the electric field is increasing or decreasing. The hysteresis effects can be minimized by:

- avoiding operation under high voltages,
- using hard piezoceramics that switch polar directions at very high electric fields,
- maintaining a fine grain size in processing the ceramics [23], and

- position control of the actuator, using a position sensor that feeds back the displacement to a controller. The controller sends a corrected signal to the amplifier driving the actuator. This configuration has the added advantage of avoiding drift and it is shown in Figure 5.4 [29].

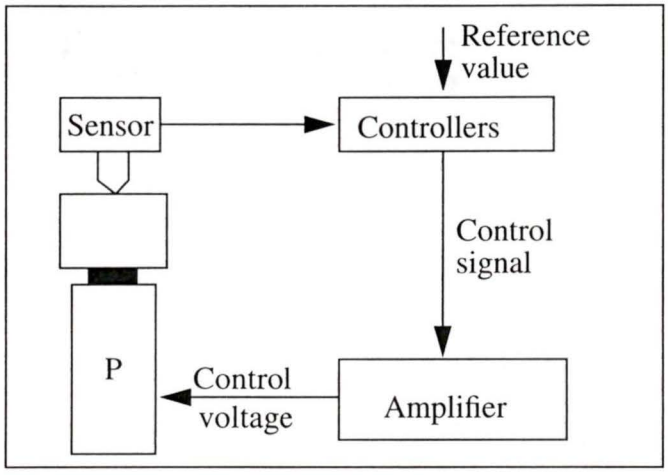

Figure 5.4: Closed positioning loop involving an external sensor

5.4 Actuator Design

Piezoactuators are designed in different shapes and configurations to achieve maximum displacement, forces and accuracy in the shortest time. In this section, we examine three of these designs along with their construction, advantages and disadvantages.

5.4.1 Stacked Actuators

A stacked actuator is a column of thin,cylindrical piezoelectric ceramic discs. They are arranged in a stack separated by metallic electrodes as shown in Figure 5.5. The stack is placed in a metal casing for protection. This configuration has the advantage of being able to produce high pushing force in short periods of time and withstanding high pressure. Its low pulling capability can be increased by using springs to provide pre-loading. Although

a stacked actuator provides more displacement than a single element, its displacement is less than other configurations such as bimorph or moonie.

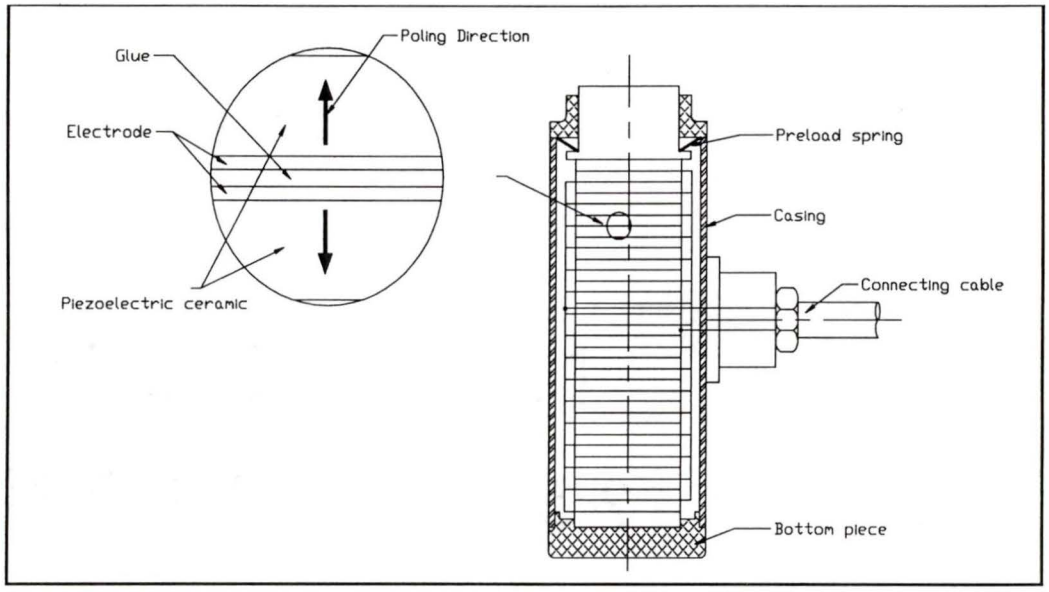

Figure 5.5: Stacked actuator design

5.4.2 Bimorph Design

A bimorph actuator is composed of two oppositely polarized plates bonded together as shown in Figure 5.6. When an electric field is applied, one plate will expand while the other will contract, causing the bimorph structure to take the shape of an arc. If the thickness of the material joining the two planes is less than one fifth of the beam thickness, the displacement can be calculated as [6]

$$\Delta z = \frac{3}{2}\left(\frac{L}{H}\right)^2 d_{31} V \tag{5.11}$$

Generally, bimorph actuators produce high displacements, weak forces and slow response times.

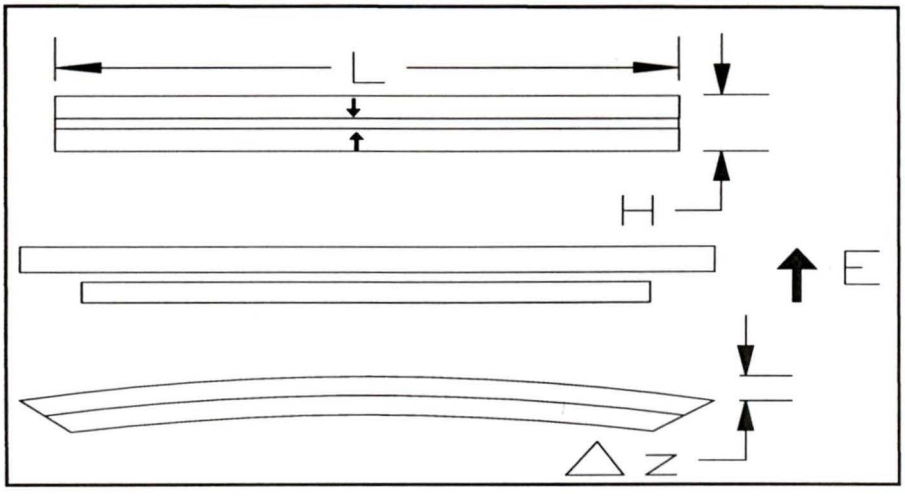

Figure 5.6: Bimorph design

5.4.3 Moonie Design

This relatively new device consists of a thin multilayered piezoelectric elements and two metal plates with moon shaped cavities bonded together as shown in Figure 5.7. This cap makes the displacement contribution from the planer piezoelectric modes add instead of subtract. The moonie design has the advantage of combining the characteristics of multi-layered and bimorph actuators, thus providing large displacement in a short response time [24].

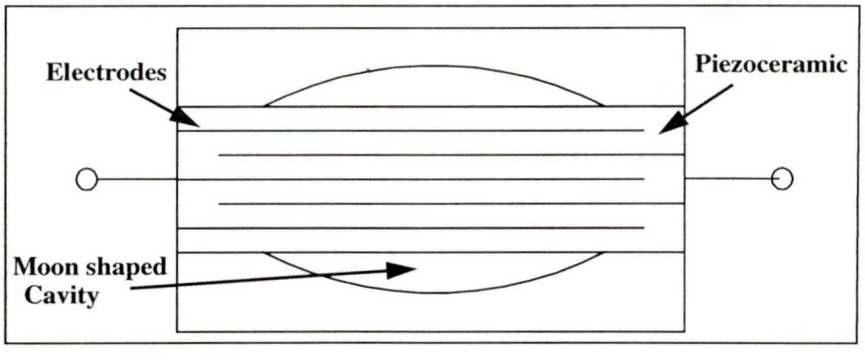

Figure 5.7: Moonie design

6 Introduction to the Processing of PZT

6.1 Introduction

This chapter provides an overall view of the materials processing technique by which PZT powder is prepared and processed into actuators. This process is accomplished in three major steps: data handling, ceramic processing and characterization. A brief discussion of data handling is followed by the examination of the processing parameters and their effects on the properties of the resulting piezoactuators. A short description of the laboratory layout and the reasons behind its design is then discussed. This is followed by a brief description of the experiments that were conducted to establish the processing procedure for desirable piezoceramics. The following chapters provide detailed discussion of this process, the processing equipment, the experiments conducted and their implementation.

6.2 Data Handling

The processing of PZT is a critical and complicated process involving numerous parameters that must be constantly evaluated, monitored and recorded. Several spread sheets were developed, one for each processing step, to serve as a data base and processing software. They are used to calculate the processing parameters according to the users input, default guides and/or the data collected from previous experiments. After processing, they are used to manipulate the data in order to examine the effect of the processing parameters on the final properties of the processed piezoceramics. To help understand and use these spread sheets, a spread sheet legend table was developed as shown in Table 6.1.

Table 6.1: Spread sheet legend

Symbol	Ruling	Meaning	Status
:	Single	User input is expected	Can be changed
>	Single	This is a value that is carried over from anther field	Should only be changed under special circumstances
!	Single	Remark	Can be changed
=	Double	This is a calculated value	Should never be changed

A detailed description of each spreadsheet will be presented when the corresponding process is discussed.

6.3 Ceramic Processing

The processing of PZT can be summarized as shown in the flowchart in Figure 6.1. The process is divided into three main parts:

Powder Preparation: The raw materials used to make PZT are the oxides of its constituents (PbO, TiO_2 & ZrO_2) which are purchased as high purity (99.9%) powders. PZT powder that is ready for pressing can also be purchased. When we start the process by using the oxides as raw materials, we begin by evaluating their volatility and purity through literature and supplier specifications. The weight of each oxide is then determined according to the amount needed for a stoichiometric composition. The powders are then mixed and the particle size of the mixture is reduced using a grinding machine (ball-mill). The powder particle size is evaluated using sieving or elutriation techniques. The solid solution of PZT is produced by reacting the oxides for an hour at 850 ^oC in a high temperature furnace. This process is called "calcination" and it is followed

by more ball-milling and particle size evaluation until the desired particle size for pressing is achieved. Raw materials and powder preparation are discussed in detail in Chapter 7.

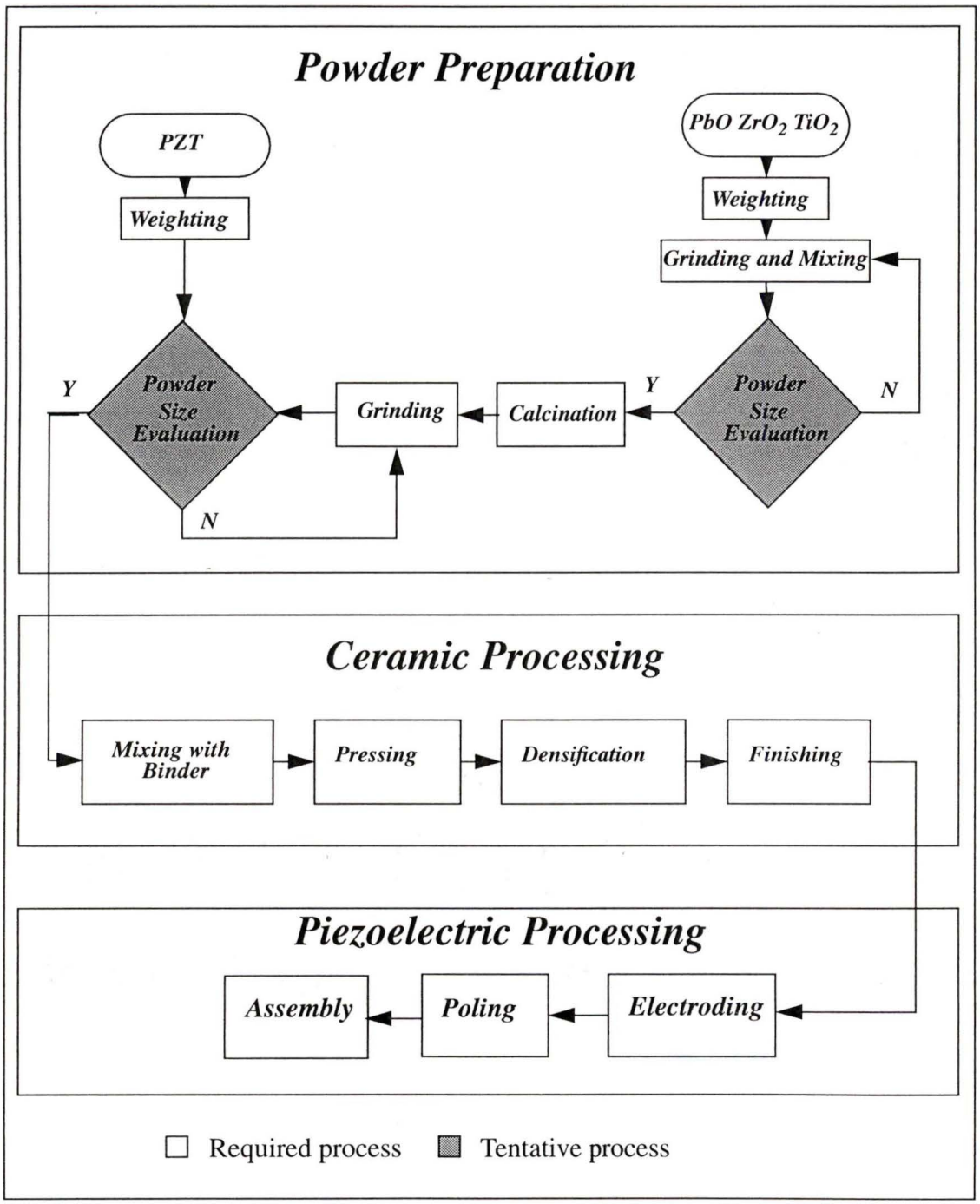

Figure 6.1: Flowchart of the processing of PZT powder and actuators

Conventional Ceramic Processing: This is the traditional ceramic processing which changes the loose free-flowing powder into a dense ceramic. The preparation of the PZT powder for pressing is started by mixing it with a binder. The pressing is done in a locally designed die using a 10 ton hydraulic press. The resulting "green" is then fired (densified) in the furnace, producing the ceramic. This ceramic is then finished to the exact dimensions needed for the actuator using a surface grinding machine. Chapter 8 is a detailed description of conventional ceramic processing techniques of PZT.

Piezoelectric Processing: The PZT ceramic is electroded by applying a thin metal layer to its surface. It is then poled by applying a very high voltage across its electrodes in an oil bath. The resulting piezoceramics are then bonded together in the desired configuration to form an actuator.

6.4 Characterization

Characterization is the set of measurements conducted to determine the piezoelectric, electric and mechanical properties of the processed piezoceramics. It is an important part of both the research and industrial processes. These measured properties are evaluated, recorded (in a spread sheet) and used as feedback to improve the process. The characterization of piezoceramics is discussed in Chapter 10.

6.5 Material Properties Controlled by Processing Parameters

Certain properties of PZT are intrinsic in the material itself, but others can be controlled through the processing parameters. The following is a list of these properties which will help us design the process and choose its parameters.

Piezoelectric Properties: As we know, maximizing of the piezoelectric properties is the prime objective of processing. These properties, such as d_{33}, are highly dependant on the processing parameters and can be enhanced by exact stoichiometry, donor doping, high density and optimal poling.

Dielectric Properties: The manufacturing process should be geared towards maximizing the resistivity and dielectric strength of piezoceramics.

Grain Size: Grain size has a direct effect on hysteresis, reliability and reproducibility of a ceramic. It can be controlled during the firing process.

Homogeneity: The density and grain size of the ceramic should be homogeneous throughout the specimens to avoid internal stresses and inaccuracy. This is achieved through the careful design of the forming die.

Actual Density: The maximum displacement of an actuator is directly proportional to the density of the ceramic. Ceramics of density less than 95% of their theoretical density[1] will have open pores which will cause dielectric losses, low dielectric strength and a dependence of the volume resistivity on moisture. It could also cause a change in apparent impedance due to absorbing of water in the finishing process [5]. Actual density is a function of the particle size, pressing pressure, calcination temperature and duration.

---

1. The theoretical (volume) density of a ceramic is calculated using its crystal structure, atomic radii and masses. This is done by dividing its unit cell mass by volume [12].

6.6 Laboratory Setup

The piezoceramic processing laboratory was set-up as shown in Figure 6.2. The following considerations were taken into account in the design of the layout:

Safety: The laboratory was designed with safety as the primary concern. For example:

- The poling station where high voltages are applied was placed far from the windows (a source of humidity) as well as any equipment where water is used to avoid electric shocks.
- The furnace was placed next to a window, to allow any fumes to escape the room.
- The laboratory was provided with goggles, gas masks, gloves and lab coats for the safety of the staff.
- To avoid contaminating the public sewage system, the laboratory was also equipped with its own sink, pump, filter and tap.

Contamination Avoidance: The processing of piezoceramics is a delicate process where any slight contamination of the input chemicals can lead to inaccurate results. Great care was taken in separating processes that could lead to contamination. This was done by isolating powder preparation equipment (scale and ball-mill) in the far corner away from other equipment.

Ease of Operation: In order to save time and energy, the laboratory's layout reflects the natural flow of processing.

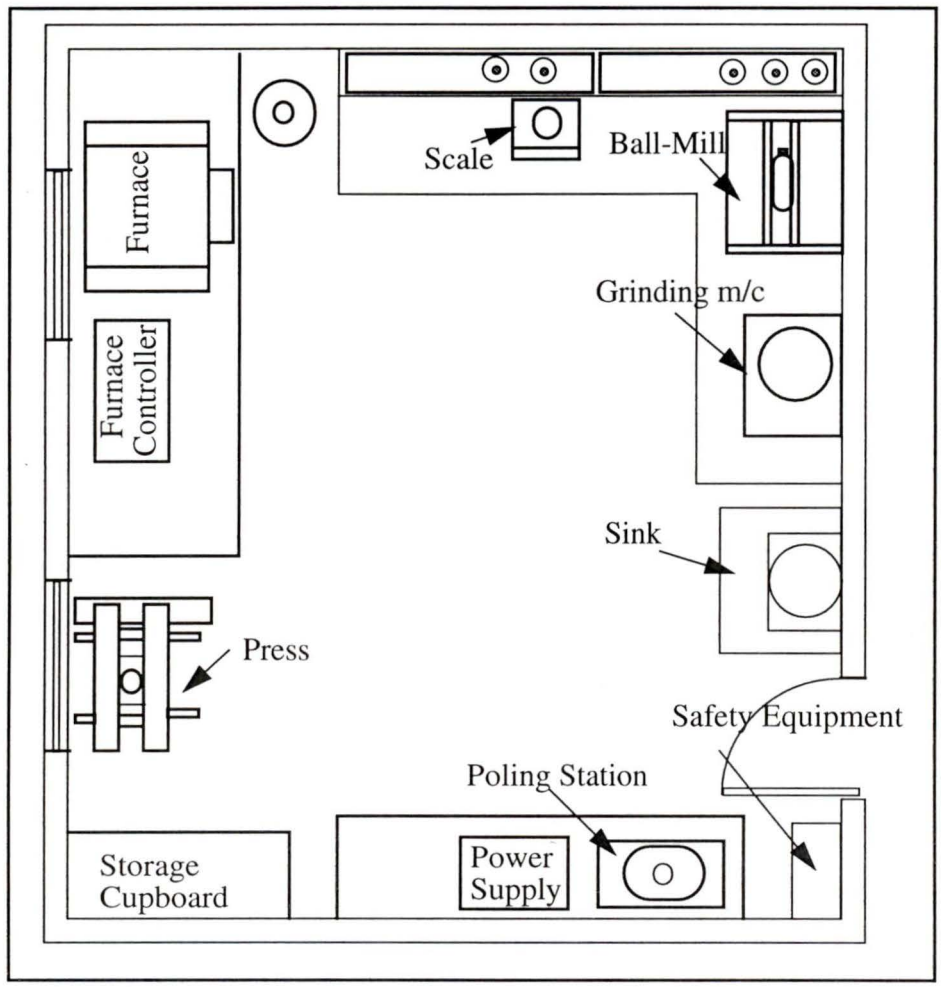

Figure 6.2: Layout of the processing laboratory

6.7 Experiments Conducted

Nearly ten batches of PZT were processed in an effort to understand and perfect the processing parameters. The starting value for each parameter was that listed in literature such as [5], [6], [4] and [26]. Some of these parameters needed improvement because of the difference between the raw materials and equipment used by the authors and those used in our laboratory. The processing parameters and results from the last two batches, described briefly below, are presented in the next four chapters.

Batch 9: This batch contained two hundred grams of the ready-made PZT powder which was supplied by BM Hi-Tech. The PZT powder BM 527 was chosen because of its high d_{31}[1], and it was mainly used for comparison with PZT-5 processed in our laboratory.

Batch 10: As we saw in Chapter 3, PZT-5 was chosen for our application. Thus two hundred grams of $Pb_{0.988}(Ti_{0.48}Zr_{0.52})_{0.976}Nb_{0.024}O_3$ (commercially known as PZT-5), were prepared as batch 10.

These two batches were chosen because:

- They represented the two choices our research group has to evaluate: ready-made powder and that prepared in our laboratory.
- They produced the best results, as we will see later, their characteristics were very close to the expected values.

1. High d_{31} is important for Bimorph Mirrors which are the subject of research in our research group.

7 Powder Evaluation and Preparation

7.1 Introduction

The raw materials used in the preparation of PZT are the oxides of its constituting ions. They are lead, zirconium, titanium and small amounts of dopants such as niobium. These raw materials are available as high purity powder oxides and the first step of processing is to weigh and evaluate them in their powder form. In the first part of this chapter, we see how these raw materials are evaluated with respect to their purity, volatility and particle size. In the second part, the methods and equipment by which these raw materials are processed into PZT powder are examined.

7.2 Purity Evaluation

Purity is a very important property of raw materials since small amounts of undesired (uncontrolled) impurities can tremendously change the properties of a piezoceramic. Impurities change these properties by altering the position of the metamorphic phase boundary (M.P.B.). This inhibits the reactivity during calcination, preventing the solution from achieving stoichiometry. As a result, the dielectric, conductive and piezoelectric properties of the resulting ceramic are adversely affected [5].

7.2.1 Types of Impurities

Impurities are those elements, other than lead, zirconium and titanium, that find their way into the ceramic. There are two kinds of impurities: controlled and uncontrolled impuri-

ties. On one hand, controlled impurities are added to the composition in exact amounts for certain purposes. In PZT the following are common controlled impurities:

- The amount and distribution of **dopants** is especially important as any slight variation can poison their effect and produce defective samples.
- **Binders** are necessary for pressing so they are added in precise amounts. They are burnt-off before densification.

On the other hand, uncontrolled impurities usually come with the raw materials and from the environment. If they do not burn-off during firing they can adversely affect the properties of the ceramic.

7.2.2 Methods of Reducing Contamination

The purity of the resulting PZT is a function of the quality of the used oxides, the handling equipment and the skill of the operators. Thus the following steps are taken to reduce contamination:

- Choosing high quality suppliers for the oxides to ensure they are up to the specifications (mainly purity and particle size).
- Using clean handling equipment such as crucibles and steering rods that do not react with the ceramic. This is especially important during high temperature processes as calcination and densification.
- Care must be taken in the ball-milling operation as the danger of contamination is especially high. This is due to the excessive wear suffered by the container and the balls.

Note: These precautions are revisited during the discussion of each process.

7.2.3 Supplied Materials

The basic constituents of PZT, lead and titanium oxides, and dopants such as niobium, are available with 99.9% purity. Zirconium oxide is supplied with a 2% HfO_2 impurity. However, this impurity does not cause any problems due to the chemical and physical similarity between zirconium and hafnium [6].

7.3 Volatility Evaluation

The presence of volatile ingredients in raw materials has an important effect on the properties of PZT. Thus, volatile materials should be identified through the literature and supplier specifications. Their ignition losses should also be calculated and compensated to maintain stoichiometry. In our case, lead was found to be volatile at high temperature (>900 ^oC). Consequently, extra amounts (3-5% by weight) of lead oxide are added to compensate for its loss.

7.4 Particle Size Evaluation

Another crucial property of raw materials is their particle size. Ceramic powder consists of millions of particles that are evaluated according to their shape and size. Most large particles are nearly spherical while smaller sized ones tend to have irregular shapes. Powders are usually a mixture of three types of particles:

Primary particles: These are crystalline structures bound together by extremely strong molecular bonding.

Aggregates: They are several primary particles tightly bound together by atomic or molecular bonding at their points of contact. Usually a large force is needed to separate them.

Agglomerates: They are primary particles or aggregates loosely bound together by weak Van der Waals forces [17].

Small particle size (less than 5 μm and greater than 1 μm) is desired for raw materials (oxides) because their presence:

- assists the attainment of chemical equilibrium during calcination, and
- the achievement of higher density during pressing and densification.

Particles are classified according to their equivalent spherical diameter. The following are the most common methods of particle size and shape evaluation:

7.4.1 Microscopy

This is an absolute means of measuring the size and shape of individual particles by magnifying them under a microscope. It has the advantage of very high sensitivity but it can only examine a very small number of particles at a time. Consequently, the representativeness of the sample has a great effect on the results. Optical microscopes are used to evaluate particles in the 150 - 0.8 μm range. Particles bigger in size can be seen by a simple magnifying glass. Smaller ones can only be accurately measured by an electron microscope [17].

7.4.2 Sieving

It is the simplest and most obvious means of particle sizing. A technique known since the time of the ancient Egyptians, it has been advanced and standardized in the last century. Basically, sieving is a process where the powder is passed through several meshes of different hole sizes. The sieves are stacked in descending order, with largest on top, on a vibrator as seen in Figure 7.1. In this configuration, particles of sizes greater than that of the holes remain in the corresponding sieve. The particle size distribution is determined by the weight of powder remaining in each sieve after a certain duration. Ordinary woven wire sieves can sort powders in the 20 μm to 125 mm range, while micromesh sieves can go down to the 5 μm sizes.

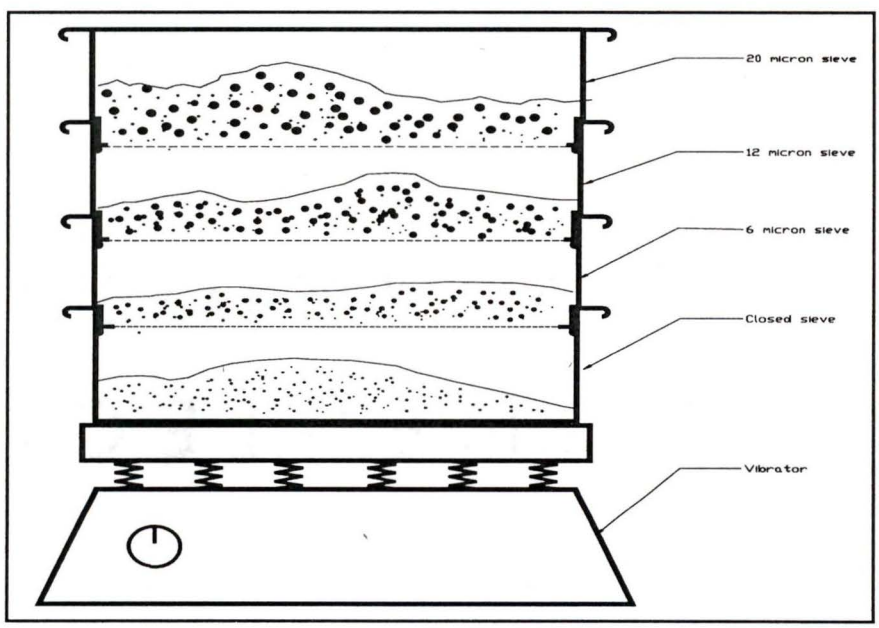

Figure 7.1: Typical sieving setup

7.4.3 Elutriation

Particles fall (under the effect of gravity) through fluids at different speeds according to their size. This fact is used in particle size determination by relating the size (diameter) of a particle to its terminal velocity in the fluid.

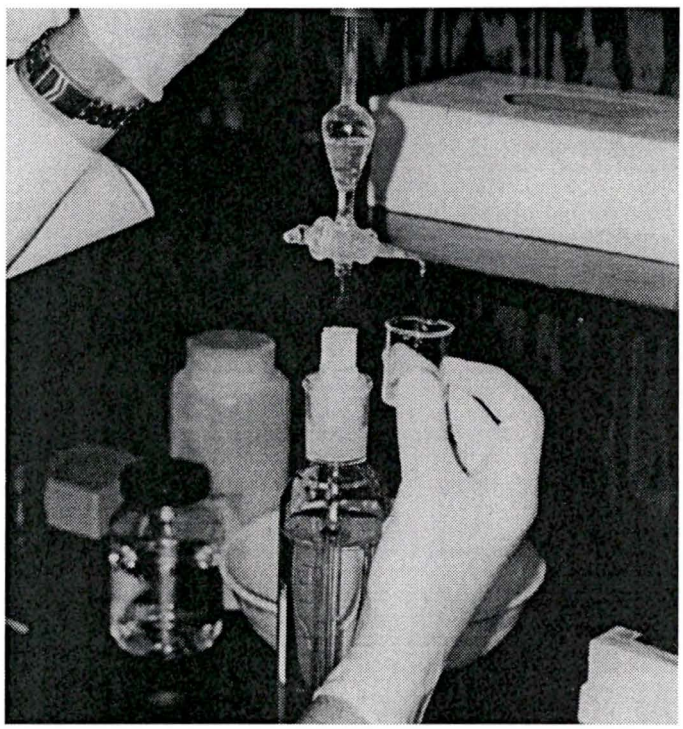

Figure 7.2: Anderson pipet

The Anderson pipet is a popular method of evaluating powder size by elutriation. Powder suspended in distilled water is poured into the apparatus and shaken well. A sample of 10 *ml* is drawn out and poured into a weighing vessel at fixed time intervals (about 20 seconds). The vessels are dried and weighted to find the weight of powder in each. Since larger particles will pass the tip first, each sample drawn has a smaller size of grain. The

particle size distribution is then calculated using Stokes' Law[1] which relates particle size (radius) to the falling velocity of the particle [17].

7.4.4 Experimental Results

These three methods were used in the first stages of our experiments to evaluate the raw materials and determine the optimum milling time. In that effort, the particle sizes of raw material were found to be satisfactory. The optimal milling time was found to be about seven to eight hours at tumbling velocity[2]. Accordingly, in later batches such as 10, the particle size was assumed to be in the correct range after 8 hours of ball-milling.

7.5 Weighing

The composition of a piezoceramic is usually given in the form of a chemical formula. This formula is equivalent to molar ratio between the ions of its constituents. The composition PZT-5 is represented as: $Pb_{0.988}(Ti_{0.48}Zr_{0.52})_{0.976}Nb_{0.024}O_3$, thus the ratio of *Pb:Ti:Zr:Nb* is, respectively 0.988:0.468:0.508:0.024. This ratio is converted into a weight ratio by using the expression

$$Wr\,(X) \;=\; \frac{\text{Mol. Wt. of X} \times \text{Mol. Frac. Required}}{\text{Total Mol. Wt. of Compostion}} \tag{7.1}$$

The actual weight [*Wt(X)*] of each oxide is calculated by multiplying the weight ratio [*Wr(X)*] by the total weight needed. Excess amount of volatile materials are added to maintain stoichiometry (3% by weight of *PbO* was added to batch 10).

---

1. Stokes' Law, which describes the interaction between particles and fluids in a gravitational field, is discussed in Chapter 7 of [17].
2. See "Ball-Milling Variables:" on page 71.

$$Wt_{TiO_2} = \text{Total Wt. needed} \cdot Wr(TiO_2) \qquad (7.2)$$

Equations (7.1) and (7.2) were implemented in Spread sheet 7.1 to facilitate weighing calculations.

Spread Sheet 7.1: Weighting Calculations (batch 10)

Sample #		1
Date		19/1/96
Total Wt Needed	g	200.000
Mol Wt of Comp	g	323.667
Excess Lead	%	3

Compound	% elm wt	Mol wt	Mol Frc	Wt of Elm	Wt 0f Ox
PbO	0.928315	207.19	0.988	126.4903	140.346
TiO2	0.599508	47.9	0.469	13.86682	23.130
ZrO2	0.740309	91.22	0.508	28.60604	38.641
Nb2O5	0.699043	92.906	0.024	1.377801	1.971
O2	0.5	15.9994	3	29.659	N/A
Total				200	204.0877

The upper spread sheet holds the sample number, date of processing, total weight of PZT required, the molecular weight of PZT and the percentage of lead oxide added to compensate for its volatility. The inputs to the lower part are each element's (*Pb, Ti, Zr* and *Nb*) required molecular fraction in the final compositions and the molecular weight of their oxides in the fourth and third columns respectively. The spread sheet calculates the required weight of each element and that of its oxide listed in the fifth and sixth columns respectively. The total weight of the oxides (204) is usually greater than the required weight of PZT (200) because of the extra lead oxide added.

Weighing Practice: A high accuracy (0.001 *g*) scale and special plastic weighing vessels are used in weighing. The oxides, especially those of the dopants, should be weighed very carefully to produce a stoichiometric solid solution with the desired properties. The total

weight should be more than that needed for the final ceramic sample to account for losses of powder in milling, firing and handling.

7.6 Powder Size Reduction (Comminution)

If the evaluation methods listed earlier show an undesirable particle size distribution, a comminution process is needed to reduce the powder's particle sizes. This is done by means of crushing or milling, which reduces the maximum size of the particles. It also changes their shapes, breaks up agglomerates, aggregates and reduces the porosity of the particles. Before calcination, ball-milling is also used to mix the powders.

7.6.1 Grinding Mechanism

Particles are subjected to shear and compressive forces during milling which reduces their size. Shear occurs when a particle is squashed between two of the grinding media moving at different velocities. Consequently, attrition is caused by the resulting frictional stresses. The energy produced during the impact, is a function of both the weight and velocity of the grinding media given as

$$\text{Energy}=\Delta\left(\frac{1}{2}mv^2\right) \tag{7.3}$$

This shows that heavy, fast moving, grinding media is needed for maximizing impact energy [18].

7.6.2 Ball-Mill

There are several types of mills used for grinding ceramics including ball, vibratory and attrition mills. The ball-mill used in our laboratory, shown in Figure 7.3, was designed by

our research team and manufactured in the mechanical engineering machine-shop. It is powered by a RELIANCE ELECTRIC servo-motor, which is controlled by an LA-5600 linear amplifier. This motor can supply a peak torque of 960 OZ-IN and a maximum continuous speed of 1850 rpm (with no load). It is connected by a rubber belt to an aluminum roller. A disposable plastic jar-shaped container is filled with grinding media and ceramic powder otherwise known as "feed" and placed horizontally on rollers. In this configuration, it rotates about its central axis causing a tumbling action which impacts the powder particles. Milling can be done either wet or dry. However, wet milling is used to achieve smaller particle sizes.

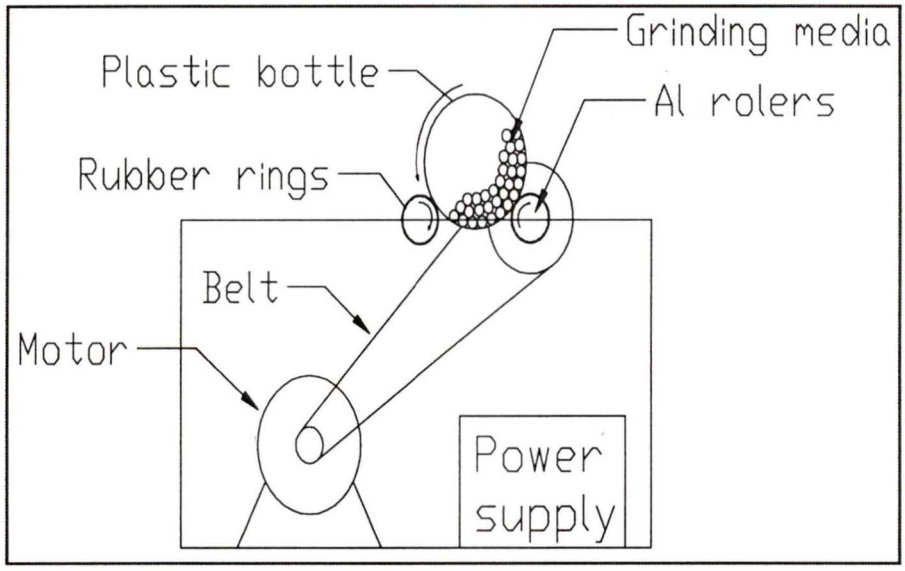

Figure 7.3: Schematic diagram of the ball-mill

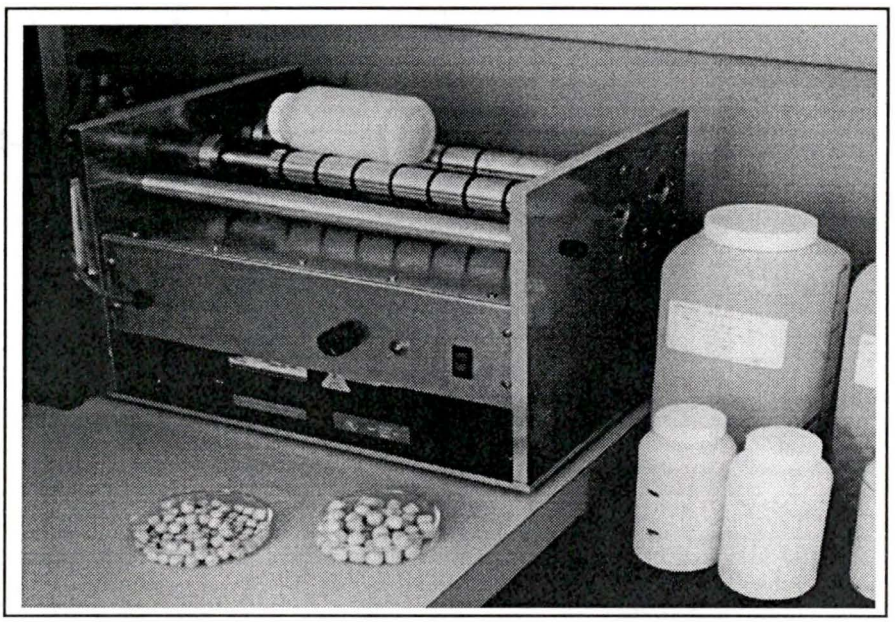

Figure 7.4:Ball-mill

Ball-Milling Variables: The reduction in particle size is controlled by:

- **Radius and rotational velocity of the cylinder**

  The rotational velocity is limited by its critical value (ω_{cr}) shown in Equations (7.4) and (7.5). This velocity causes centrifuging, when very limited crushing occurs. The lower limit on velocity is that causing excessive tumbling [18].

$$\omega_{cr\,(\mathrm{Dry})} = 0.5R^{-0.5} \tag{7.4}$$

$$\omega_{cr\,(\mathrm{Wet})} = (0.65 - 0.85)\,\omega_{cr\,(\mathrm{Dry})} \tag{7.5}$$

  where R is the radius of the cylinder in meters

- **The ratio of the size of the grinding media to that of the feed particle size**

  This ratio should always exceed 25:1 [4].

- **The relation between the volume of feed and that of media**

The media should occupy 50% of the volume of the jar, with the feed filling a volume slightly exceeding that of the voids between the media. This ratio is a good balance between the media and wall rate of wear and grinding efficiency. More feed can be added if breaking agglomerates and mixing are the only purposes of the milling [4].

- **Physical properties of the grinding media**

It should be made of dense, non porous, wear resistant materials in the shape of rods, short cylinders, spheres or pebbles. The two kinds of grinding media used in our mill are described in Table 7.1.

Table 7.1: Grinding media used in ball-mill

Diameter	Shape	Material	density
1.3 *mm*	Cylindrical	Zirconia	5.5 Mg/m^2
0.6 *mm*	Cylindrical	Zirconia	5.5 Mg/m^2

Zirconia was used as grinding media since it is a material similar to that of the powder being milled. This helps avoid contamination. Cylindrical media pack densely thus increasing the probability of particle impact [4].

- **Agglomeration of the feed**

The powder should be as separate as possible before it is fed into the mill.

- **Milling time (Number of revolutions)**

The milling time or number of revolutions is directly proportional to the mean particle size and the narrowness of its distribution.

- **Viscosity of the slurry in wet milling**

  A liquid (distilled water in our case) is added in milling to increase the solid loading in slurry and disperse agglomerates. The slurry should be viscous enough to form a film around the grinding media, holding the particles in the impact zone. It should also minimize slippage between media and the wall of the mill to reduce wear [4].

7.7 Mixing

Mixing distributes additives, disperses agglomerates, intermingles and combines batch materials differing in chemical and physical properties. The mechanism should be strong enough to break up aggregates in the raw materials. It is a crucial process since any lack of homogeneity could cause loss of piezoelectric properties [18]. Mixing the components (lead, zirconium, titanium oxides and dopants) of PZT before calcination is performed, along with powder size reduction, in the ball-mill.

7.8 Calcination

As mentioned in previous chapters, to obtain PZT of maximum piezoelectric properties, the two phases ($PbTiO_3$ & $PbZrO_3$) must be present in equal quantities. This solid solution of exact stoichiometry is obtained by: properly mixing and weighing powder lead, zirconium and titanium oxides, then heating them in the furnace[1]. This process is called calcination, and besides being the chemical reaction, it is considered to be the final part of mixing and the first part of densification. During calcination, constituents interact by interdiffusion of their ions and the following takes place:

1. The furnace used in the laboratory will be described in section 8.3.2.

- Water[1], Carbon dioxide and volatile impurities are removed.
- The desired PZT solid solution is formed by reacting the raw materials as shown in Figure 7.5.

7.8.1 Chemical Reactions During Calcination

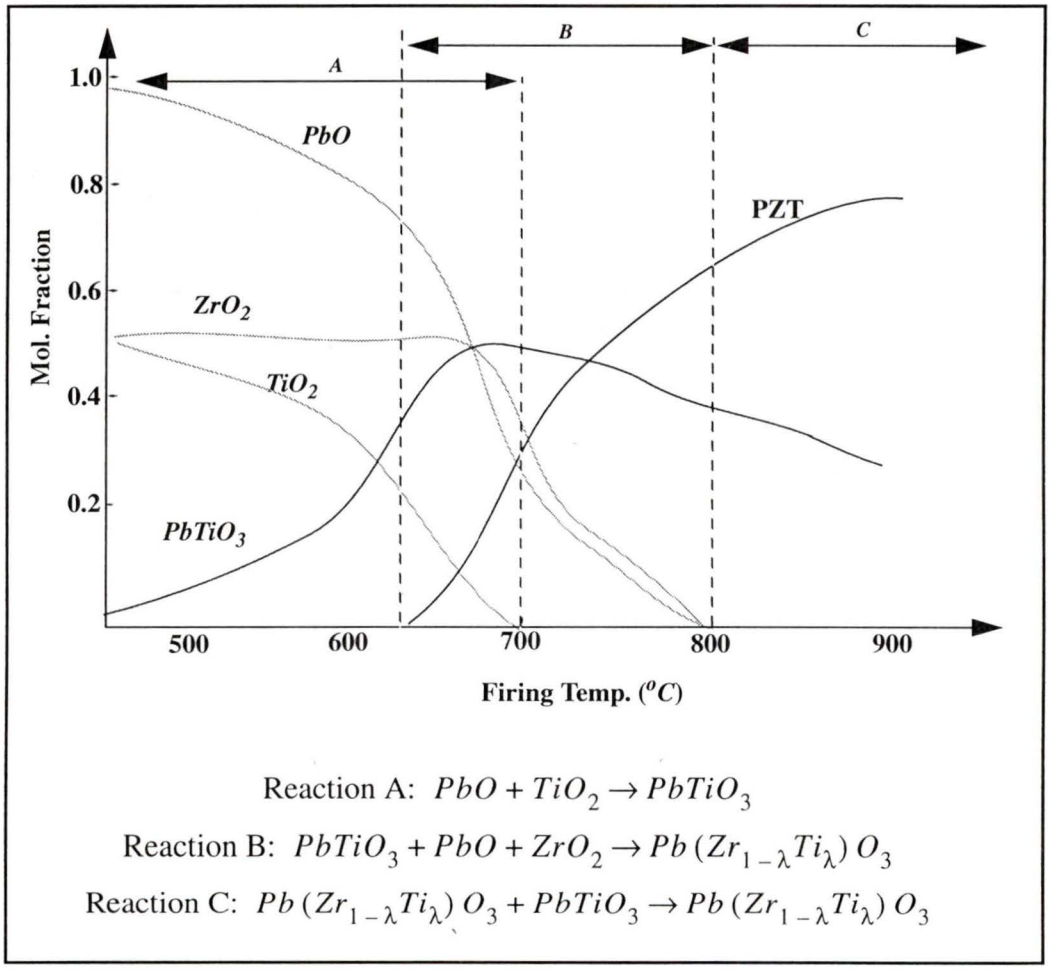

Figure 7.5: Chemical reactions during calcination (Adapted from [5])

The chemical reactions needed to produce PZT are dependent on particular properties of the chemicals used, mainly their particle size, purity and reactivity. Several scenarios of

1. Water could be present as a result of wet mixing or ordinary dampness.

the reaction can occur but the most probable is shown in Figure 7.5. The solid state reaction usually starts by the formation of lead titanate solid solution. This is followed by the remaining lead and zirconium oxide reacting into the lead titanate to form the desired $Pb(Ti,Zr)O_3$ [5].

Note: The presence of free zirconium oxide in the final powder is usually the result of excessive lead oxide loss [5].

7.8.2 Calcination Practice and Precautions

The practice of calcination can be summarized in the following points:

1. The powder is placed in a ceramic container made of alumina. This crucible withstands high temperatures without reacting with the powder.
2. The container should be covered to avoid the loss of volatile constituents (lead oxide).
3. The calcination temperature should be high enough to foster the reaction. However, it should be low enough not to cause too much loss of volatile oxides or hamper subsequent grinding operations. For PZT this temperature should be in the range of 800 to 850 ^oC.
4. Ceramic powders usually have low thermal conductivity. Therefore, a uniform thermal distribution can only be achieved for a few centimeters depth for a heating duration of one to two hours. A typical heating profile for making PZT is shown in Figure 7.7.

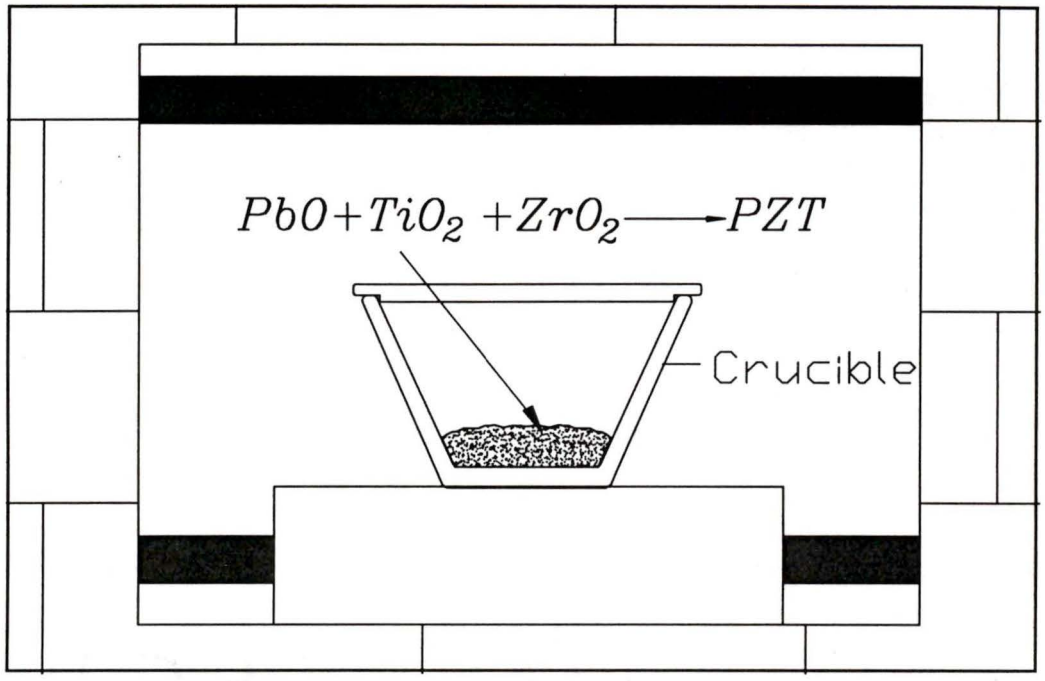

Figure 7.6: Calcination

5. Calcined materials usually undergo a limited amount of sintering so they must be milled afterwards to obtain the free flowing powder needed for pressing.

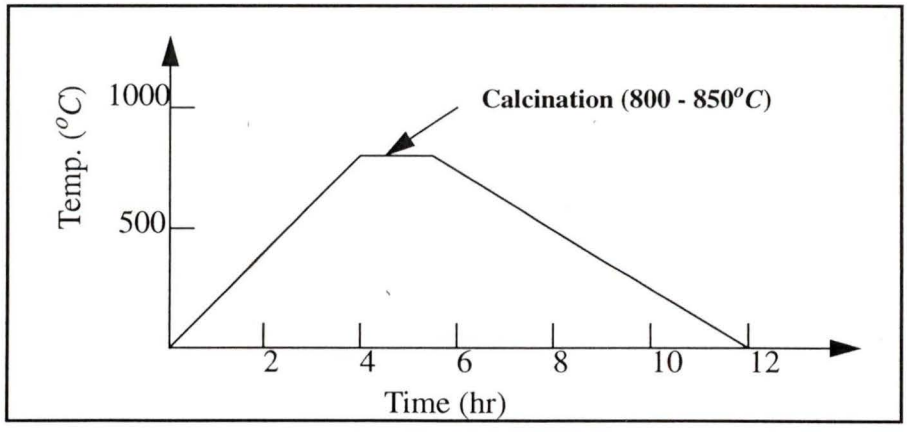

Figure 7.7: Calcination heating profile

7.9 Data Acquisition

The Spread sheet 7.2 was prepared for monitoring the powder preparation process. It was divided into three steps (two ball-milling operations and one calcination).

Spread Sheet 7.2: Powder preparation

Ball-Milling

Step		1		3
Sample #		10		10
Run	:	Befor Cal	:	After Cal1
Date	:	19/1/96	:	5/10/95
Water Content (ml)	:	0.25	:	
Input Wt. (g)		200		189
Ball Sieze (mm)	:	big	:	small
Rotaional Speed (rpm)	:	tm	:	tm
Duration (hr)	:	8	:	8
Output Wt (g)	:	194	:	181
Wt Losses (g)		6		8

Calcination

Step		2
Sample #	:	10
Date	:	
Input Wt (g)		194
Heating Rate (C/min)	:	5
Soak Temp (C)	:	850
Ramp Time (min)		170
Duration (min)	:	90
Coling Rate (C/min)	:	fast
Output Wt (g)	:	189
Wt Losses (g)		5

The chronological order of these processes are expressed by the step number. Thus we start with a ball-milling operation followed by calcination then another ball-milling. The inputs to the ball-milling operations are the sample number, date of processing and water content which shows the fraction of water added in wet-milling. This is followed by input sample weight, size of grinding media, rotational speed (where *tm* indicates the tumbling velocity) and duration of milling. The weight of powder recovered from the jar is used to calculate the losses. These losses are due to powder sticking to the jar walls and are used

to estimate the weight of raw materials required for subsequent batches. The calcination spread sheet uses the input heating rate and soak temperature to calculate the ramp time required to program the furnace. It also lists the duration of heating and the cooling rate where (fast) means the power to the furnace is completely turned off. In the case of calcination the volatilization of *Pbo* is the main cause of weight loss that should be monitored to ensure stoichiometry.

7.10 Conclusion

The preparation of raw materials is of vital importance to the manufacturing process. If evaluation, weighing, mixing, grinding and calcination are carried out carefully, we should obtain reproducible PZT powder possessing:

- homogeneously distributed composition and density,
- correct powder size (smaller than 5 μm and free flowing), and
- stoichiometric composition.

This PZT powder will be the input of the following process which is pressing. Any mistakes in the preparation can adversely effect the mechanical, dielectric and piezoelectric properties of the resulting samples. Great care must be taken in powder preparation, as the correcting of these mistakes in later stages is very difficult or impossible.

8 Ceramic Processing

8.1 Introduction

In this chapter, the process by which PZT powder is processed into a dense ceramic of exact dimensions is discussed. Ordinary ceramic forming operations such as uniaxial pressing are used to compact and shape the PZT powder. The forming process should ensure the homogeneity of the resulting "green" sample. The next step is to densify the pressed sample by firing it in the furnace. The ceramic is then finished by a process of surface grinding.

8.2 Forming

This process involves the compacting of piezoceramic powder into a desired shape. Uniaxial pressing is the most suitable forming process for our experiment. This is due to the simple shape of the samples required. Another advantage is that pressing tends to be more economical at low production rates.

8.2.1 Optimal Particle Size for Pressing

The following should be considered in determining the optimal powder size for pressing piezoelectric PZT powder:

- The size must be small enough to increase the reactivity in the densification process.
- Particle sizes should be available in a range that maximizes the packing process.
- Small particle sizes reduces the time and duration of the densification process.

- Very small particles cause logistical problems, since when they become air-born they are difficult to handle and pose a threat to the health of operators [4].
- A high concentration of elongated or flat particle can cause bridging during forming. The resulting irregularly shaped pores are difficult to remove during sintering [5].

For our application, we need PZT powder with a range of particle sizes smaller than 5 μm and greater than 1 μm. Its distribution should be diverse enough to produce optimal compacting. This is achieved in the ball-milling operation performed before pressing.

8.2.2 Binders

Since the pressed part should be sufficiently strong to survive ejection from the die, organic additives called binders are used to consolidate the green sample. The binder is then removed during presintering. Binder content should be as low as practically possible to reduce gas release. The most suitable binder for use with PZT is polyvinyl alcohol. It is obtained in powder form and the following describes how it is prepared and used:

1. PVA powder (5% by weight) is slowly added to hot water (60 - 70 ^{o}C).
2. After about an hour of stirring and heating, the PVA is poured through a strainer to remove the undissolved powder.
3. The container is marked with the date as the PVA solution is only good for one month.
4. The solution is added (5% by weight) and thoroughly mixed with the dry powder before pressing.

8.2.3 Uniaxial Pressing

It is the compaction of powder along one axis, by means of a rigid punch into a die. During pressing, the powder is crushed and redistributed. High pressures are required to ensure the breakdown of the granules and uniform density. Pressing machines are categorized according to the source of pressing force. Mechanical presses have higher production rates with pressure up to 100 tons. Hydraulic presses can produce higher pressures of up to 5000 tons, but at a lower production rate. The following problems should be avoided in the design of the pressing setup:

Cracks: They are usually associated with bad die design, especially not accounting for air entrapment or rebound during ejection. Surface cracks can be readily visible. However, internal cracks are more difficult to detect. In that case, the ceramic has to be subjected to X-ray examination.

Density Variation: The variation of density in different parts of the compacted green, shown in Figure 8.1, is probably the biggest drawback of uniaxial pressing. It results in distortion during firing as lower density areas will exhibit more shrinkage, therefore causing flaws. This results in a final product with non-uniform mechanical and, more importantly, electrical properties or simply a cracked sample. Density variation is caused by the friction between powder particles as well as the particles and the die wall. It can be reduced by:

- the addition of lubricants to the powder to reduce friction and help with the flow of the powder in the die during pressing,
- the design of samples with low thickness to diameter ratio, and

- the application of pressure from both directions as shown in Figure 8.1.

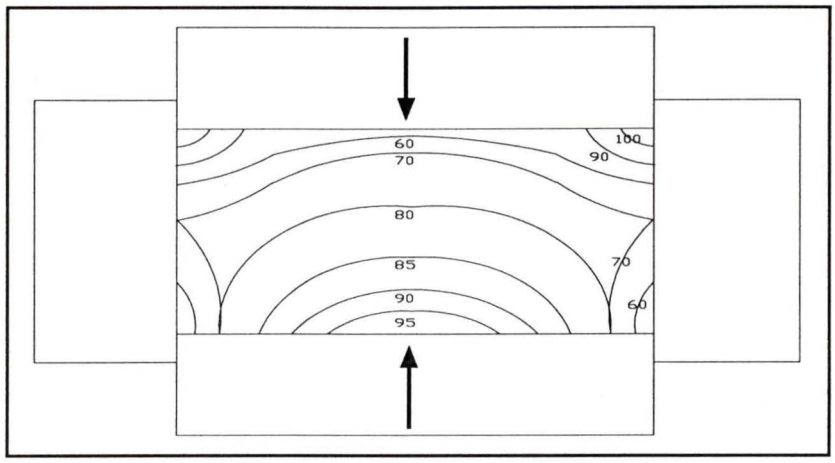

Figure 8.1: Density distributions in uniaxial pressing

8.2.4 Sample Size

The following points were considered in the choice of the sample size and shape:

- It should be suitable for making actuators and characterization purposes[1].
- The maximum diameter (D_{smax}) of a sample is a function of the maximum force (F_{max}) that can be applied by the available press and the pressure needed to achieve uniform compactness (P_c). Our press can supply 99640.2 N force and P_c should be greater than 100 MPa for technical ceramics such as PZT.

$$D_{smax} = \sqrt{\frac{4F_{max}}{\pi \cdot P_c}} = \sqrt{\frac{4 \times 99640.22}{\pi \times 100 \times 10^6}} = 0.0356m \tag{8.1}$$

A suitable sample diameter was calculated at D_s=25.4 mm.

1. See "Sample Shape:" on page 120.

- The minimum thickness of the sample should be small enough to achieve uniform properties without leading to breakage [4].

$$H_{smin} = 0.1D_s = 2.54mm \tag{8.2}$$

- The limit on the maximum height of the sample is the maximum voltage that can be applied during poling and the desired electric field. In our laboratory, the power supply maximum voltage is 20 *KV* and for PZT, the optimal poling electric field is 2.5 *KV/mm,* which yields a maximum height of:

$$H_{smax} = \frac{20KV}{2.5KV/mm} = 8mm \tag{8.3}$$

8.2.5 Die Design

Material Selection: The main requirements for die and plunger materials are:

- high yield strength to withstand the applied pressure,
- high modules of elasticity to avoid buckling, and
- rust resistance to avoid contamination.

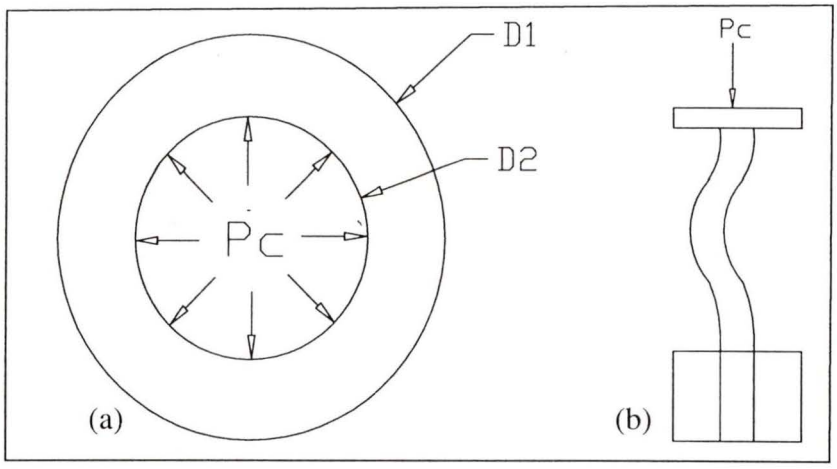

Figure 8.2: Modes of failure due to external load a) Radial and tangential stresses. b) Buckling in upper or lower plungers

The best material for the die and plungers is ultra-high strength steel. Due to its high cost, a combination of stainless and hardened steel were used instead.

Design Objectives: Flexibility is the main objective in the design as it is intended for low volume experimental production. The following are the general guidelines in the design of the die:

- It should produce a thin disc-shaped sample with low thickness to diameter ratio.
- The force must be applied in two directions.
- It must include an ejection mechanism for getting the fragile compact out intact.
- It must be easy to clean to avoid contamination.

Figure 8.3 is a sketch of the die showing the different dimensions. The following is a list of these dimensions and the design constraints associated with each:

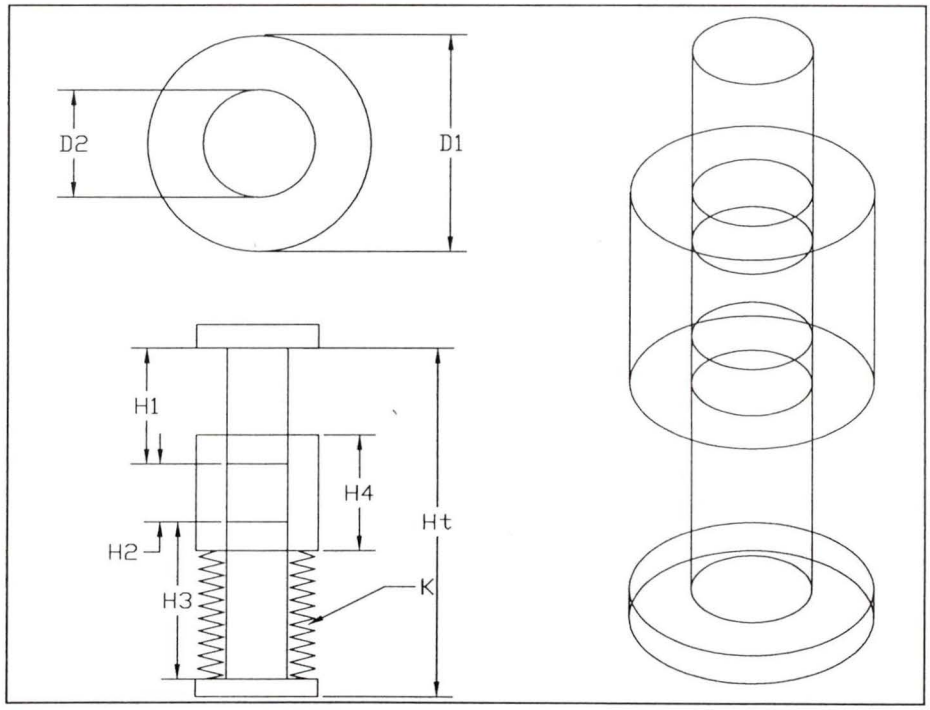

Figure 8.3: Preliminary die design

D2: The internal diameter of the die is also the diameter of the upper and lower plungers and that of the resulting green (D_s). The diameter of the plunger should be large enough so it will not buckle or bend under the compressive force of the press.

T: The tolerance of D2 should be arranged so the plunger fits easily in the die with enough space for any air to escape. The maximum clearance should not be too large that it will cause the jamming of the plunger or the escape of too much air-born powder. Reed [18] suggests a clearance of 10 - 25 μm when pressing micron-sized powder. He also suggests a (< 10 $\mu m/cm$) tapered die wall to facilitate ejection.

D1: The thickness of the die depends on the yield strength (Y_s) of its material and the maximum pressure applied.

H2: The length of the cavity should be long enough to hold the amount of uncompressed powder needed to produce a sample of maximum thickness (H_{smax}). The compression ratio for PZT is about 2, therefore H2 should be twice the maximum sample length.

H4: The total length of the die should be greater than H2 plus at least twice the diameter of the plungers. This interference is necessary for balance and prevention of buckling. It should also be shorter than the lower plunger H3, to facilitate ejection as shown in Figure 8.6. To avoid the need for a long plunger, the die was divided horizontally into two parts.

K of the spring: The stiffness (K) is calculated so the spring would compress a distance D2 (desired interference) under the weight of the die.

These constraints were used to calculate the die dimensions. The die and plunger were manufactured in the mechanical engineering machine-shop.

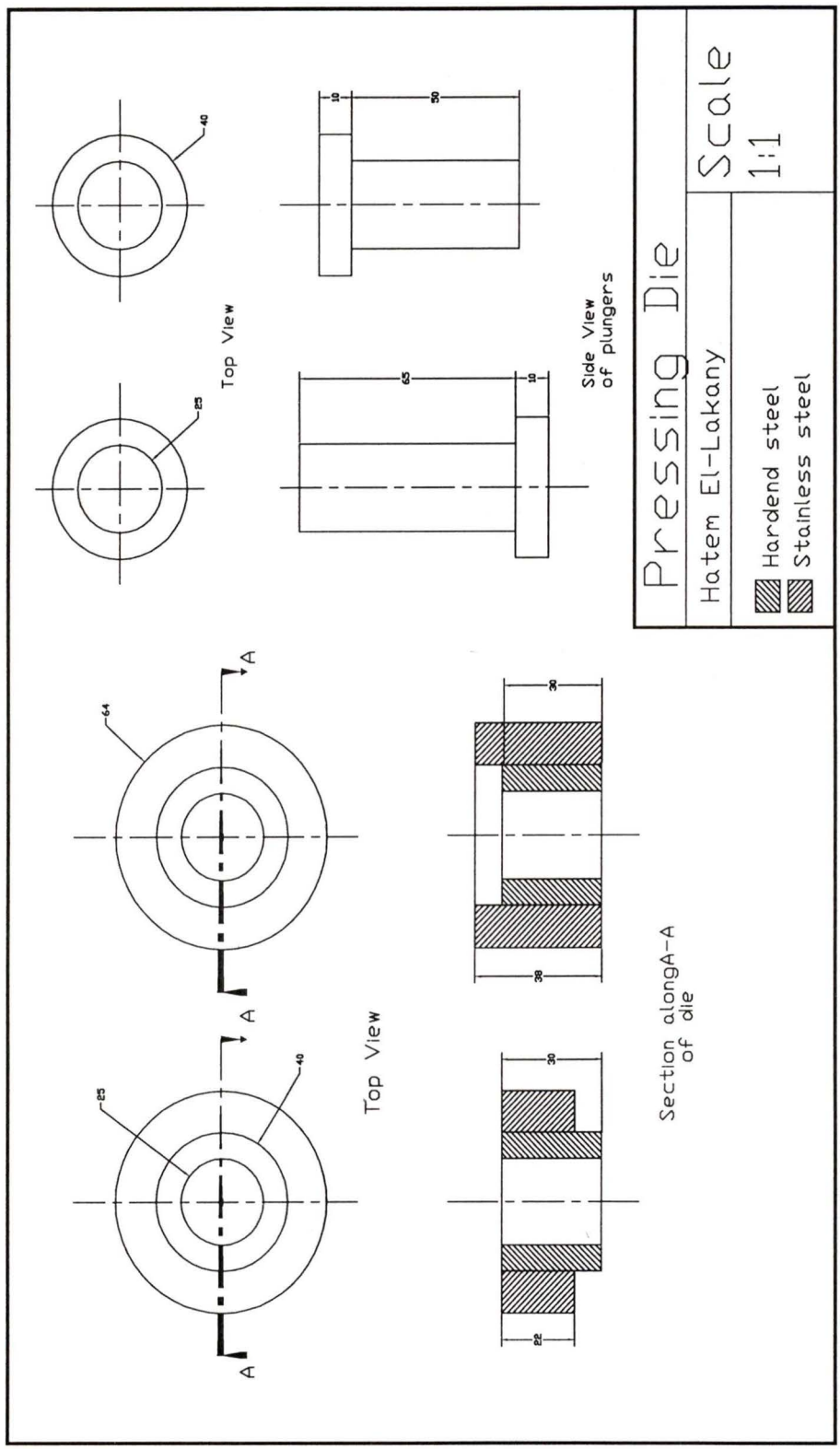

Figure 8.4: Die Drawings

8.2.6 Pressing Equipment and Practice

The press chosen was the 10 ton floor press shown in Figure 8.5. It is equipped with a manual hydraulic pump which can supply up to 99640.22 Newtons of force with a ram range of 3 inches. Its frame is made of steel and has a movable bed-flat to adjust the distance Ht. This press, which was assembled in the laboratory, was the most suitable for the low volume of production and the limited budget of our experimental facility.

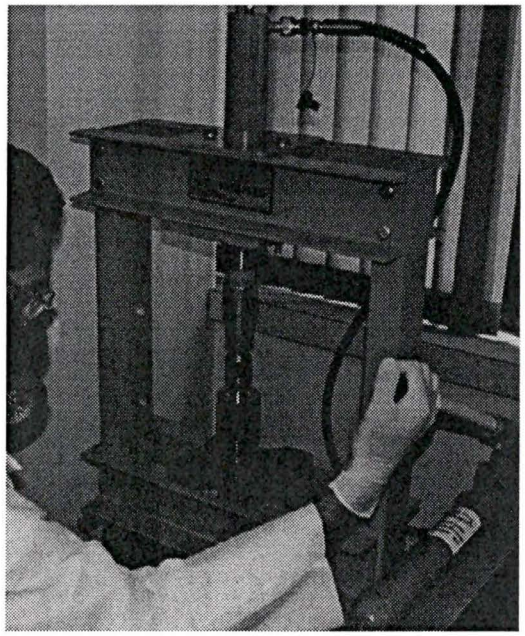

Figure 8.5: The hydraulic press

The following steps are taken during pressing:

1. The powder is weighed according to the desired thickness (H_s) by

$$W_t = H_s \cdot W_f \tag{8.4}$$

where W_f is a weighing factor usually equal to 2 to 3 *g/mm* for PZT

2. The lower plunger and the die are assembled and the powder is poured into the die.

3. The die is jolted to level the powder and then covered with the upper plunger.

4. The pressure is applied for about ten seconds, then released.

5. The upper plunger and top part of the die are replaced by an inverted steel cup. The pressure is applied again until the sample is ejected as shown in Figure 8.6.

6. The green sample is removed and its surface is examined for cracks. The excess powder around its edges is carefully removed.

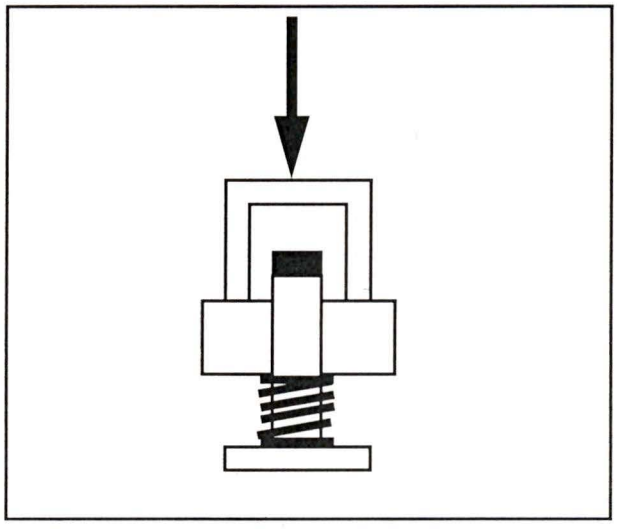

Figure 8.6: Sample ejection mechanism

8.2.7 Data Acquisition and Experimental Results

A spread sheet was prepared to assist the processes of pressing. It uses the intended height and compaction ratio of the sample to calculate the required weight of powder using Equation (8.4). The pressing of batches 9 and 10 was achieved successfully. The processing parameters and results are listed in Spread sheets 8.1 and 8.2. In this spread sheet the pow-

der sample 9 is divided into three disc samples (9.1, 9.2 and 9.3). The actual compression ratio, calculated in the last row, is used as input for the subsequent batches.

Spread Sheet 8.1: Forming of batch 9

Forming

Sample # (Powder)	:	9				
Total Wt Needed (g)	>	43.2				
Sample #	>	9.1	9.2	9.3	Average	Expected
Date	:	22/1/96	22/1/96	22/1/96		
Intended Hight (mm)	:	4.5	4.5	4.5	4.50	
Comp. Ratio (g/mm)	:	2.4	2.4	2.4	2.40	
Required Wt	=	10.8	10.8	10.8	10.80	
					0.00	
Applied Force (Tons)	:	10	10	10	10.00	
Duration (sec)	:	10	10	10	10.00	
Output Wt (g)	:	10.26	10.134	10.4	10.26	
Output hieght (mm)	:	4	4.08	4.22	4.10	
Output Diam. (mm)	:	25.2	25.2	25.2	25.20	
Remarks	!					
Actual Comp. Ratio (g/mm)	>	2.57	2.48	2.46	2.50	

Spread Sheet 8.2: Forming of batch 10

Forming

Sample # (Powder)	:	10				
Total Wt Needed (g)	>	43.2				
Sample #	>	10.1	10.2	10.3	Average	Expected
Date	:	22/1/96	22/1/96	22/1/96		
Intended Hight (mm)	:	4	4	4	4.00	
Comp. Ratio (g/mm)	:	2.7	2.7	2.7	2.70	
Required Wt	=	10.8	10.8	10.8	10.80	
Applied Force (Tons)	:	10	10	10	10.00	
Duration (sec)	:	10	10	10	10.00	
Output Wt (g)	:	9.336	10.432	9.72	9.83	
Output hieght (mm)	:	3.38	3.76	3.48	3.54	
Output Diam. (mm)	:	25.2	25.2	25.2	25.20	
Remarks	!					
Actual Comp. Ratio (g/mm)	>	2.76	2.77	2.79	2.78	

8.3 Densification

Sintering is increasing the density of a pressed powder by firing. Densification occurs by the removal of pores between particles. The objective of sintering is to densify the green sample from about 60% to more than 95% of its theoretical density [3]. This is achieved by solid state sintering at an elevated temperature (1200 - 1300 ^{o}C for PZT) [5]. The resulting PZT ceramic should have an optimal grain size that is controlled by the temperature and duration of firing. This should be achieved with minimum losses of volatile substances (PbO) and without physical damage to the sample such as warpage or bloating [4]. The three stages of the densification process are: pre-sintering, sintering and cooling, as shown in Figure 8.7. Factors affecting them, their parameters and the problems associated with each are discussed in this section.

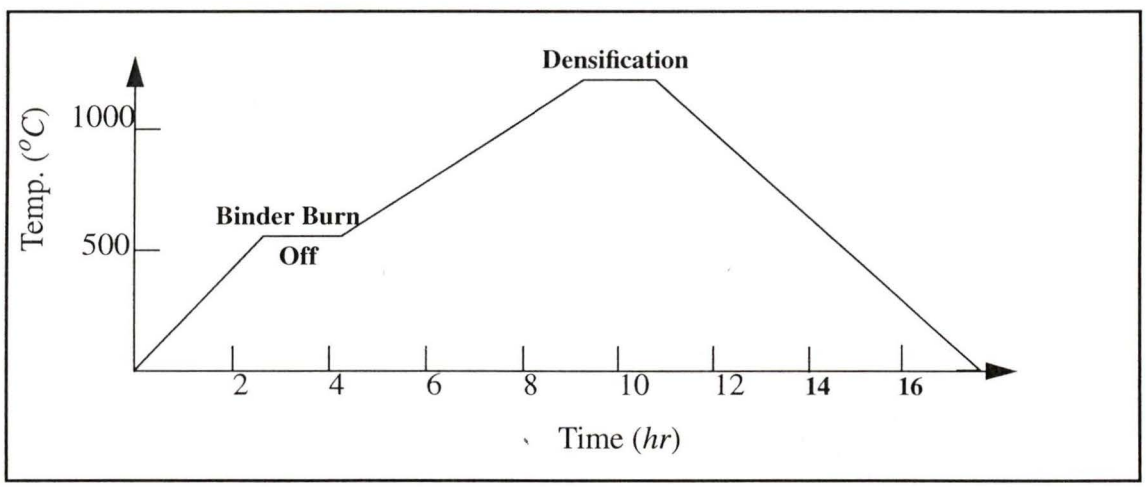

Figure 8.7: Sintering profile

8.3.1 Pre-sintering

Solid-state sintering does not start until the temperature of the ceramic reaches to about one-half to two-thirds of its melting point (670 - 890 ^{o}C for PZT). As the temperature of the ceramic climbs up to these values, several important processes take place during presintering. These processes listed below are controlled by the rate at which the temperature rises [4]:

Drying: The moisture content of the ceramic evaporates at the initial stage of presintering. Thus, it is essential that the initial temperature of the furnace be well below the boiling point of water to avoid damaging the sample.

Additive Burn-off: The burn-off of the PVA binder is the most important objective of presintering. This process is highly dependent on the kind of binder, the nature of the surrounding gas and the porosity of the sample. The adsorbed water evaporates first at temperatures less than 250 ^{o}C [18]. As the temperature increases, the decomposition of PVA takes place up to 600 ^{o}C. This temperature is maintained for about an hour to achieve complete binder burn-off. Stresses could build up in the sample due to differential expansion and gases evolving from the burnout. These stresses can cause the cracking or even fracturing of the sample [4]. Moreover, carbon residue can persist in the sample if the presintering parameters (time, temperature rise rate and atmosphere) are not adjusted carefully [4].

Grain Growth: The beginning of grain growth takes place during presintering. The rate of temperature rise should be slow enough to achieve a large grain size and correct structure. At the same time, this rate should be fast enough not lose too much *PbO*. For PZT, the optimal rate of temperature rise during presintering is about 200 - 300 $^{o}C/hr$, depending on the size of the batch and capability of the furnace.

8.3.2 Sintering

Densification is the main objective of the sintering process. For PZT, it is achieved by raising the temperature of the ceramic and holding it at 1200 - 1300 ^{o}C. The main sintering action is caused by solid state mechanism. Material transport in this mechanism results from diffusion as shown in Figure 8.8. It is driven by the difference in chemical potential or free energy between the free surfaces of particles and their points of contact [4]. This leads to:

- the elimination of pores between atoms,
- the strong bondage between adjacent particles, and
- volume shrinkage.

Note: The success of sintering is measured by the volume shrinkage achieved during the process [4].

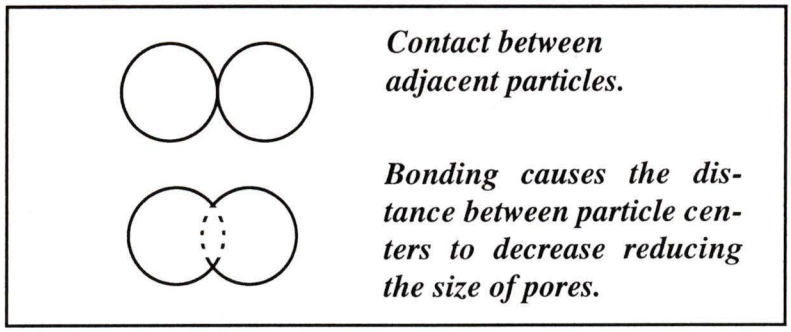

Figure 8.8: Solid state sintering [4]

Factors Affecting Sintering: The efficiency of the sintering process and the quality of the resulting ceramic depend on several factors: The maximum temperature in the furnace and the duration the sample is maintained at this temperature (soaking time). Accurate choice of these firing variables helps eliminate the problems of over- or under-firing. Their values depend on the properties of the particular PZT composition being fired, such as its doping, melting point, volatility, reactivity and the size of the sample. Over-firing or under-firing generally results in inferior mechanical and piezoelectric properties as summarized in Table 8.1 and Table 8.2:

Table 8.1: Problems associated with Over-firing [5]

Problem	**Effects**	**Detection Method**	**Prevention**
Excessive grain growth	Inferior mechanical and electric properties	Examining polished surface under microscope	Fast rate of temperature rise
Loss of volatile constituents (*PbO*)	Improper stoichiometry	Weighting sample before and after firing	Controlling firing atmosphere by adding volatile substance
Reaction with furnace structure	Damaged sample	Chemical examination	Choosing a container and furnace insulation that would not react with the ceramic
Warpage	Twisting of sample	Visual examination	Supporting the sample by Saggers
Bloating	Improper sample shape	Visual examination	

Table 8.2: Problems associated with under-firing

Small grain size	Difficulty in realigning by electric field (poling)	Examining polished surface under microscope	Slow rate of temperature rise
Presence of pores (low density)	Low dielectric strength Impairs piezoelectric quality	Chalky Appearance. Density comparison	

Sintering Atmosphere: The desired atmosphere will inhibit the loss of volatile constituents, so the following precautions are taken:

- The sample is placed in a sealed crucible during firing.
- The sample is surrounded with a setter composed of the same powder to act as an atmosphere donor. Another method is to place a pressed pallet of 70% PbO and 30% ZrO_2 with the sample during firing [26].

8.3.3 Cooling

Cooling is the final stage of sintering, in which the sample is brought down to room temperature. The rate at which this occurs should be fast enough so that the temperature goes below the volatilization point of lead as fast as possible. The cooling rate is limited by the thermal shock resistance of the ceramic, crucible and heating elements.

8.3.4 Sintering Equipment

Sintering is usually carried out in high temperature kilns or furnaces. They consist of an inner chamber insulated by refractory material. The sample is placed on special refractory supports in this chamber. The temperature inside this chamber is raised by applying electric current across heating elements. A list of different heating elements and the temperatures they can reach is given in Table 8.3. The radiant heat emitted from these elements

provides a uniform temperature distribution throughout the samples. PZT should be fired in an electric furnace because it is susceptible to reduction[1] [5]. The furnace chosen for our laboratory was a BS15 electric furnace using silicon carbide heating elements. Its temperature can reach a maximum of 1500 ^{o}C in 8 hours. This temperature and its rate of change are controlled by a UDC 3000 Universal digital controller. The main advantage of this controller is that it can be programed to store and execute heating profiles such as those shown in Figure 7.7 or Figure 8.7.

Table 8.3: Electric furnace heating elements [18]

Element	Maximum Temperature
Metal Alloys	1150°C
Silicon carbide	1550°C
Molybdenum silicide	1650°C in oxidizing atmosphere
Tungsten and graphite	1700°C in inert or reducing atmosphere

Sample Support: The fired ceramic should be positioned so the radiant heat will reach its center. It should also be properly supported to avoid warpage. The material of the container should withstand elevated temperatures and neither melt, deform nor react with the ceramic, setter or the furnace insulation. Recrystallized alumina crucibles are used for this purpose in our laboratory.

1. Reduction is the decrease of the positive oxidation number corresponding to the gain of electrons in an atom or ion [21].

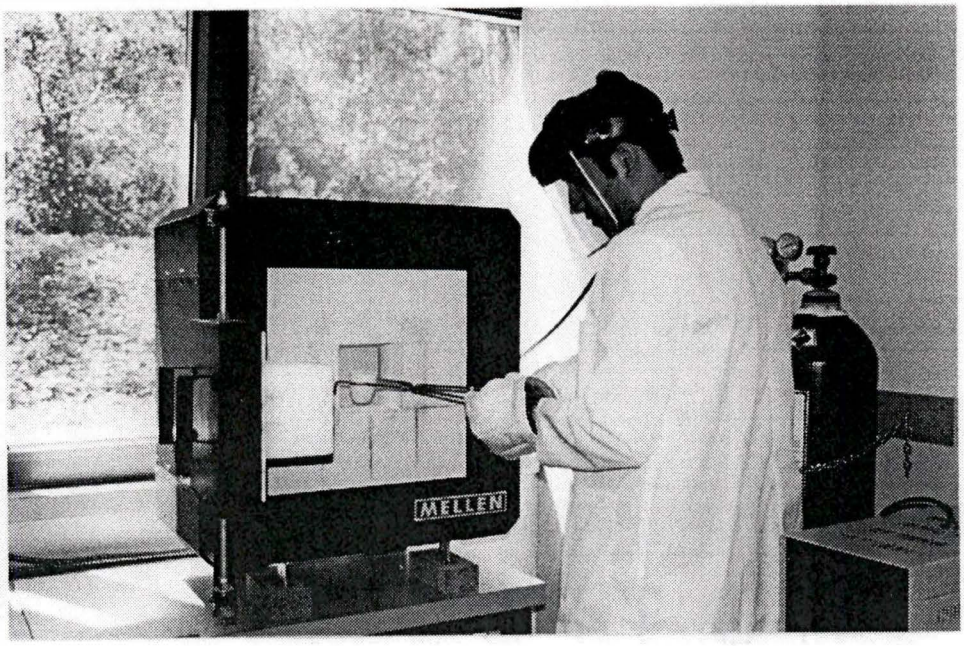

Figure 8.9: Electric furnace

8.3.5 Data Acquisition and Experimental Results

A spread sheet was prepared to assist the densification process. It uses the input soak temperatures and its desired rate of rise to generate the heating profile. The densification process was carried out for batches 9 and 10 using the parameters listed in Spread sheets 8.3 and 8.4. The densification spread sheets are similar to those of calcination but they are divided horizontally into two stages: binder burn off and densification. The data is also listed for three different discs usually fired at the same time. The heating data inputted in the table on the left are used to generate the heating profile shown on the right. This profile is used to program the furnace controller. Each sample's dimensions and weight before and after the operation are used to calculate the densification. The increase in density is a measure of the success of the process. The operation was considered a success because the density achieved in the ceramics of batches 9 and 10 were 95% and 96% of the expected[1]

value respectively, as shown in Figure 8.10, and the samples did not have any visible warpage, bolting, cracks or pores.

Spread Sheet 8.3: Densification of batch 9

Firing

Sample #	:	9.1	9.2	9.3	Average	Expected
Date	:	22/1/96	22/1/96	22/1/96		
Binder Burn Off						
Heating Rate (C/min)	:	7	7	7	7.00	
Hold Temp.(C)	:	630	630	630	630.00	
Duration (min)	:	90	90	90	90.00	
Densification						
Heating Rate (C/min)	:	2	2	2	2.00	
Hold Temp.(C)	:	1250	1250	1250	1250.00	
Duration (min)	:	90	90	90	90.00	
Cooling Rate (C/min)	:	fast	fast	fast	0.00	
Output Wt (g)	:	9.677	9.788	10.4	9.96	
Output Hight (g)	:	3.52	3.54	3.7	3.59	
Output Diameter (mm)	:	21.9	21.9	21.9	21.90	
Remarks	!					
Input Volume (cc)	=	2.00	2.03	2.10	2.04	
Input Desity (g/cc)	=	5.142762	4.980005	4.941171	5.02	
Output Volume (cc)	=	1.33	1.33	1.39	1.35	
Output Density (g/cc)	=	7.298271	7.340279	7.46197	7.37	7.8
Densification %	=	29.53452	32.1551	33.78194	31.82	

Prompt	Function	Segmen	Value
STRT SEG	Start Seg		1
END SEG	End Seg		6
RECYCLES	# Recycles		1
SOAK DEV			0
SEG1RAMP	Ramp Time	1	90.00
SEG2SP	Soak Time	2	630
SEG2TIME	Soak sp	2	90
SEG3RAMP	Ramp Time	3	310
SEG4SP	Soak sp	4	1250
SEG4TIME	Soak Time	4	90
SEG5RAMP	Ramp Time	5	0
SEG6SP	Soak sp	6	50
SEG6TIME	Soak Time	6	1
STATE			
PROGEND			
RAMP UNIT			

Spread Sheet 8.4: Densification of batch 10

Firing

Sample #	:	10.1	10.2	10.3	Average	Expected
Date	:	22/1/96	22/1/96	22/1/96		
Binder Burn Off						
Heating Rate (C/min)	:	7	7	7	7.00	
Hold Temp.(C)	:	630	630	630	630.00	
Duration (min)	:	90	90	90	90.00	
Densification						
Heating Rate (C/min)	:	2	2	2	2.00	
Hold Temp.(C)	:	1250	1250	1250	1250.00	
Duration (min)	:	90	90	90	90.00	
Cooling Rate (C/min)	:	fast	fast	fast	0.00	
Output Wt (g)	:	8.768	9.799	9.183	9.25	
Output Hight (g)	:	3	3.38	3.2	3.19	
Output Diameter (mm)	:	22.22	22.14	22.22	22.19	
Remarks	!					
Input Volume (cc)	=	1.69	1.88	1.74	1.77	
Input Desity (g/cc)	=	5.538003	5.56274	5.600104	5.57	
Output Volume (cc)	=	1.16	1.30	1.24	1.24	
Output Density (g/cc)	=	7.537048	7.530433	7.400424	7.49	7.8
Densification %	=	26.52292	26.12988	24.32726	25.66	

Prompt	Function	Segmen	Value
STRT SEG	Start Seg		1
END SEG	End Seg		6
RECYCLES	# Recycles		1
SOAK DEV			0
SEG1RAMP	Ramp Time	1	90.00
SEG2SP	Soak Time	2	630
SEG2TIME	Soak sp	2	90
SEG3RAMP	Ramp Time	3	310
SEG4SP	Soak sp	4	1250
SEG4TIME	Soak Time	4	90
SEG5RAMP	Ramp Time	5	0
SEG6SP	Soak sp	6	50
SEG6TIME	Soak Time	6	1
STATE			
PROGEND			
RAMP UNIT			

1. The expected values are those listed in literature (see [5] and [6]) and BM 527 manuals.

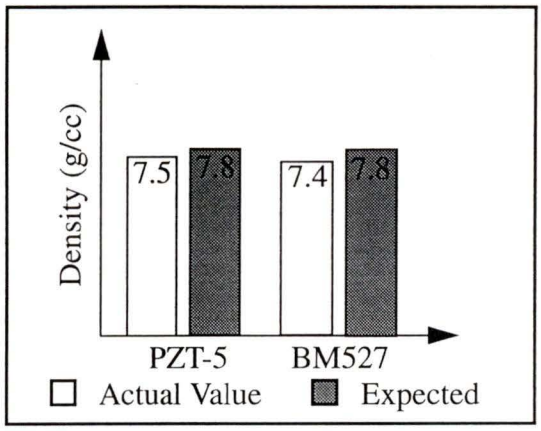

Figure 8.10: Density of resulting ceramics

8.4 Dimensioning and Finishing

8.4.1 Introduction

Finishing is the final step of conventional ceramic processing. Material could be removed from the surface of a ceramic by mechanical, chemical or thermal action. The objective of finishing is to produce a ceramic with:

Smooth Flat Surface that is Free of Flaws: This is required for successful electroding, i.e., to obtain a good contact between the electrode and the ceramic. A flat surface is also crucial in most of our actuation applications such as deformable mirrors.

Tight Tolerances: Most piezoelectric applications require high precision actuating, poisoning or sensing. This can only be achieved by an actuator manufactured to very tight dimensional tolerance.

Very Low Thickness: Some applications require piezoceramics in the shape of very thin plates in the sub-millimeter range. For technical reasons discussed earlier, this kind of thickness cannot be achieved by conventional pressing operations. The required thickness is thus accomplished by machining.

High Mechanical Strength: A ceramic used as an actuator is usually subjected to high stresses and thus the machining should improve (or at least not diminish) its mechanical properties.

The machining of ceramics is a difficult and expensive task because of its hardness and brittleness, especially after firing. A tool that is harder than the ceramic must be used to remove material from its surface without overstressing it. The most common method of machining ceramics is the use of high precision surface grinding machines with abrasive particles such as SiC, Al_2O_3 or industrial diamonds as cutting tools.

8.4.2 Grinding Mechanism

Grinding is achieved by the action of mounted abrasive particles sliding against the ceramic surface as shown in Figure 8.11. This results in the following effects:

- The removal of material directly in the particle's path due to the high stress and temperature. The resulting grooves in the surface of the ceramic account for most material removal.
- Plastic deformation of the material adjacent to the groove is caused by the compressive force of the abrasive particles.

7. Machining also causes cracks, which reduces the strength of the ceramic [4].

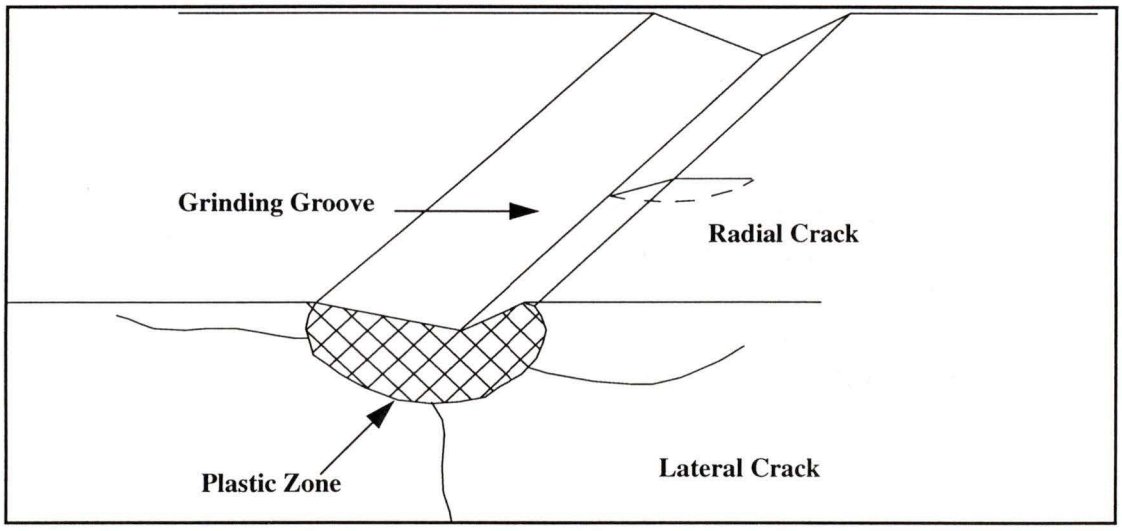

Figure 8.11: Schematic diagram of the effects of surface grinding

In surface grinding, the material removal rate depends on:

- the grain size and hardness of the ceramic,
- the size, density and hardness of the grinding media, and
- the grinding time.

8.4.3 Grinding Equipment

The surface grinding machine used in our laboratory is shown in Figure 8.12. It is driven by a motor which rotates an interchangeable grinding disc. Two 8" industrial diamond grinding discs are used: a 125 μm for roughing and a 74 μm for final finishing. The sample is bonded to a thick glass disc and placed between it and the grinding media. The glass disc is continuously rotated and swayed by the U-shaped arm while the grinding disc rotates in the opposite direction.

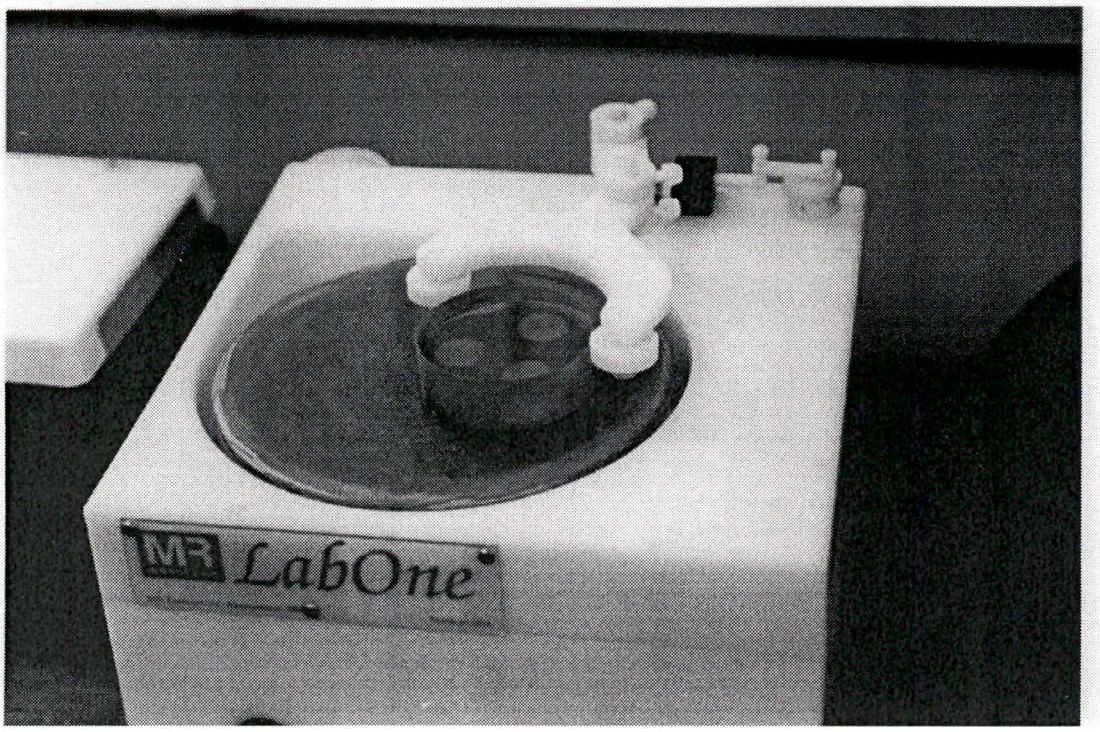

Figure 8.12: Surface grinding machine

9 Piezoelectric Processing

9.1 Introduction

The final stage of processing PZT is transforming the ordinary ceramic into a piezoelectric actuator. Piezoelectric processing starts by the application of a thin layer of metal on its surface to act as electrodes. The next step is inducing the piezoelectric effect in the ceramic by applying a high electric field to realign its dipoles. This process is called "poling", and it is the most critical step in processing piezoelectric ceramics. Finally, the ceramic elements are assembled according to the application they are intended for. In practice, the order of electroding, poling and assembly can be changed according to the application.

9.2 Electroding

For a ceramic disc to be used as an actuator, its two faces must be covered by electrodes as shown in Figure 9.1. Typically, a thin layer of silver in paste or dispersed liquid form is applied to the ceramic. It is then sintered at $500^{o}C$ to form a continuous, uniformly conductive and closely bonded layer. Temporary electrodes can be used if the application calls for a poling direction different from the driving direction [5]. The functions of electrodes are:

- applying a uniform electric field across the ceramic during poling,
- applying the driving electric signal when the ceramic is used as an actuator, and
- conducting the output potential if the ceramic is used as a sensor.

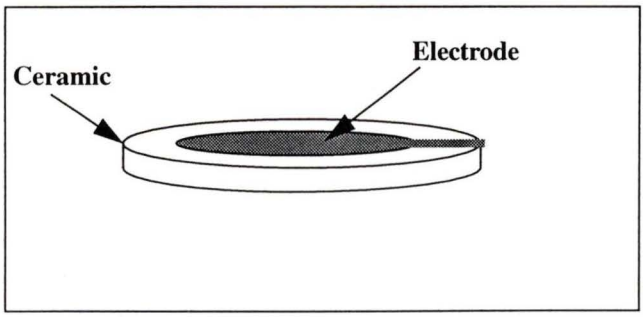

Figure 9.1: Schematic diagram of an electroded ceramic sample

9.2.1 Electrode Material

The material chosen as an electrode should have the following qualifications:

- It should adhere strongly to the ceramic surface. An air gap acts as a low valued series capacitor that reduces the effective capacitance of the ceramic transducer.
- It should be applicable as very thin film while maintaining its chemical and physical durability under cyclic electrical and mechanical loading.
- Low (practically zero) electrical resistance is another essential property.
- It should also be easy to solder lead on the electroding material.

The most commonly used electrode material are:

- Silver.
- Fired on gold, platinum or palladium.
- Vacuum-evaporated gold or platinum.
- Electroless nickel or copper.

9.2.2 The Application of Silver Electrodes

Silver can be applied to a ceramics in a variety of ways depending on their number, shape, size, surface quality and application. For the flat surface of a disc, one method is to apply the liquid silver by spray painting as shown in Figure 9.2. More accuracy and uniformity can be achieved by applying silver paste using a print-screen. For more complicated shapes such as tubes, dipping is used. Great care must be given to the prevention of paint leakage to the side of a sample. This could cause a short circuit during poling.

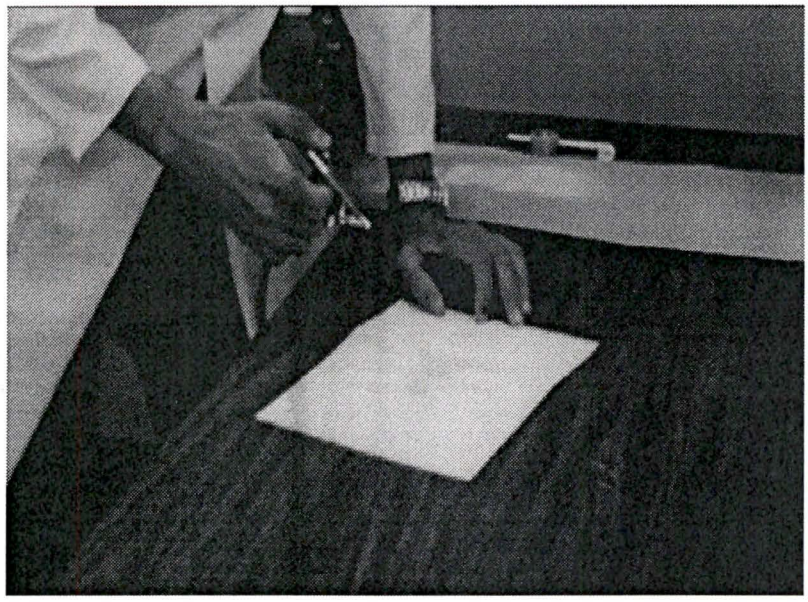

Figure 9.2: Spray-painting silver electrodes

9.3 Poling

In this critical process, a strong electric field is applied to the ceramic to reorient its dipoles and give it piezoelectric properties. The theoretical background behind poling is discussed in details in Section 2.2.2 on page 7. Optimum piezoelectric properties are achieved by correct adjustment of the poling conditions. These conditions along with the processing procedure and the equipment used in poling PZT are presented in this section.

9.3.1 Poling Conditions

Successful poling can only be achieved under special conditions. These conditions should be adjusted according to the composition (specially doping), breakdown strength and application of the ceramic. These conditions are the:

- electric field strength, i.e. voltage per unit thickness of ceramic,
- direction of the electric field,
- duration it is applied, and
- the temperature at which it is applied. Generally, the poling field required decreases with the temperature increase [5].

These conditions are optimized to obtain the highest piezoelectric properties. The electric field should be higher than the coercive field of the ceramic. It is limited by the dielectric strength of the sample which depends on its composition, porosity, thickness and shape. Generally, the breakdown voltage of a ceramic disc can be calculated from the following empirical formula [5]:

$$E = ct^{-0.39} \tag{9.1}$$

where E is the breakdown voltage in *KV/cm*, t is the thickness in *cm* and c is an experimentally determined constant

9.3.2 Poling Problems

Numerous problems are usually faced during the poling process. The following table lists some of these problems and the suggested solutions:

Table 9.1: Poling problems and their solutions

Problem	Solved by
Low dielectric strength of air	Poling in an oil bath
Dielectric breakdown of sample	Avoiding cracked, porous and very thin samples
Deformation up to 0.2% in PZT, which can lead to mechanical failure [5]	Avoiding curved and thick walled tube samples

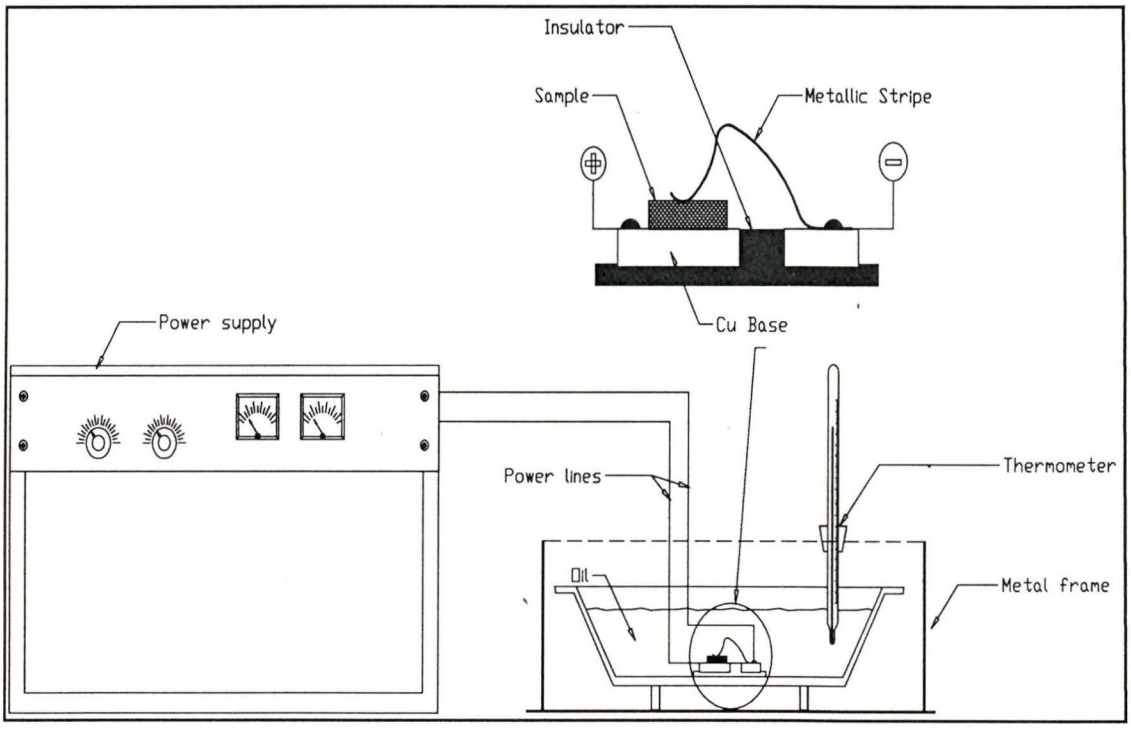

Figure 9.3: Schematic drawing of the poling setup

9.3.3 Poling Equipment

As seen in the Figure 9.3, the poling setup consists of the following equipment:

Clamp: It is used to support the disc-shaped sample and apply the poling electric field. It consisted of a copper metallic base connected to the power supply and insulated from the pot. The base is also insulated from a flexible metallic strip. This strip is connected to the ground and holds the sample in place. The connections to the power supply are two water-proof high voltage cables. The clamp material should be a very good conductor of electric current and stable under high temperature. Copper was found to be the most suitable material for this application. The advantage of this locally designed and manufactured clamp is that it can accommodate many samples of different shapes and sizes.

Power Supply: It provides the electric field necessary for poling. The power supply chosen is an Acopian high voltage model with the following features:

- It can supply a maximum potential difference of 20 *KV,* which means it can pole samples up 8 *mm* in thickness at 25 *kV/cm.*
- It possesses controls over the voltage and current as well as gages to show their values.

Oil Pot: This pot acts as a container for holding the oil and as a heat source to raise its temperature. It must be able to raise and control the temperature of the oil to that required for optimal poling (approximately 120 ^{o}C for PZT). It must also be made of a material that is stable under high temperature, so as not to contaminate the sample. A common cooking pot can be used because it satisfies these requirements and is readily available in stores.

Thermometer: It is used to measure the temperature of the oil (up to 150 ^oC).

9.3.4 Poling Practice

A typical poling setup is shown in Figure 9.3 in which the following steps are taken to pole PZT:

1. The electroded ceramic sample is fitted in the clamp.
2. The upper and lower poles of the clamp are connected to those of a high voltage power supply.
3. The clamp is submerged into the oil-filled pot. This oil must have a high dielectric strength at elevated temperatures.
4. The oil is heated until it reaches the temperature of optimal poling (120 ^oC *for PZT).*
5. An electric potential of 25 *kv/cm* is then applied for 20 to 30 minutes.
6. The sample is then carefully[1] removed and dried.

9.4 Assembly And Configuration

Most piezoelectric applications require the assembly of several piezoelectric ceramic elements in a certain configuration. Section 5.4 on page 50 describes some of these configurations. In this section, we will see how piezoceramic elements are connected to form these designs. After a design is chosen, the assembly process is usually divided into two parts:

1. Bonding of the elements in certain configurations using special adhesives.

---

1. The sample might hold a very high charge, so it must be shorted before being handled.

2. Placing them in a casing to provide protection from the environment. This is especially important as the case insulates the ceramic from the temperature rise and/or fluctuation outside. As discussed earlier, a stable moderate operating temperature is essential for reducing inaccuracies.

9.4.1 Adhesives

For configurations using multiple elements, such as stacked actuators, a bonding agent is needed to fix them together. The adhesives used in bonding piezoelectric ceramic should be:

- very good conductors of electric current,
- as thin as possible when applied,
- mechanically durable under repeated loading,
- electrically and chemically stable under high voltages and temperatures, and
- provide strong adhesion between the ceramics [5].

9.5 Experimental Results

The six ceramic samples of batches 9 and 10 were electroded and poled successfully. Their electroding and poling parameters are listed in Spread sheets 9.1 and 9.2.

Spread Sheet 9.1: Electroding and poling of batch 9

Electroding

Date	:	23/1/96	23/1/96	23/1/96		
Paint type	:	silver	silver	silver		
Firing Temp.	:	500	500	500	500.00	

Poling

Date	:	24/1/96	24/1/96	24/1/96		
Electric Field (KV/cm)	:	25	25	25	25.00	
Duration (min)	:	20	20	20	20.00	
Applied Volage (KV)	=	8.8	8.85	9.25	8.97	

Spread Sheet 9.2: Electroding and poling of batch 10

Electroding

Date	:	23/1/96	23/1/96	23/1/96		
Paint type	:	silver	silver	silver		
Firing Temp.	:	500	500	500	500.00	

Poling

Date	:	24/1/96	24/1/96	24/1/96		
Electric Field (KV/cm)	:	25	25	25	25.00	
Duration (min)	:	20	20	20	20.00	
Applied Volage (KV)	=	7.5	8.45	8	7.98	

10 Characterization

10.1 Introduction

Characterization is the measurement of various properties of processed piezoceramics. These properties, such as the piezoelectric coefficient (d_{33}) determine how the ceramic will perform as an actuator. Characterization plays an important role in both the research and mass-production of piezoceramics. This is because processing piezoceramics is a very delicate process which involves many variables. These variables are difficult and sometimes impossible to control. For example, any change in the quantities or type of impurities in the raw material can tremendously alter the properties of the processed ceramics. Also, their nonlinear nature and absence of precise theoretical modeling makes experimental determination of their properties essential. Consequently, each sample is characterized during and after processing in order to:

- reject any sample that does meet the customer's specifications, and
- provide the customer with the specific properties of each ceramic. This is especially important in high precision applications which constitute a large segment of the piezoceramics market.

Moreover, characterization is very important as a research tool. It is much more elaborate and involves the determination of some properties that are not usually required by customers. In a research setting, characterization is used as feedback to improve the properties and reproducibility of piezoceramics. In our research, actuation is the primary interest, so properties that indicate how a ceramic acts as an actuator are emphasized. These include

the physical, electrical, mechanical and most importantly piezoelectric properties. In this section, the equipment used in measuring these properties and their theory of operation are discussed.

10.2 Choosing Characterization Equipment

For characterization equipment to function efficiently in a research or industrial setting, they must have the following assets:

Versatility: Piezoceramics are manufactured in different shapes and sizes. Characterization equipment should be able to perform tests on as many configurations as possible without affecting the accuracy of measurements. This concern is usually addressed in the design of the clamping devise. Another aspect of versatility is the ability of the equipment to measure several properties without much modification.

Accuracy and Reliability: The extent of the required accuracy is determined by the application of the ceramics. Most piezoceramics are used for high precision applications, therefore great emphasis is put on the reliability of the equipment.

Ease of Operation: Simplicity is preferred for characterization equipment, especially in industry. This is due to the high cost of skilled labor. Simplicity of operation includes ease of loading, unloading, and straight-forward readings[1].

1. Some readings require extensive calculations. This is not desirable in an industrial setting.

Compatibility with Industrial Standards: There are several industrial standards for characterizing piezoceramics. However, the most popular are those of the IRE[1], so the selected equipment and calculations must adhere to these standards.

10.3 Physical Measurements

Certain properties of a ceramic are determined to evaluate the physical effect of processing and for use in other calculations. These physical properties and the method they are evaluated in our laboratory are presented in this section.

10.3.1 Size and Shape

Accurate measurement of the dimensions of a sample (mainly radius and thickness) is performed by a high precision (0.02*mm* accuracy) caliber. The shape of the sample is also scrutinized by measuring the parallelism of its surfaces.

10.3.2 Weight and Density

As mentioned previously, the density of a ceramic measures of the success of firing and is directly proportional to the strength of the piezoelectric effect. The actual density is also used in the calculation of some other properties. There are two methods of measuring density which are the dry and wet methods. The former is simply measuring the weight of the sample in air and dividing it by the volume (calculated from its dimensions). This method is adequate for samples of simple shapes but a more accurate method is needed for more complicated shapes. The wet method is used to avoid the inaccuracies associated with vol-

1. IRE Standards on Measurement of Piezoelectric Ceramics, 1961 are listed in [5].

ume measurements. It involves measuring the weight of the sample in air (W_a) and in water (W_w) [28]. Since

$$W_w = m_s g - \rho_w V_s g \tag{10.1}$$

where m_s and V_s are the mass and volume of the sample therefore, the density is calculated by using

$$\rho_s = m_s / V_s = \frac{W_a / g}{(W_a - W_w)/\rho_w g} = \frac{W_a \rho_w}{W_a - W_w} \tag{10.2}$$

where ρ is in g/m^3 and W is in grams

10.3.3 Grain Size

After densification, the grain size of a ceramic can be measured under a microscope. We have previously discussed the use of optical microscopy in the evaluation of particle size. The only difference here is in the preparation of the sample. Fired ceramics have to be polished or etched before being examined.

10.3.4 Composition

The composition of a fired ceramic can be evaluated by X-ray diffraction. X-rays are electromagnetic radiations of a wavelength much shorter than that of light. They are produced by colliding high-speed electrons with a metal target.

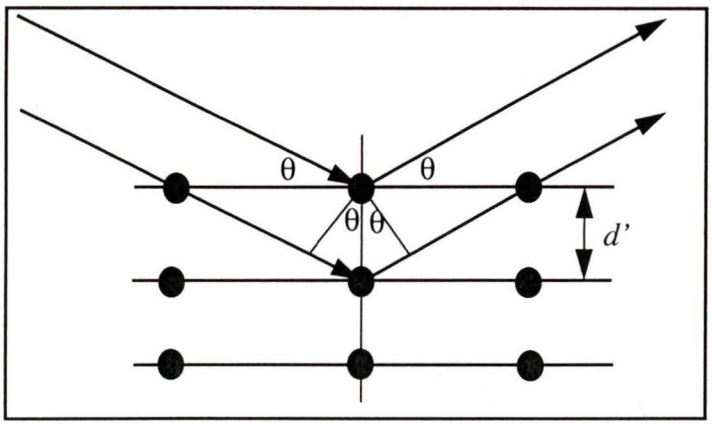

Figure 10.1: Diffraction of X-rays by crystals

X-rays of known wavelength ($\lambda = 0.5$-2.5 Angstroms) are diffracted by crystals if the conditions stated in Bragg's law, Equation (10.3), are met as illustrated in Figure 10.1 [19].

$$n\lambda = 2d' \sin\theta \qquad (10.3)$$

where n = 1, 2, 3.....

When subjecting a material made of crystals to X-rays, the result is a graph such as that shown in Figure 10.2. Each crystal shows different X-ray intensity peaks at certain angles. These angles are recorded and inputted into Spread sheet 10.1 which calculates the distance *d'*. This distance is characteristic of each compound depending on the crystal structure of its phases. Consequently, its composition can be identified by comparing the results to those of the suspected compounds.

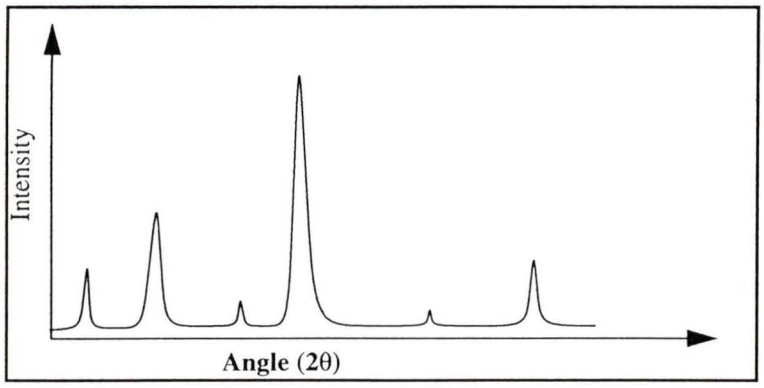

Figure 10.2: X-ray diffraction output

Spread Sheet 10.1: X-ray diffraction calculations

Phase		PbZr52Ti4		PbO		PbTiO3		Pb2TiZrO		PbZrO3	
Lambda		1.5418		1.54059		1.5418		1.9373		1.7902	
2 Theta:	Theta(rad)	d=	Match=	d=	Match=	d	Closest	d	Closest	d	Closest
21.4	0.18675	4.15207	4.146	4.1488		4.15207		5.21715		4.82101	
28.6	0.249582	3.12107		3.11861		3.12107		3.92168		3.6239	
29.2	0.254818	3.05829		3.05588		3.05829		3.84279		3.55101	
30.9	0.269653	2.8938	2.89	2.89152		2.8938		3.63611		3.36002	
38.2	0.333358	2.35592	2.351	2.35407		2.35592		2.96026		2.73549	
42.4	0.37001	2.13177		2.13009		2.13177		2.67861		2.47522	
43.7	0.381354	2.07132	2.073	2.06969		2.07132		2.60265		2.40503	
46.7	0.407534	1.94501		1.94349		1.94501		2.44395		2.25838	
49.2	0.429351	1.85188	1.844	1.85042		1.85188		2.32691		2.15023	
54.6	0.476475	1.6808		1.67948		1.6808		2.11196		1.9516	
54.8	0.47822	1.67514	1.677	1.67383		1.67514		2.10485		1.94502	
55.2	0.481711	1.66395		1.66264		1.66395		2.09078		1.93203	
64.2	0.560251	1.4507		1.44956		1.4507		1.82283		1.68442	1.681
68.2	0.595157	1.37504	1.38	1.37396		1.37504		1.72776		1.59657	

Experimental Results: An X-ray diffraction test was conducted on the PZT-5 ceramic processed in our laboratory. The results listed in Spread sheet 10.1 show the close similarity to the profile of $PbTi_{0.48}Zr_{0.52}O_3$ extracted from a material database. No significant matches were found in the literature with other suspected compounds such as $PbTiO_3$ or PbO.

10.4 Electrical Measurements

10.4.1 Capacitance (*C*)

As dielectric materials, piezoceramics have high capacitance which has to be determined, especially in high frequency applications. Furthermore, its value is used in the calculations of other mechanical and piezoelectric properties. Capacitance is measured using a BK Precision 810A digital capacitance meter. The sample is clamped in the same clamp used for the resonance measurements.

10.4.2 Dielectric Constant (ε)

The relative dielectric constant is the ratio between the charge developed on the electrodes of a material to that developed across vacuum when they are subjected to the same voltage [5]. It can be calculated from the electrode area (*A*), thickness (*t*) and capacitance (*C*) of the sample using [26]

$$\varepsilon = \frac{Ct}{0.08854A} = \frac{14.38Ct}{D^2} \tag{10.4}$$

where ε is dimensionless ratio, C is in pF, t and diameter D in cm

10.5 Piezoelectric Measurements (Resonance Method)

An effective method of evaluating the electromechanical coupling factor (*k*) is the resonance method. In this technique, the characteristic frequencies are determined by applying an alternating current to a piezoceramic of specific shape and size (usually thin disks). The frequency is changed and the phase difference[1] is monitored to determine the resonance

1. The phase difference is between the voltage on the ceramic and that on the resistance R_c.

and antiresonance frequencies (f_r and f_a). These frequencies and the dimensions of the sample are used to calculate the coupling factor (k) of the material.

10.5.1 Theoretical Background

The piezoelectric effect can excite elastic waves in a ceramic. These waves manifest the interaction between the mechanical resonance and the electric behavior. The behavior of a piezoceramic can be approximated by the circuit shown in Figure 10.3 as long as:

- the input frequency is close to its resonance frequency, and
- the parameters of the circuit (C_1, C_o, R and L) are independent of the input frequency. This occurs when there are no other vibrational modes near the one of interest.

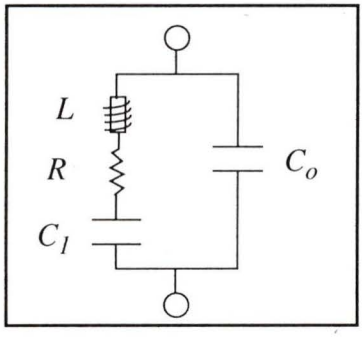

Figure 10.3: Equivalent circuit near resonance

At f_r the total impedance of the first branch is equal to the relatively low mechanical resistance (R). This is because the impedances caused by L and C_1 are equal in magnitude and opposite in direction as shown in Equation (10.5). In this case, R is in parallel with the electric capacitance (C_o), so the circuit exhibits minimum impedance. This is called the resonance frequency and it corresponds to zero-field conditions. As the input frequency increases, the first branch becomes inductive. Maximum impedance (anti-resonance) will

occur when its series impedance is equal and opposite to the impedance caused by C_o [6]. This state of parallel resonance corresponds to open-circuit conditions. This pattern will be repeated again as the sample goes through other resonance modes as shown in Figure 10.4.

$$\text{at } f_r: \qquad 2\pi f_r L = -\frac{1}{2\pi f_r C_1} \qquad (10.5)$$
$$Z_1 = R$$

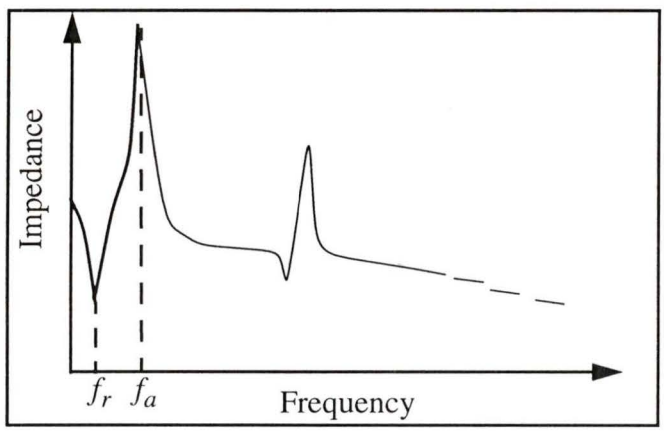

Figure 10.4: Characteristic frequency measurements[1]

The coupling factor can be related to the characteristic frequencies by the elastic compliance at zero-field and open-circuit conditions. It is calculated from the characteristic frequencies of the primary mode and the sample shape factors. For example, the coupling factor of a piezoceramic disc can be calculated using [26]

1. This plot is a reproduction of results obtained on an impedance analyzer for a PZT disc obtained with the permission of the BM Hi-Tech company in Collingwood.

$$1/k_{33}^2 = 0.405\left[\frac{f_r}{f_a - f_r}\right] + 0.810 \qquad (10.6)$$

where k_{33} is a dimensionless ratio and f is in KHz

10.5.2 Measurement Setup

Sample Shape: A ceramic disc of diameter at least six times its height is usually chosen because [5]:

- it shows strongly exited modes,
- a homogeneous disc will have fundamental radial resonance free from interfering modes, and
- they can be easily and cheaply manufactured.

Connections: The equipment needed for measuring the characteristic frequencies of a ceramic are: a function generator, clamp and oscilloscope. The function generator should have an output impedance lower than the minimum impedance of the piezoceramic. The oscilloscope is used to show phase difference between the output signals. The equipment is connected as shown in Figure 10.5 [26].

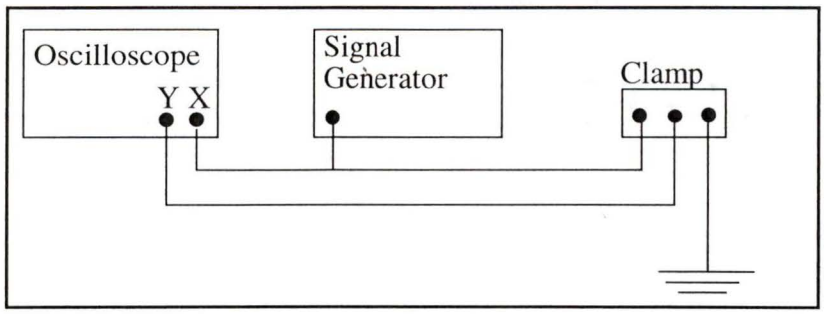

Figure 10.5: Connection of Characteristic frequency measuring equipment

The clamp: As shown in Figure 10.6a, it applies the input alternating current to the specimen and resistance. To obtain accurate measurements, the design of the clamp should not change the mechanical characteristics of the sample.

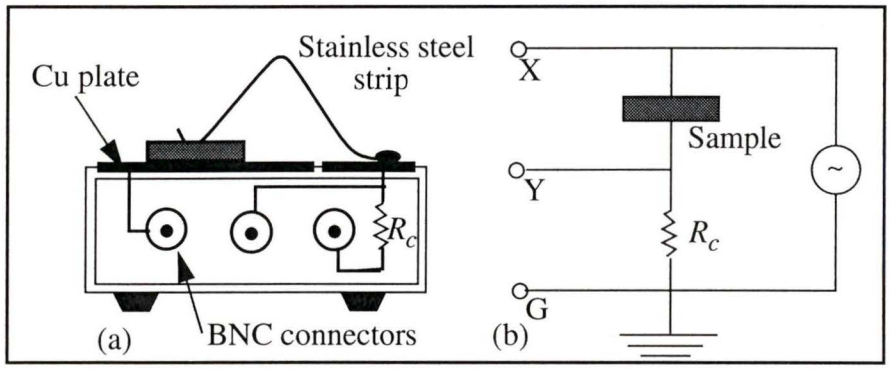

Figure 10.6: Clamp design a) implementation b) electric circuit

Measurement Procedure: After the equipment is connected, the frequency is set to a low value of about 100 *Hz*. The sample will act as a capacitance, so the oscilloscope will show an ellipse. The ellipse, shown in Figure 10.7a, is a result of a phase difference between the two signals. The input frequency is then gradually increased. At the resonance frequency the sample acts like as a resistance, so the phase angle diminishes to 0^{o}. Thus, the ellipse narrows down to a single line at 45^{o}, as shown in Figure 10.7b. At the frequency of anti-resonance, the voltage across the resistance will diminish. This is because the sample impedance will be very high compared to that of R_c. The output appears as a single horizontal line on the oscilloscope screen, as shown in Figure 10.7c [26].

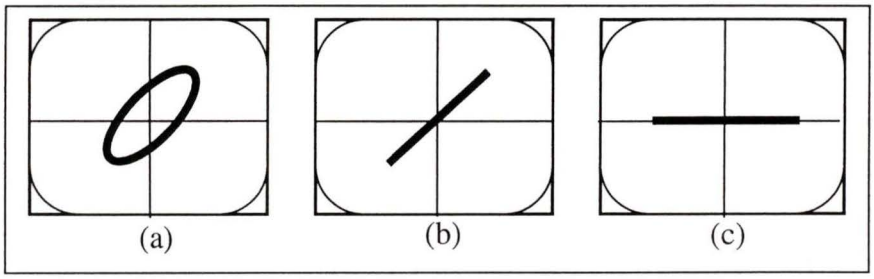

Figure 10.7: Oscilloscope in X-Y mode a) All other frequencies b) Resonance c) Anti-resonance

10.5.3 Alternative Method (Impedance Analyzer)

A more accurate method of determining the characteristic frequencies is to use an impedance analyzer. In this case, the characteristic frequencies can be readily read on a graph of the frequency versus impedance such as that shown in Figure 10.4.

10.6 Piezoelectric Coefficient (d_{33}) Measurement

As mentioned previously, the piezoelectric coefficient (d) is the most important measure of the piezoelectric effect. It is defined as ratio between the applied stress and the resulting dielectric displacement. The most important of these coefficients for our actuator applications is d_{33}. It is the measure of the indirect effect which represents the displacement of an actuator in an electric field. There are several ways of measuring the coefficient d_{33}, but we choose the Berlincourt type for its simplicity, versatility and accuracy.

10.6.1 Theory and Operation

The force head part of the "d_{33} Tester" applies an oscillating low frequency force which places the specimen under the stress (T_3). A high accuracy voltmeter measures the voltage

across its electrodes (V). From the constitutive equation listed in Section 2.4.2 on page 17, we can express the piezoelectric coefficient as:

$$d_{33} = \left[\frac{\delta D_3}{\delta T_3}\right]_E$$
$$d_{33} = \frac{Q/A}{F/A} = \frac{Q}{F} = \frac{CV}{F} \tag{10.7}$$

where A is the area stressed by the force F, C is the capacitance and V is the voltage generated.

Simplification: The need for measuring the capacitance is avoided by placing two identical capacitors in parallel with the sample and "standard". These capacitors have a much greater capacitance than that of the sample and standard. This will also decrease the effect of stray capacitance on the output [27].

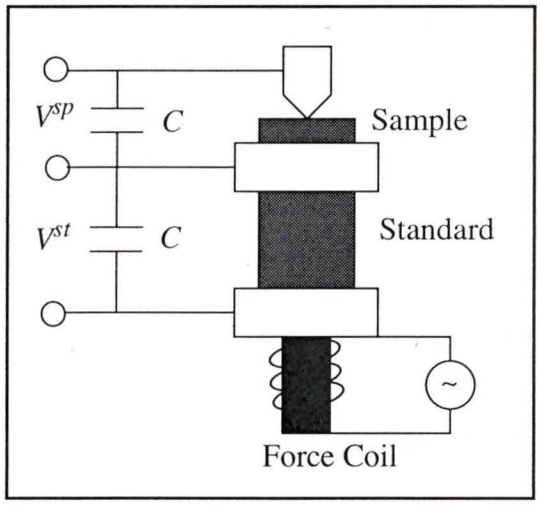

Figure 10.8: Force head construction

In order to simplify the calculations further, the same force is applied across the standard piezoelectric sample of known d_{33} in series with the sample being tested as shown in Figure 10.8. The magnitude of the force, which is equal on both ceramics, can then be adjusted so that the voltage across the standard is equal to its known d_{33}. In this case, the

ratio of capacitance to force is set to one. Since the sample has the same capacitance, the voltage across its poles will therefore be equal to its d_{33} as shown in Equation (10.8) [27].

$$\begin{aligned} d_{33}^{st} &= \frac{CV^{st}}{F} \\ \text{if} \quad & C/F = 1 \\ \text{then} \quad & d_{33}^{sp} = V^{sp} \end{aligned} \tag{10.8}$$

where d_{33} is in C/N x 10^{-12} and V is in Volts

10.6.2 Construction and Operation

The d_{33} tester setup consists of four main parts connected by BNC cables as shown in Figure 10.9. The frequency generator supplies a sinusoidal alternating current of a nominal 200 KHz frequency at a low amplitude. This signal is amplified and controlled in the main box then fed to an electromagnet (force coil). The voltages across the sample and standard (V^{sp} and V^{st}) are directed back to the main box. Using the main box, the d_{33} of the sample is measured by:

- directing the voltage V^{st} across the standard to the multimeter (DMM),
- changing the magnitude of the input force until the DMM shows the d_{33} of the standard, then
- switching the DMM reading to show the voltage across the sample V^{sp} which is its d_{33}.

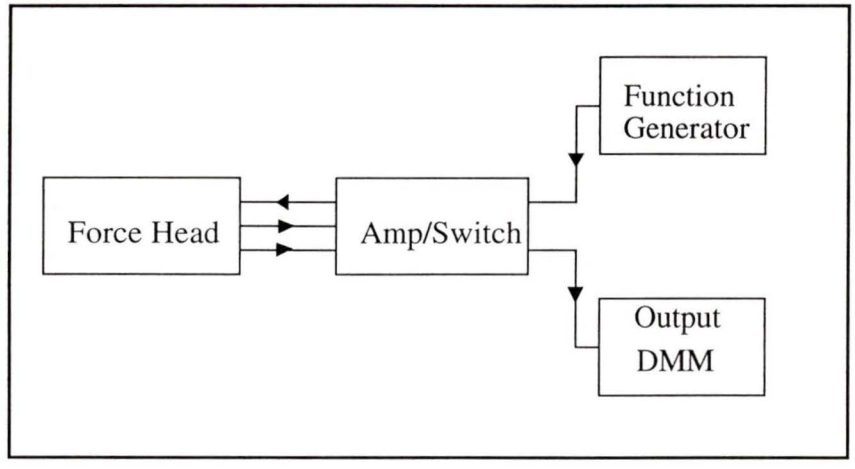

Figure 10.9: Layout of the d_{33} tester

10.7 Experimental Results

All the characterization techniques discussed in this chapter were applied to batches 9 and 10 ceramic samples. The results were entered into Spread sheets 10.2 and 10.3 which performs the required calculations. The average piezoelectric coefficient (d_{33} in C/N x 10^{-12}) measured for both batches was very close to the values listed in literature for PZT-5 and in the BM527 manual indicating the success of processing. The dielectric constant (ε) calculated using Equation (10.4) was also close to the expected value. On the other hand, the electromechanical coefficient (k_{33}) was 83% of the expected value for both ceramics. This is probably due to a slight deviation from stoichiometry caused by excessive loss of lead oxide during densification. Another important note is that sample 9.2 did not show an anti-resonance frequency. This was probably due to an internal crack that occurred during firing or poling.

Spread Sheet 10.2: Characterization of batch 9

Charachterization

Sample #	:	9.1	9.2	9.3	Average	Expected
Date	:	25/1/96	25/1/96	25/1/96		
Fr (Hz)	:	88.8	93.7	90.1	90.87	
Fa (Hz)	:	105.4		105.2	105.30	
Piezoelectric Coff d33	:	474	479	490	481.00	480
Capacitance C (nFr)	:	2.36		2.08	2.22	
Fa -Fr	=	16.6		15.1	15.85	
K33	=	0.61005		0.584114	0.60	0.72
E Youngs Mod (N/m2)	=	6.13E+09		6.45E+09	4.2E+09	
Dielectric Const.	=	2490.722		2307.468	2399.10	2750

Spread Sheet 10.3: Characterization of batch 10

Charachterization

Sample #	:	10.1	10.2	10.3	Average	Expected
Date	:	25/1/96	25/1/96	25/1/96		
Fr (Hz)	:	90	89.7	89.5	89.73	
Fa (Hz)	:	105.1	104.6	104.4	104.70	
Piezoelectric Coff d33	:	365	384	372	373.67	374
Capacitance C (nFr)	:	1.96	1.74	2.01	1.90	
Fa -Fr	=	15.1	14.9	14.9	14.97	
K33	=	0.584375	0.58203	0.582553	0.58	0.7
E Youngs Mod (N/m2)	=	6.69E 09	6.59E 09	6.5E 09	6.59E 09	
Dielectric Const.	=	1712.569	1725.32	1873.341	1770.41	

11 Conclusion

11.1 Introduction

This chapter is an overview of the research effort at-hand. It gives a brief recount of the achievements and some obtained results of this research. Then it introduces the problems encountered during the experimental phase. Several suggestions on how to improve the processing and characterization facilities in our laboratory are then offered along with suggestions for future work.

11.2 Contribution

11.2.1 Theoretical Study of Piezoelectricity

A comprehensive literature survey was conducted on the subject of piezoelectricity with special emphasis on piezoceramics. The following points were examined and documented in detail:

- The understanding of the piezoelectric effect in atomic scale.
- The derivation of governing equations (linear and non-linear).
- The relevant piezoelectric material physical, mechanical, electrical and piezoelectric properties (e.g. the piezoelectric constant d_{33}).
- The design and properties of piezoceramics actuators.
- Sources of inaccuracy in their operation and methods of avoiding and/or correcting them (e.g. Hysteresis).

- The influence of external effects on the performance of piezoactuators.
- The composition and doping of piezoceramics.

11.2.2 Material Selection

The piezoceramic PZT, a solid solution of lead titanate and lead zirconate, was chosen after careful comparison of all the available piezoelectric materials and consideration of the nature of applications our research group is involved in.

11.2.3 Processing of PZT

The next step was to design and implement the experimental setup for producing piezoceramics. This was achieved by:

- A general literature survey on the processing techniques of ceramics in particular those of PZT.
- Field trips to piezoceramics processing facilities[1].
- Selection and ordering of some equipment such as the furnace, poling power supply, d_{33} tester and press.
- The design and manufacture of some required equipment, including the clamps for poling and characterization, the pressing die and the ball-mill.
- Design of the laboratory layout.
- Installation, testing and calibrating of the equipment in the laboratory.

---

1. Two visits were made to BM HI-Tec. company in Ontario to examine their processing facilities.

11.2.4 Characterization

A laboratory for evaluating the piezoelectric properties of ceramics was established. The following properties can be directly measured by the available equipment:

- The piezoelectric coefficient (d_{33}).
- The resonance and anti-resonance frequencies.
- The Capacitance.

11.2.5 Experiments Conducted and Results Obtained

Ten batches of PZT were processed in an effort to improve the processing parameters. The starting value for each parameter was taken from the literature such as [5] and [6]. However, some of the processing parameters needed improvement. This was because of the differences between our facilities and those used by the authors of the cited literature. These inconsistencies are usually in the raw materials and equipment.

The results from batches 9 and 10 are discussed here because they were the most successful. As shown in Figure 11.1, the piezoelectric coefficient (d_{33}) obtained for both batches was very close to the values listed in literature for PZT-5 and in the BM527 manual indicating the success of processing. On the other hand, the electromechanical coefficient (k_{33}) was 83% of the expected value for both ceramics. This is probably due to a slight deviation from stoichiometry caused by excessive loss of lead oxide during densification.

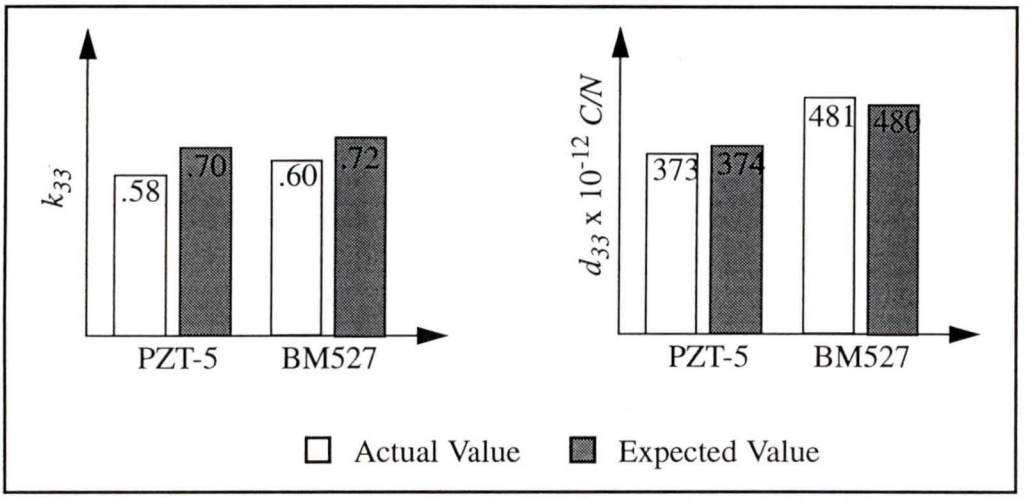

Figure 11.1: Experimental results for batches 9 and 10

11.3 Problems Encountered

The following problems were faced during the experimental phase of this research effort:

- Long delays in the delivery of equipment which prolonged the experimental phase.
- The secrecy surrounding the composition and doping of advanced PZT ceramics. Naturally, this meant that we had to start our research from basic compositions of inferior qualities.
- The difference in properties between raw materials received from different suppliers w leads to the continuous need for the readjustment of the processing parameters. The variation are usually in the amounts of impurities and particle size of the raw materials. The later can be overcome by careful particle size evaluation and readjusting the ball-milling time accordingly. The presence of impurities is a much more complicated matter and suggestions on overcoming it are presented in Section 11.4.2 on page 131.
- The limited temperature rise rate in the furnace, especially at high temperatures, led to excessive loss of lead oxide and small grain size.

- Poor ventilation in the furnace during binder burn-off and sintering of silver.
- The limited electric field that can be supplied by the poling station (20 *KV*) restricted the maximum thickness of samples to 8*mm*.

11.4 Recommendations

11.4.1 Equipment

It is suggested that the following modifications and equipment should be added to the laboratory:

- A new ventilation system for the existing furnace or a new low temperature (up to 600^oC) furnace with specialized ventilation for binder burn-off and silver sintering.
- Pressing dies for making square, tube and cylindrical-shaped samples.
- Many problems are associated with using wax as a binder in surface grinding. Thus, a new clamp should be designed to replace the glass cylinder.
- Although impedance analyzers are very expensive, they are essential for more advanced characterization research.

11.4.2 Future Research

It is suggested that our research in the arèa of piezoelectric materials processing and characterization should take the following directions:

- Theoretical and experimental work on the improvement of the piezoelectric properties of PZT-5. This can be done by studying the effect of different quantities (0.05 to 5 at.%), kinds (*Bb, Ta, Sb, La, Bi* and *Nd*) and combinations of donor dopants.

- The improvement of the existing theoretical piezoelectric models by incorporating non-linear effects and experimental results.
- Improving the reliability and consistency of piezoceramics by isolating their final properties from variations in the raw materials. This can be done by:

  i) studying the effect of raw material impurity on the final properties,

  ii) devising methods of identifying these impurities in raw materials, and

  iii) developing a model that would use the previous two points to predict the changes to the processing parameters needed to maintain the final properties.
- Research into new piezoelectric materials such as single crystals and polymers.

11.5 Final Note

This application-oriented research has established the required background and expertise that will make it possible to repeatedly process the piezoceramic PZT in our laboratory. The successful processing of PZT (batches 9 and 10) is considered as the essential first step in the IRIS project for future research in materials and applications.

Appendix A

Due to the experimental nature of this research effort several items were purchased for use in the laboratory. These equipment and raw materials along with their suppliers are listed in this appendix to facilitate future work.

TABLE 11-1 List of suppliers

Item	Supplier	Phone	Fax
PZT powder (BM527, 500, 532 and 800)	BM Hi-Tech[a]	(705)444-1440	(705)444-6787
d_{33} Tester	BM Hi-Tech	(705)444-1440	(705)444-6787
Silver paint screen	BM Hi-Tech	(705)444-1440	(705)444-6787
Lead, zirconium and titanium oxides	Alfa AESAR (Johnson Matthey)	1-800-343-0660	1-800-322-4757
Electric furnace	Mellen[b]	(603) 648-2121	(603) 648-2177
Hydraulic press	Princess Auto	(604) 860-6191	(604) 861-8372
Anderson pipet	Fisher Scientific	(604) 872-7641	(604) 872-5819
Stirring hot-plate	Fisher Scientific	(604) 872-7641	(604) 872-5819
Ultrasonic cleaner	Fisher Scientific	(604) 872-7641	(604) 872-5819
Alumina crucibles	Fisher Scientific	(604) 872-7641	(604) 872-5819
Surface grinder	LECO Instruments	(905) 564-6577	(905) 564-6582
Diamond grinding discs	LECO Instruments	(905) 564-6577	(905) 564-6582
Silver Paint	Lakeside electronics	(905) 668-2981	(905) 666-0153
Power supply	Acopian	(610) 258-5441	(610) 258-2842
Capacitance meter	BK Precision	(604) 273-2911	(604) 273-7360

a. Contact: Dr. E. Prasad

b. Contact: R. Berliner

Bibliography

1. W. Cady. *Piezoelectricity Vol. 1.* Dover Publications, New York. 1964.

2. W. Cady. *Piezoelectricity Vol. 2.* Dover Publications, New York. 1964.

3. J. Shields. *Basic Piezoelectricity.* Eastmidlands, Bucks. 1966.

4. D. W. Richerdson. *Modern Ceramic Engineering.* Marcel Dekker Inc, New York. 1982.

5. B. Jaffe, W.R. Cook, H. Jaffe. *Piezoelectric Ceramics.* Academic Press, London 1971.

6. A. J. Moulson, J. M. Hurbert. *Electroceramics Materials Properties Applications.* Chapman and Hall, New York. 1990.

7. H. F. Tiersten. *Linear Piezoelectric Plate Vibration.* Plenum Press, New York. 1969.

8. K. Ragulskis. *Vibromotors For Precision Microrobots.* Hemishere Publishing, New York. 1988.

9. A. C. Eringen. *Mechanics of Continua.* Robert Publishing Company New York. 1980.

10. V. Z. Parton, B. A. Kudryavtsev. *Electromagnetoelasticity.* Gordon and Breach Science Publishers, New York. 1988.

11. M. Farag. *Selection of Materials and Manufacturing Processes for Engineering Design.* Prentice Hall, London. 1989.

12. W. F. Smith. *Material Science and Engineering.* McGraw-Hill, New York. 1990.

13. M. A. Omar. *Elementary Solid State Physics.* Addison Wesly, London. 1975.

14. G. Kino. *Acoustic Waves.* Prentice Hall. Englewood Cliffs. 1987.

15. V. Bottom. *Introduction to Quartz Crystal Unit Design.* Van Nostrand, New York. 1982.

16. C. DeSilva. *Control Sensors And Actuators.* Prentice Hall, Englewood Cliffs. 1989.

17. T. Allen. *Particle Size Measurement.* Chapman and Hall, London. 1990.

18. J. S. Reed. *Introduction to the Principles of Ceramic Processing.* Wiley Interscience Publication, New York. 1985.

19. B. D. Cullity. *Elements of X-ray Diffraction.* Addison-Wesley Publishing, Massachusetts. 1978.

20. G. A. Maugin. *Continuum Mechanics of Electromagnetic Solids.* Elsevier Publishers, Amsterdam. 1988.

21. W. H. Nebergall. *General Chemistry.* Raytheon Education Company. 1968.

22. W. B. Carlson, S.E. Trolier, A. Safari, R. E. Newman, L.E. Cross. Multilayer Actuator Design. *IEEE 6th International Symposium on Applications of Ferroelectrics,* 641, 1992.

23. K. Uchino. Ceramic Actuators: Principles and Applications. *MRS Bulletin,* 42. 1993.

24. S. Trolier-McKinstry, R.E. Newnhan. Sensors, Actuators, and Smart Materials. *MRS Bulletin,* 27. 1993.

25. H. Ohigashi. Piezoelectric Polymers-Material and Manufacture. *Japanese Journal of Applied Physics.* Vol. 24. Supplement 24-2, pp. 18-22. 1985.

26. BM HI-Tec. "Characterization of Piezoceramics".

27. BM HI-Tec. "d_{33} Tester Manual".

28. Royal Military Collage. "Characterization of Piezoelectric Ceramics".

29. Physik Instrument. Products for Micropositioning". CAT 108-12/90.14, West Germany.

30. ASTM E11. *Annual Book of ASTM Standards*. American Society for Testing and Materials, Philadelphia, 1970.

VITA

Surname: El-Lakany Given Name: Hatem

Place of Birth: Vancouver, British Colombia, Canada Date of Birth: 30 August 1969

Educational Institution Attended:

University of Victoria	1993 to 1996
The American University in Cairo	1987 to 1992

Degrees Awarded:

B.Sc.	The American University in Cairo	1992

Honors and Awards:

University of Victoria Fellowship	1994
High Honors Gradation Status	1992

PARTIAL COPYRIGHT LICENCE

I hereby grant the right to lend my thesis to users of the University of Victoria Library, and to make single copies only for such users or in response to a request from the Library of any other university, or similar institution, on its behalf or for one of its users. I further agree that permission for extensive copying of this thesis for scholarly purposes may be granted by me or a member of the University designated by me. It is understood that copying or publication of this thesis for financial gain shall not be allowed without my written permission.

Title of Thesis:

The Processing and Characterization of Piezoelectric Ceramics

Author [redacted]

Hatem El-Lakany

1996